ABSTRACT

Title of Dissertation: THE ROLE OF THE MECHANICAL ENVIRONMENT ON CANCER CELL TRANSMIGRATION AND MRNA LOCALIZATION

Susan M. Hamilla, PhD. 2016

Dissertation directed by: Associate Professor, Helim-Aranda Espinoza
Fischell Department of Bioengineering

Most cancer-related deaths are due to metastasis formation, the ability of cancer cells to break away from the primary tumor site, transmigrate through the endothelium, and form secondary tumors in distant areas. Many studies have identified links between the mechanical properties of the cellular microenvironment and the behavior of cancer cells. Cells may experience heterogeneous microenvironments of varying stiffness during tumor progression, transmigration, and invasion into the basement membrane. In addition to mechanical factors, the localization of RNAs to lamellipodial regions has been proposed to play an important part in metastasis. This dissertation provides a quantitative evaluation of the biophysical effects on cancer cell transmigration and RNA localization.

In the first part of this dissertation, we sought to compare cancer cell and leukocyte transmigration and investigate the impact of matrix stiffness on transmigration process. We found that cancer cell transmigration includes an additional step,

'incorporation', into the endothelial cell (EC) monolayer. During this phase, cancer cells physically displace ECs and spread into the monolayer. Furthermore, the effects of subendothelial matrix stiffness and endothelial activation on cancer cell incorporation are cell-specific, a notable difference from the process by which leukocytes transmigrate. Collectively, our results provide mechanistic insights into tumor cell extravasation and demonstrate that incorporation into the endothelium is one of the earliest steps.

In the next part of this work, we investigated how matrix stiffness impacts RNA localization and its relevance to cancer metastasis. In migrating cells, the tumor suppressor protein, adenomatous polyposis coli (APC) targets RNAs to cellular protrusions. We observed that increasing stiffness promotes the peripheral localization of these APC-dependent RNAs and that cellular contractility plays a role in regulating this pathway. We next investigated the mechanism underlying the effect of substrate stiffness and cellular contractility. We found that contractility drives localization of RNAs to protrusions through modulation of detyrosinated microtubules, a network of modified microtubules that associate with, and are required for localization of APC-dependent RNAs. These results raise the possibility that as the matrix environment becomes stiffer during tumor progression, it promotes the localization of RNAs and ultimately induces a metastatic phenotype.

THE ROLE OF THE MECHANICAL ENVIRONMENT ON CANCER CELL TRANSMIGRATION AND MRNA LOCALIZATION

By

Susan M. Hamilla

Dissertation submitted to the Faculty of the Graduate School of the
University of Maryland, College Park, in partial fulfillment
of the requirements for the degree of
Doctor of Philosophy
2016

Advisory Committee:
Associate Professor Helim Aranda-Espinoza, Chair
Appointed Faculty, Voula Mili
Associate Professor, Ian White
Assistant Professor, Kimberly Stroka
Associate Professor, Garyk Papoian (Dean's Representative)

Dedication

This work is dedicated to my parents, Ellen and David Hamilla, and also to my sister Sandy Hamilla.

Acknowledgements

I want to thank my advisor, Dr. Helim Aranda-Espinoza for the opportunity to work in the Cell Biophysics laboratory, welcoming me into his lab, and mentoring me throughout the duration of my tenure at the University of Maryland. I want to give a special thanks to my co-advisor and mentor at the NIH, Dr. Voula Mili who introduced me to RNA localization. None of this work would have been possible without her guidance. Her advice and mentorship has been a crucial aspect of my development as a scientist. I am grateful for both Helim and Voula who have provided me with so many opportunities, for continuously challenging me to be a better scientist, and for supporting me every step of the way.

I want to thank my committee members for all of their support and comments, especially Kimberly Stroka who introduced me to cancer transmigration. I want to also like to thank my colleagues, friends and students for many useful discussions, comments, and suggestions. I want to especially like to thank Tianhong from Voula Mili's lab as she helped me with some of the confocal imaging.

I want to thank my fiancé Carlos Luna, for his emotional and intellectual support. Seeing his continuous drive, devotion, and ingenious thinking has inspired me to become a better scientist.

I would like to acknowledge the generous funding I have received over the last five years:(1) the NCI-UMD Partnership for Integrative Cancer Research which funded me for two years and introduced me to Dr. Voula Mili, (2) Dr. Aranda-Espinoza's NSF

and HHMI funding and Dr. Voula Mili's NIH funding and (3) various travel grants which have allowed me to travel to international and national conferences.

Table of Contents

List of Tables

Chapter 3

Chapter 4

List of Figures

Chapter 1

Chapter 2

Chapter 3

Chapter 4

Chapter 1: Introduction and Background

1. Introduction

Cancer is a major health concern that affects millions of people worldwide. The main contributing factor to the deadliness of the disease is cancer metastasis, the ability of cancer cells to break away from the primary tumor site, migrate through the vasculature, transmigrate through the endothelium, and then form secondary tumors in distant areas of the body. Thus far, much research has been dedicated to analyzing cancer cells' molecular and biochemical capabilities, but less is known about regulation and localization of genetic factors during transmigration and how mechanical properties of the microenvironment influence metastasis formation.

There are many steps where the mechanical properties of the extracellular matrix influence cell behavior during the metastatic cascade. As tumors progress, they display desmoplasia, a fibrotic state characterized by increased deposition, increased post-translation modifications of extracellular matrix proteins, and altered organization [1, 2]. This increases local matrix stiffness and ultimately leads to a phenotype promoting migration away from the tumor [3]. Similarly, once the tumor cell migrates away from the primary tumor, it encounters mechanical properties within the blood stream. Blood vessel stiffness likely varies based on tissue location and type. The effects of stiffness are relevant in the context of cancer metastasis from primary tumor formation, to transmigration, and finally to secondary tumor formation. The effects of subendothelial

matrix stiffness and mechanisms governing cancer cell transmigration, however, were poorly understood prior to our work.

On a more molecular level, we wanted to understand the role of localized RNAs in the context of cancer and their response to extracellular matrix stiffness. During cellular migration, cells polarize such that at the leading edge, actin polymerization and formation of new adhesions drive the cellular extensions forward. At the trailing edge, contractile forces and adhesion disassembly propel the cell forward [4]. Localized mRNAs are prominently observed during this process. RNAs accumulate at sites of new integrin engagement [5], at lamellipodia [6, 7], and at sites of early or persistent protrusion formation [8, 9]. Localization of RNAs in lamellipodial regions has been proposed to play an important role during metastatic progression [10], however, the identity and functional significance of these localized mRNAs has been investigated only in few cases [11]. Furthermore, mRNA localization at adhesion sites is influenced by mechanical tension, which is adjusted by cells as a function of the mechanical properties of the cell environment [5]. **The objective of this dissertation was to understand the mechanisms and effects of matrix stiffness on cancer cell transmigration and mRNA localization.**

In the first part of our objective, we examined the mechanisms of cancer cell transmigration and how it is affected by subendothelial matrix stiffness. We formed endothelial cell monolayers on extracellular matrix coated (ECM) hydrogels. The stiffness of the matrix was varied to in order to mimic physiological tissue and vasculature stiffness. We found that cancer cell transmigration is unique from leukocyte

transmigration, and that it includes an additional step, incorporation into the endothelium (Chapter 2). Secondly, we found that it was independent of matrix stiffness and endothelial cell activation (Chapter 2) for melanoma cells and breast cancer cells. Pancreatic cells, however, were sensitive to endothelial cell activation and subendothelial matrix stiffness. These results indicate that the place where cells exit the blood stream is cell specific. It is likely a combination of cell-specific properties such as adhesion molecules and their sensitivity to extracellular matrix stiffness that determines homing mechanisms of cancer cells.

Our next objective was to gain a better understanding of molecular factors involved in cancer metastasis. We decided to focus on RNA localization and the effect of matrix stiffness on RNA localization. In one pathway, the tumor suppressor protein Adenomatous Polyposis Coli (APC) is required for localization of RNAs at cell protrusions. The APC-dependent localization pathway was the focus of our work. Interestingly, we found that substrate stiffness enhances RNA localization (Chapter 3). We hypothesized that increased actomyosin contractility contributed to localization. We found that myosin II inhibition reduced localization on stiff substrates and that increasing contractility on soft substrates (with lysophosphatidic acid (LPA)) induces RNA localization (Chapter 3). The subset of RNAs we were examining is located at the tips of detyrosinated microtubules. Thus, our next goal was to examine the effect of substrate stiffness and contractility on microtubule detyrosination (Chapter 4). We found that contractility enhances microtubule detyrosination and that detyrosinated microtubules are necessary and sufficient for RNA localization. Finally, we wanted to look at the

interplay between actomyosin contractility and detyrosinated microtubules (Chapter 4). We found that the effects of myosin II inhibition (reduced RNA localization) could be recovered by increasing the amount of detyrosinated microtubules. Similarly, we found that on soft substrates inhibiting detyrosinated microtubules could reverse RNA localization after increasing contractility. Thus, actomyosin contractility through modulation of the detyrosinated microtubule network drives RNA localization to cellular protrusions. Likely, this effect is mediated through RhoA and a downstream effector mDia that signals the formation of detyrosinated microtubules. The results of this research have implications in cancer metastasis. **We envision a scenario where as the microenvironment stiffens during tumor progression, it drives the localization of RNAs to cellular protrusions** where they may play roles in cancer cell adhesion and migration, and ultimately promote the metastatic phenotype.

1.2. Background: Cancer cell transmigration and RNA localization

1.2.1 Cancer Metastasis

Cancer is a public heath concern that affects people all over the world. In the United States alone, 1 in 4 deaths is attributed to cancer [12]. The cause of death attributed to primary tumors accounts for only 10% of cancer death, while the remaining 90% are caused by secondary tumors [13]. In particular, cancer metastasis, the ability of cancer cells to break away from the primary tumor site, enter the lymph and/or blood vessels, circulate through the body and invade surrounding tissue where they then form secondary tumors is the main contributing factor to the deadliness of the disease. However, diagnosis of cancer is usually not made until it becomes life-threatening and

the cancer has already metastasized. Therefore, it is critical to emphasize research that will lead to improved diagnostic and therapeutic targets for the disease.

1.2.2 Cancer Cell Transmigration

One of the main steps in the metastatic cascade is the adhesion of tumor cells to the endothelium lining the blood vessels, transmigration through the endothelial cell monolayer, and migration into the basement membrane. Immune cells routinely transmigrate through the endothelium to reach sites of injury and inflammation. The signaling mechanisms underlying this process are well characterized [14]. The mechanisms governing cancer cell transmigration, however, are less understood. In principle, the general process of extravasation is presumed to be the same. In the first step, cells loosely adhere to the endothelium, an event that is mediated by endothelial expression of selectins [14]. Due to the slack attachment, the cells are still pulled along by the blood flow, resulting in a rolling motion across the endothelial surface. This process is called 'rolling". Eventually cells form a tight attachment to the endothelium using specific receptors. Then, they subsequently transmigrate through the endothelial cell barrier in a process called diapedesis [14].

The function of the endothelium in cancer cell transmigration is a crucial aspect because it can actively modulate extravasation by allowing or blocking adhesion [15-17]. As a main pathway of tumor-endothelial interaction, adhesion receptors and integrins facilitate tumor-cell invasion. During the rolling process, tumor cells use adhesion molecules to loosely tether to the endothelium. Several groups have found that tumor

cells express ligands for E-selectin [18-20]. The expression of E-selectin ligands correlates with a high potential of bone metastases [18, 19]. E-selectin is a receptor that becomes expressed by endothelial cells upon exposure to inflammatory cytokines and helps mediate the rolling process. N-cadherin has also been identified as another molecule to mediate the rolling of breast cancer cells and also been identified to play a role during the transmigration step [21]. To facilitate tight adhesion to the endothelium, cancer cells use integrins. Expression of αvβ3 integrin has been shown to be associated with the metastatic potential of tumor cells [15]. Furthermore, animal models have shown that αvβ3 integrin on melanoma cells enhances interactions with vascular endothelial adhesion molecule-1 (VCAM-1) [22, 23]. Other adhesion molecules have also been identified to facilitate tumor adhesion to the endothelium. Galectins are one group that has been identified on tumor cells to increase metastatic potential by increasing their adhesion to endothelial cells [24, 25]. While many adhesion molecules have been identified to play a role during transmigration, the actual process of diapedesis of tumor cells through the endothelium still remains elusive.

During the process of diapedesis, leukocytes cross the endothelium without damaging its integrity. Leukocytes can either move between endothelial cells in a paracellular route, or through the endothelial cell itself, in a transcellular route. For cancer cells, the route of transmigration through the endothelium is largely unknown. It is also unknown whether tumor cells leave the endothelium intact or induce apoptosis in neighboring endothelial cells. Based on this, one of the goals of this dissertation was to examine the mechanism of cancer cell transmigration through the endothelium.

Another question that remains largely unanswered is what signals guide tumor cells to extravasate. For leukocytes, they are guided by inflammatory cytokines such tumor necrosis factor alpha (TNF-α) which is produced by stromal cells. Additionally, we have shown previously that leukocytes are mechanosensitive to the subendothelial matrix stiffness and increase their transmigration rates with stiffer subendothelial matrix stiffness [26, 27]. It is currently unknown how cancer cells respond to subendothelial matrix stiffness and chemokines such as TNF-α; thus another goal of this dissertation was to elucidate these questions.

1.2.3 Cellular mechanotransduction

Most cells in multicellular organisms are attached to much softer environments than the glass and plastic materials that are commonly used in vitro. Most common attachment sites for cells such as the extracellular matrix have elastic moduli between 10-10,000 Pa [28, 29]. Consequently, cell functions as well as morphology depend strongly on the substrate stiffness.

As cells migrate, they probe elasticity as they anchor and pull on their surroundings. Such processes are dependent on myosin-based contractility and transcellular adhesions to transmit forces to the substrates [30]. Cell-exerted forces promote a feedback loop of inside-outside-in signaling that couples to the elasticity of the extracellular microenvironment to intracellular responses [30]. Therefore, cells alter their behavior based on the substrate they are plated on. For example, NIH 3T3 fibroblast cells alter their spreading behavior, exertion of traction forces, as well as their motility on

soft flexible polyacrylamide gels compared to stiffer substrates [31, 32]. Substrate stiffness also affects the motility of smooth muscle cells [33], mouse fibroblasts [34], as well as neutrophils [35, 36]. Fluorescence imaging also reveals more F-actin organization and stress fiber formation on increasingly stiff substrates in fibroblasts. Focal adhesions are also affected by the stiffness of the matrix. On soft gels (<1kPa), fibroblast cells show diffuse and dynamic adhesion complexes. On stiff gels, cells show stable adhesions similar to those observed on glass [31].

Furthermore, evidence implicates a role of signaling in stiffness sensing. Tyrosine phosphorylation of many proteins, including paxillin, is enhanced on stiff substrates [31]. However, inhibition of actomyosin contractions largely eliminates focal adhesions and stimulation of contractility drives integrin aggregation into adhesions [37]. Additionally, myosin inhibitors such as the myosin II inhibitor, blebbistatin, have provided evidence of the role of contractility in substrate sensing [31, 38]. Myosin II has a well-established role on rigid substrates in adhesion and cytoskeletal organization [37, 39], spreading [39], as well as cell tension [40]. Activator proteins of the Ras superfamily, especially Rho subfamily members, are known to regulate the cytoskeleton, cell growth and contractility. Rho stimulated contractility drives stress fiber and focal adhesion formation and upregulation of alpha smooth muscle actin correlates with contractility on rigid substrates [37, 41].

Cancer cells also respond to the mechanical properties of their microenvironment. Ample evidence implicates alterations in the signaling pathways that regulate the response of cells to microenvironmental cues as critical events in tumor initiation,

progression, metastasis, and perhaps tumor dormancy [42]. Additionally, the increase in tumor tissue rigidity due to the accumulation of dense, cross-linked collagen matrix locally is a hallmark of cancer progression in soft tissues [1]. It has been shown that cancer cells modulate their gene expression in response to the mechanical properties of the substrate [43-45]. For example, the lung carcinoma cell line, A549 responded to culture on soft polyacrylamide gels by expressing the differentiated epithelial marker E-cadherin and decreasing the expression of the mesenchymal transcription factor Slug [44]. Additionally, ECM stiffness promotes invasion and metastasis. ECM stiffness promotes invadapodia formation and intensifies cancer invasion by driving focal adhesion assembly [3]. Since cells alter their behavior from morphology, to gene expression, to migration in response to extracellular matrix stiffness, it is a very important parameter to take into consideration. Specifically, a stiffened ECM promotes metastasis by fostering properties such as proliferation, angiogenesis, and motility and invasion. The interplay between localized RNAs and the stiffened matrix may be a contributor to the progression of metastasis.

1.2.4 RNA Localization

The ability to form pseudopodial protrusions is closely related to cancer cell invasiveness and metastatic properties. A number of asymmetrically localized RNAs have been observed in pseudopodial protrusions or at the leading edge of migrating cells [7, 46]. In some cases the evidence suggests that they have a functional role in cell migration [11, 47]. Furthermore, deregulation of RNA binding proteins involved in

localization pathways has been implicated in cancer metastasis [10, 48, 49]. Therefore, to gain a better understanding of molecular factors that influence cancer metastasis, we decided to focus on RNA localization in migrating cells. The next sections focus on the regulation of RNA localization, and RNA localization pathways in migrating cells.

Subcellular localization of mRNAs can give rigorous control over where protein products are synthesized and operate. Localized mRNAs are present in a wide range of cell types and they play central roles in many cellular events. The asymmetric distribution of mRNAs was first visualized when in-situ hybridization techniques were used to detect β-actin mRNA in embryos [50]. Since then, high-throughput approaches have allowed for identification of numerous localized RNAs and revealed that it is more common than previously assumed. In *Drosophila* embryos, for example, 70% of expressed RNAs were classified as asymmetrically distributed [51]. Recent high-throughput screens have also identified hundreds of mammalian RNAs are enriched in protrusions of fibroblasts [8], in neuronal processes [52, 53], or on spindles [54]. These studies indicate that mRNA localization has a prominent role in the spatial recognition of gene activity.

There are many advantages to localizing RNAs rather than proteins. Transport costs are reduced because many proteins can be translated from a single mRNA molecule. Transporting mRNAs also prevents proteins from acting prematurely before they reach the appropriate site. Localization of mRNAs can also facilitate incorporation of proteins into macromolecular complexes by generating high local protein concentrations and then allowing the co-translation of different subunits. Lastly, a major

advantage of mRNA targeting is that it allows control of gene expression in both space and time. For example, it allows activation of localized mRNA translation specifically at their destination, in response to certain extracellular cues [55].

1.2.5 Cellular Mechanisms Underlying mRNA Localization

The targeting of RNAs involves multiple steps. The cellular "address" of transcripts, or 'zip code', is encoded by *cis*-acting elements in the RNA, or localization elements. Usually, these elements are located in the 3' untranslated region (UTR), but in some cases can be found in the 5'UTR or in the coding sequence. Depending on the nature of the factor they bind, localization elements can consist of single stranded stretches or double-stranded stem loops [56]. Localization elements are recognized by specific RNA-binding proteins (RBPs) that often function in RNA localization and translation regulation. While the molecular mechanisms underlying the recognition of zip codes by RBPs has remained difficult to find, there has been some progress in identifying specific patterns or structures. For example, the RBP ZBP1 recognizes a 54-nucleotide (nt) sequence that contains two RNA motifs to target β-actin mRNA in fibroblasts [57, 58].

There are three different mechanisms that are thought to contribute to mRNA localization after their transcription: (i) localized protection from degradation, (ii) diffusion-coupled entrapment, and (iii) directed transport along a polarized cytoskeleton (Figure 1.1). Localized protection from degradation occurs when non-localized RNAs are degraded and the localized RNAs are protected and has been observed in Drosophila

[59]. The mechanisms governing protection of certain RNAs from degradation are unknown. Diffusion coupled local entrapment occurs when RNAs freely diffuse and are entrapped at specific sites. Diffusion coupled entrapment of mRNA transcripts plays a role in restricting the transcripts to the germ plasm in Drosophila and embryos [60]. Motor-based transport along the cytoskeleton seems to be the predominant mechanism in animal cells. This is because it provides a rapid method for translocation of large ribonucleoprotein complexes through the crowded cellular environment. In mammalian oligodendricytes and neurons, mRNAs are bound to microtubule motors that switch between periods of motion in the plus and minus end directions [61-63]. Some RNAs may even associate with microtubule and actin based motors [64].

Once RNAs are transported, they are usually 'anchored' at their destination to prevent diffusion away from the site of need. In the case of Drosophila oocytes, xenopus oocytes, and dividing yeast cells, static anchoring relies on cortical actin and actin binding proteins [65-67]. Other mechanisms that involve anchoring have also been discovered. In migrating fibroblasts, accumulation of transcripts depends on Adenomatous polyposis coli (APC) [8]. When no 'anchor' is present, localization can be maintained by short bursts of active transport [68].

In order to produce proteins locally, translation suppression is needed to avoid mRNAs being translated before delivery to their specified site. Translational repressors associate with transport RNPs by binding RNA regulatory sequences and blocking translation. Phosphorylation of the repressor at the destination stage can decrease their affinity for the RNAs, allowing the RNAs to be translated at the localization site. The

RNA binding protein, ZBP1 has been shown to exhibit this behavior [69]. Expressing a non-phosphorylatable form of ZBP1 reduces β-actin RNA accumulation at the cell periphery.

Taken together, these mechanisms ensure tight regulation of mRNA localization within the cell.

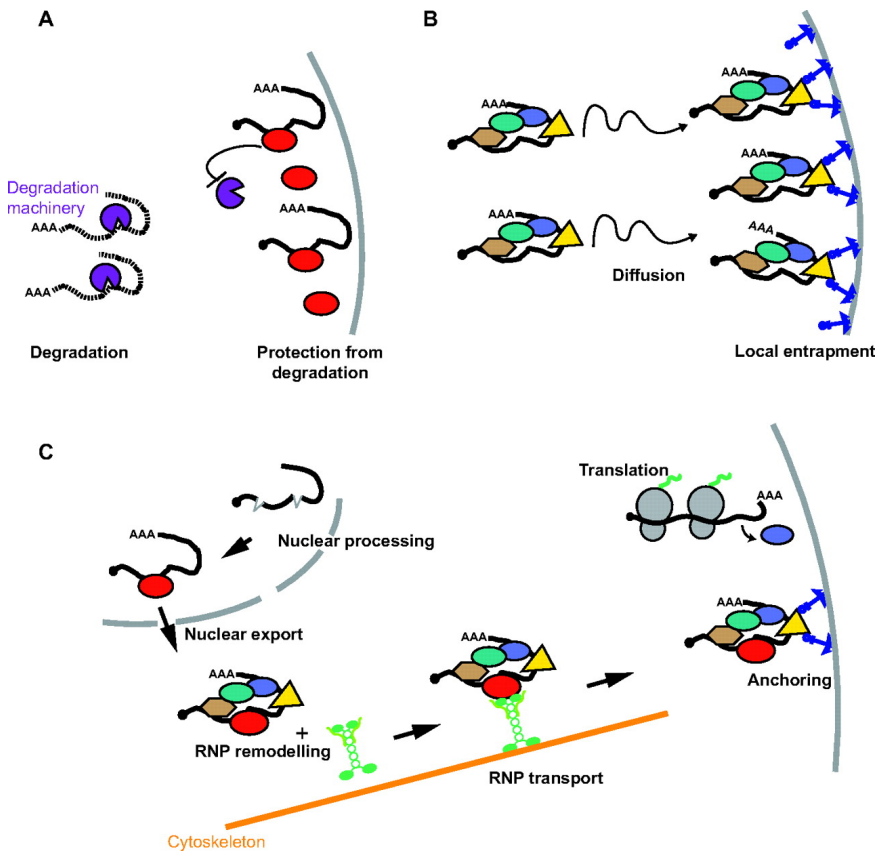

Figure 1.1. There are three distinct mechanisms underlying mRNA localization. (A) Localized protection from degradation (B) Diffusion-coupled local entrapment (C) Directed transport along a polarized cytoskeleton. In (A) localized RNAs are protected from degradation machinery whereas non-localized transcripts are not. In (B) mRNAs diffuse to their destination and are locally entrapped. In (C) mRNAs are recognized by trans-acting factors in the nucleus. When exported to the cytoplasm, cytoplasmic factors recruit molecular motors to facilitate transport along the cytoskeleton. Once at their destination, RNAs are anchored and their translation is activated. Figure adapted from [70].

1.2.6 RNA Localization during Migration

As cells migrate, there is the establishment of front-back cell polarity. Particularly, in mesenchymal-like cells, the front portion of the cell is protrusive and characterized by a network of actin filaments while the back end is retractile towards the cell body in the direction of migration. Most of the proteins that are asymmetrically distributed between the front and back of the cell are associated with the actin cytoskeleton [71]. For example, actin is polymerized at the leading edge by formins and the actin nucleating factors Arp2/3. Similarly, mRNAs are differentially distributed in the rear and leading edge of a migrating cell [7, 8, 72]. Through using a fractionation approach to separate the cell bodies from the protrusions in transwell plates, laser-capture dissection, or microfluidic chamber-mediated isolation, over 700 protrusion localized RNAs have been identified in neurons, cancer cells, astrocytes, and fibroblasts [8, 73-76]. There are at least two main pathways that localize RNAs to protrusions in migrating cells: (1) ZBP1-mediated localization and (2) APC-dependent localization pathway.

1.2.6.1 ZBP1-mediated localization

To date, the localization of β-actin mRNA to the leading edge is one of the most studied pathways in migrating cells. A crucial factor is the RNA-binding protein ZBP1 (zip code binding protein 1 (ZBP1) (also called IMP1 in humans, or CRD/BP in mice)), which associates with β-actin RNA during transcription in the nucleus and accompanies it to the cytoplasm [77]. It is localized in the protrusions of fibroblasts and myoblasts, and in the growth cone of neurons [78, 79]. The localization of β-actin requires the presence

of serum and activation of Rho GTPase and Rho downstream effector myosin IIB [7, 77, 78, 80, 81]. Recent evidence suggests that β-actin mRNA may rely on both actin and microtubules for transport, perhaps in different stages [82, 83]. The microtubule motors KIF11 and KIF5A have been shown to play roles in the transport of β-actin mRNA [83, 84]. ZBP1 binds β-actin mRNA in the nucleus, suppresses translation, and mediates its transport [69, 72, 81, 82]. Once at the destination, β-actin mRNA is anchored at its destination on actin filaments through EF1α, which is a translation elongation factor and an actin binding protein [85]. The translation of β-actin mRNA at the leading edge is regulated by Src kinase that phosphorylates ZBP1/IMP1 causing the dissociation from the mRNA [69]. Once ZBP1/IMP1 has been dissociated from the RNA, translation initiates.

Another example of protrusion-localized mRNAs mediated by ZBP1 is the transcripts encoding the actin polymerization nucleator Arp2/3 complex. The Arp2/3 protein complex regulates the actin cytoskeleton and is localized to the leading edge in migrating cells [86]. All of the RNAs encoding the seven subunits of the Arp2/3 complex are localized n primary chicken embryo fibroblasts and primary human foreskin fibroblasts [7]. This suggests a mechanism for facilitating protein complex assembly through local translation or even co-translation assembly [7]. The protrusion localization is dependent on serum, actin and microtubule cytoskeleton, and activation of Rho and myosin II [7, 87].

1.2.6.2 APC Localization Pathway

In addition to β-actin mRNA, and the Arp2/3 mRNAs, a pathway targets numerous RNAs to the protrusions in migrating cells and depends on the tumor suppressor adenomatous polyposis coli (APC) for accumulation in the protrusions [8] **(Figure 1.2)**. **The APC localization pathway in migrating fibroblasts is the focus of this dissertation.**

Using a fractionation scheme to isolate the cell bodies from the protrusions, about 50 transcripts were found to be enriched in the protrusions of NIH/3T3 cells using a genome wide approach [8]. At the tips of protrusive areas, APC associates with multiple RNAs, including Discoidin Domain Receptor 2 (*Ddr2*), which will be the main focus for this dissertation. Many of the RNAs discovered were found to encode for proteins involved in various functions including membrane trafficking, cytoskeletal organization, microtubule-based transport and RNA metabolism. When comparing the transcripts, no structural motifs appeared to be shared among them, suggesting that their localization signals are defined by a combination of primary sequences and higher order structure. Furthermore, it was found that these transcripts are stably anchored in the protrusions and do not exchange rapidly with free cytoplasmic RNA molecules. It was also found that they do not associate with P-bodies, focal adhesions, or cortical actin or actin stress fibers. However, it was found that they associated with microtubules. The fact that the transcripts appeared to be relatively stable over time, led to the conclusion that the transcripts associate with stable microtubules which are post-translationally modified. Specifically, it was found that they associated with detyrosinated (or Glu) microtubules

(Figure 1.2). At the ends of detyrosinated microtubules, APC also associates with proteins such as FMRP and PABP1 to form APC-containing ribonucleoprotein complexes **(Figure 1.2)** [8, 88]. The translation of APC-associated mRNAs is regulated by the RNA-binding protein Fus/TLS which promotes translation in the protrusions [88].

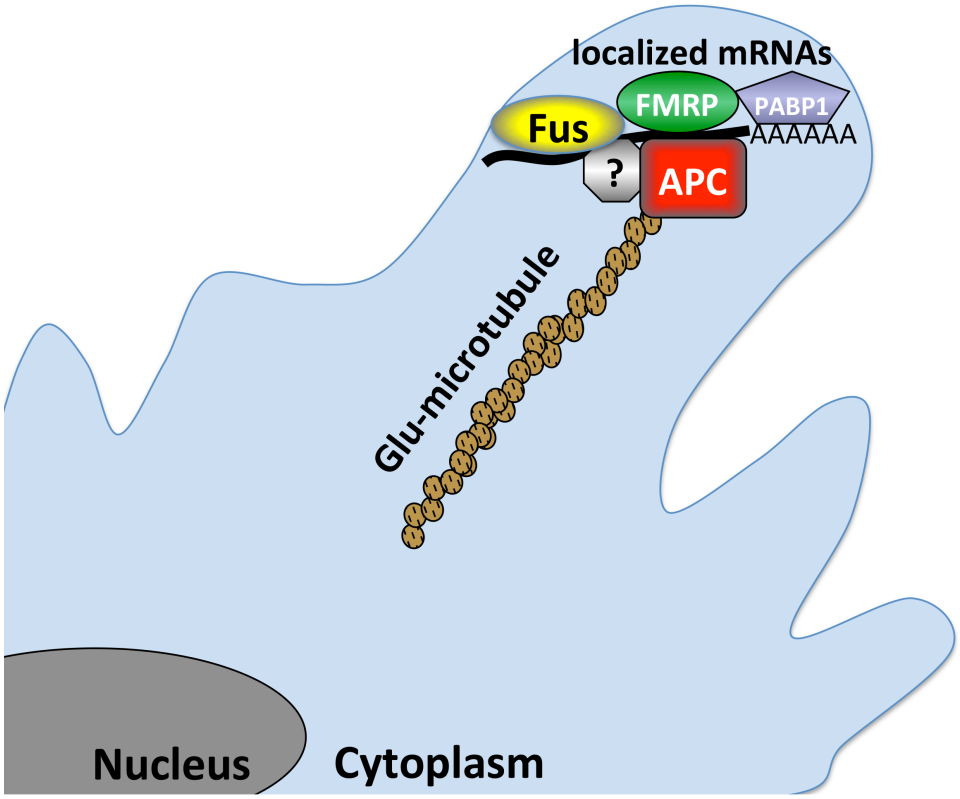

Figure 1.2. APC dependent RNA localization pathway. RNAs are stably anchored at the plus ends of detyrosinated microtubules. Their anchoring requires the tumor suppressor protein adenomatous polyposis coli (APC) for anchoring. APC also associates with proteins such as FMRP and PABP1 to form APC-containing ribonucleoprotein complexes at the ends of detyrosinated microtubules.

1.2.7 APC-associated RNAs

Transport of these mRNAs to the cellular leading edge is dependent on the APC protein, which plays a role in anchoring the mRNAs to the plus ends of detryrosinated MTs. These mRNAs have previously been identified to be isolated to protrusions in various cell types based on genome wide screens. The proteins that they encode are also implicated in processes relating to cellular migration and metastatic progression. Therefore, localization or not of these RNAs might have functional relevance.

1.2.7.1 Rab13

During epithelial morphogenesis, the development and organization of cell symmetry requires the assembly of functional tight junctions. Epithelial polarity also depends on the continuous sorting of proteins and lipids into distinct cell surface domains. A family of small GTPases, Rab proteins, is involved in regulating tight junction dynamics. Recent work suggests that RAB13 regulates the assembly of functional tight junctions and the role of Rab13 in polarized vesicular transport from the trans-Golgi network to the cell surface is distinct from other Rab proteins [89-91]. Functional tight junctions play a crucial role in regulating paracellular transport across cells and maintenance of epithelial polarity. Modulations of tight junction structure and function have been shown in epithelial tumorgenesis, mostly the loss of cellular polarity and paracellular permeability [92]. Furthermore, it has been shown that RAB13 is required for epithelial cell scattering, one of the first major steps in metastasis [92]. RAB13 knockdown has been shown to reduce spread of cancer cells *in vivo* and reduces

cancer cell migration and invasion *in vitro[93]*. *RAB13* mRNA has also been found in breast cancer protrusions [75].

1.2.7.2 Pkp4

PKP4, or plakophilin 4/p0071 is a member of the armadillo family of proteins. PKP4 is located at desmosomes and adherens junctions playing a regulatory role in the dynamics of intermediate filaments and actin cytoskeletal assemblies [94, 95]. PKP4 also have been shown to localize to the cytoplasm where it acts as a regulator for the small GTPase RhoA [95]. The *Pkp4* mRNA has been shown to be localized in protrusions of mouse astrocytes [76], NIH3T3 cells [8], and MDA-MB-231 metastatic breast cancer cells [75]. Furthermore, PKP4 is associated with different steps in carcinogenesis [94, 96-98]. Knockdown of PKP4 has been shown to affect the migratory properties of epithelial cells [94].

1.2.7.3 Ddr2

This dissertation focuses mainly on the localization of Ddr2 RNA as representative APC-dependent RNA. Discoidin domain receptor 2, or DDR2, is a homodimeric tyrosine-kinase collagen receptor that binds to triple-helical collagen fibers. When DDRs bind to collagen, it becomes activated and serves as an initiator for many signaling pathways [99]. One of the common outcomes after DDR activation is an increase in metalloproteinase secretion and collagen rearrangement [100-103]. Therefore, DDR2 has been associated with metastasis during tumor progression [100]. It

has recently been investigated that DDR2 stabilizes SNAIL1 to facilitate breast cancer metastasis [104]. A recent study by Afonso et al. showed that DDR2 regulates neutrophil chemotaxis in 3D [105].

1.2.8 RNA localization and disease

During many human disease pathologies, RNA localization pathways become defective. RNA localization pathways have been identified in neuromuscular and neurodegenerative diseases as well as in cancer. In the genetic disorder spinal muscular atrophy (SMA), the mutation leading to the disease occurs in the SMN1 gene encoding the survival of motor neuron protein (SMN). Several studies have demonstrated that SMN is localized to axonal projections and that its loss leads to impaired trafficking and translation, suggesting that mRNA localization defects contribute to SMA pathogenesis [106, 107]. Additional examples include trinucleotide repeat expansion disorders (TREDS), in which abnormal repeat amplifications either causes RNA gain or loss functions that affect normal RNA localization. A prominent example of this is fragile X syndrome (FXS), a genetic disorder that represents the most common form of inherited mental retardation [108]. Expansion of the CGG repeats in the 5'UTR of the FMR1 gene leads to transcriptional silencing and loss of function of the protein FMRP [108]. FMRP controls synaptic plasticity in response to external stimuli. FMRP disruption causes defects in mRNA trafficking and translation regulation in dendrites and these functions are also disrupted in FXS [108-110].

In addition to muscle and neurodegenerative diseases, flawed mRNA localization is also involved in cancer. One of the hallmarks of cancer is the loss of normal cell polarity, which is thought to be a causative event leading to tissue disorganization, invasion and metastasis. Taking into account that mRNA localization pathways help regulate and maintain normal cell polarity, disruption of these pathways could be an initiating event in tumorgenesis. In one mouse study, it was shown that the loss of function of the translational regulatory protein, CPEB, led to a loss of cell polarity due to defects of targeting ZO-1, a tight junction protein [111]. CPEB plays a direct role in the apical localization of ZO-1 mRNA, a process that is important for proper tight-junction targeting of ZO-1 protein for the maintenance of epithelial cell polarity. These findings are intriguing because deregulated expression and localization of ZO-1 is associated with poor prognosis in breast cancer patients [112]. Additionally, RNA binding proteins (RBPs) with known roles in mRNA localization have been shown to have clear functions in cancer. Members of the IGF-II mRNA-binding Proteins (IMP) family of RBPs are overexpressed in multiple cancers and have been shown to have oncogenic potential [113-115]. In transformed cells, IMP proteins can reside within RNP granules that are targeted to podosomes or invadopodia (actin rich protrusions that can degrade the extracellular matrix and are thought to enable cancer cell invasion) [116]. In HeLa cells, depletion of IMP factors led to a disruption of invadopodia formation and to a reduced expression of mRNAs that are involved in cellular adhesion [117]. mRNA pathways involving APC are also disrupted during cancer progression. Loss of function of the APC tumor suppressor protein is a main event in colorectal cancer progression. APC

associated mRNAs have also been identified in protrusions of metastatic MDA-MB-231 cells [75].

1.2.9 Microtubule Post-Translational Modifications: Microtubule Detyrosination (Glu-MT)

The focus of this dissertation is on the APC-dependent RNA localization pathway in migrating cells. APC-dependent RNAs are localized to the tips of the protrusions in fibroblasts at the ends of detyrosinated microtubules (Glu-MT) [8]. Thus, this next section focuses on the post-translational modification that gives rise to detyrosinated microtubules and their diverse functions within the cell.

Tubulin and microtubules are subject to post-translation modifications (PTM). Many of these modifications are found concurrently, leading to a diverse population of microtubules. Post-translation modifications affect not only the dynamics, but also their organization and interaction with cellular components. Tubulin PTMs are found in all types of cells. Tubulin may be modified as soluble dimer or in a microtubule. There are many PTMs that can take place, such as detyrosination, acetylation, glutamylation, and phosphorylation to name a few [118].

In the case of detyrosinated microtubules, the posttranslational modifications are associated specifically with tubulin polymerized in microtubules. Newly-synthesized α-tubulin contains a terminal tyrosine. The terminal tyrosine is removed by an unknown cytosolic carboxypeptidase to expose a glutamate. The tubulin tyrosine ligase (TTL) then tyrosinates detyrosinated tubulins released from the microtubules. TTL rapidly and

exclusively adds the tyrosine back to the soluble α/β-tubulin dimers such that newly assembled microtubules are primarily tyrosinated MTs [119-121].

Detyrosinated microtubules are considered to be more stable microtubules as they can persist for hours before turnover. They are much less dynamic than tyrosinated microtubules. However, it is important to note that the Glu-tubulin does not confer stability to the MTs rather that it is the stable microtubules that accumulate Glu-tubulin [122-124]. Factors have been identified that regulate the selective stabilization of microtubules. LPA, for one, has been shown to induce Glu-MT formation and that Rho-GTPase is sufficient for the stabilization of MTs [124, 125].

The interactions of proteins with tyrosinated/detyrosinated MT define distinct cellular compartments and generate a platform for cellular signaling by regulating protein interactions with MTs [126]. For example, although the plus-end tracking protein EB1 binds MT independent of tyrosination, other plus-end tracking proteins require both EB1 and tyrosinated tubulin to localize to MT plus ends [127]. Tyrosination also affects the activity of spastin, a MT severing protein [128]. It preferentially cleaves deytrosinated MT, despite the association of detyrosinated MT with longevity. The detyrosination/tyrosination cycle also recruits molecular motors. Kinesin-1 preferentially binds to detyrosinated microtubules over tyrosinated MT, possibly enabling it to preferentially move various cargos along detyrosinated MT [129].

Detyrosinated microtubules play a role in an array of cell functions, and this dissertation explores the relationship between detyrosinated microtubules and RNA localization.

1.2.10 Conclusions

Cancer metastasis is a complex process that requires cells to undergo a range of changes as they migrate away from the primary tumor, invade the blood stream, and form secondary tumors at distant sites. Cancer cell transmigration through the endothelium plays a critical role in metastasis formation. It is evident that this process may share similarities with leukocyte transmigration. Thus, this thesis aims to dissect the mechanism of cancer cell transmigration through the endothelium and mechanical and biochemical factors that may influence transmigration. Since protrusion formation is a fundamental step in cancer migration and invasion, we decided to focus on localized RNAs and understand how they may play a role in metastasis formation. Specifically, as cancer progresses, the primary tumor becomes stiffer compared to healthy tissue. Thus, we aim to understand how matrix stiffness influences RNA localization and how this might play a role in metastasis.

Chapter 2: Mechanisms of Cancer Cell Transmigration[†]

2.1 Introduction

Cancer metastasis occurs when tumor cells fragment from the primary tumor site, enter the blood and lymph vessels, and spread to distant bodily organs. This process is one of the main contributing factors to the deadliness of cancer [130, 131]. Once metastatic cancer cells have entered the blood stream, they must cross the endothelial cell (EC) barrier before invading the tissue beneath in a step known as extravasation. Most tumor cells arrest by nonspecific binding of coagulation factors and by size restriction in capillary beds [132]. In some cases, specific ligands on tumor cells have been correlated with an increased metastatic potential [15, 133, 134]. Thus far, significant research has been dedicated to analyzing the biochemical and molecular capabilities of cancer cells [135-137], but the underlying mechanism of cancer cell extravasation through the endothelium remains largely unknown. Cancer cells have been observed to migrate through the EC cell body [138], and through endothelial cell-cell junctions without destroying the EC layer [139]. However, conflicting research has also shown that cancer cells do not leave the endothelium intact following extravasation [140-143]. It is

[†] This chapter was originally published as Hamilla, S.M**. Stroka, K.M**, and H Aranda-Espinoza, VE-Cadherin Independent Breast Cancer Cell Incorporation Into the Vascular Endothelium Precedes Transmigration. (2014) PLoS ONE 9(10): e109748. doi: 10.1371/journal.pone.0109748. ** Represents Co-first author.

important to note that these studies used different tumor cell lines, as well of different EC lines and *in vitro* methods, so it is possible that different combinations of various types of tumor cells and ECs may lead to diverging mechanisms of extravasation.

There are three proposed methods of cancer cell migration through the endothelium: (a) cancer cells may migrate through the EC body [138], (b) cancer cells may induce EC apoptosis [141, 142] and (c) cancer cells may migrate through endothelial cell-cell junctions without permanently destroying the EC layer [139]. In recent years, research has also shown that cancer cells also exert forces on ECs that push them deeper into the extracellular matrix during transmigration [144, 145], and that the endothelium enhances cancer cell migration [146]. These findings suggest that cancer migration through the endothelium is a complex process that requires further investigation to elucidate its mechanistic course.

Leukocytes routinely transmigrate through the endothelium and underlying layers of the vasculature to reach tissue sites of inflammation, infection, or injury. This is a well-characterized process that relies on localized biochemical signals. In leukocyte trafficking, the endothelium acts as a selective barrier that greatly reduces the invasion rate [147]. During an immune response, the chemokine tumor necrosis factor alpha (TNF-α) is produced by stromal cells, and the localized exposure of ECs to TNF-α upregulates adhesion molecules such as intercellular adhesion molecule-1 (ICAM-1) on the surface of the endothelium. Furthermore, in addition to molecular changes, TNF-α also significantly alters the structural properties of the endothelium, which induces softening, actin realignment, and an increase in overall permeability [26, 148]. An

additional factor that enhances leukocyte transmigration is the subendothelial matrix stiffness and mechanical properties of the endothelium. These vary during vascular homeostasis and in pathological conditions [26]. Neutrophils are able to mechanosense their microenvironment [26, 36, 149-151], and neutrophil transmigration increases as subendothelial matrix stiffness increases due to EC myosin light chain kinase (MLCK)-mediated contractile forces [26]. All of these changes in the EC monolayer facilitate leukocyte transmigration during an immune response.

Since leukocytes routinely transmigrate through the EC layer, it is presumed that metastatic cancer cells may share many of the same mechanisms. However, these mechanisms have yet to be investigated in greater detail. For example, the involvement of chemokines in tumor-endothelial interactions and their effects on cancer cell migration are not well understood [152]. Even more, the significant molecular and structural changes that take place in the endothelium following TNF-α treatment may enhance metastatic cancer cell transmigration. It also remains to be seen how cancer cell extravasation varies with subendothelial matrix stiffness. As observed with leukocytes [26], it is possible that cancer cell transmigration may increase with increasing substrate stiffness. Cancer cells have also been observed to push ECs into the extracellular matrix during extravasation, indicating that the mechanical properties of the ECM may play an important role. Taken together, these results indicate that both the activation status of the endothelium and subendothelial matrix stiffness may influence cancer cell extravasation.

2.2 Materials and Methods

2.2.1 Preparation of polyacrylamide gel substrates

Thin polyacrylamide gels were prepared on glass coverslips according to the method first described by Wang and Pelham [153] and described in detail in our previous publications [26, 36, 154-157]. Briefly, 280 kPa (15% acrylamide + 1.2% bis acrylamide) and 0.87 kPa (3% acrylamide + 0.1% bis acrylamide) gels were created and coated with 0.1mg/mL fibronectin (Sigma-Aldrich) as previously described [26]. Characterization of the Young's modulus of the gels was accomplished by atomic force microscopy and dynamic mechanical analysis, while analysis of surface-bound fibronectin was accomplished by immunofluorescence [36, 156]. For experiments on glass, 22x22 mm coverslips (Fisher Scientific) were coated with 0.1 mg/mL fibronectin for 2 hours at room temperature.

2.2.2 Cell culture

Human umbilical vein endothelial cells (Lifeline Cell Technology) were cultured as previously described [158]. MDA-MB-231 metastatic breast cancer cells (ATCC) and A375 melanoma cells (ATCC) were cultured in DMEM, 10% FBS and 1% penicillin streptomycin. SW1990 pancreatic cancer cells (ATCC) were cultured in DMEM, 10% FBS, and 50 ug/mL gentamicin. HUVECs (passages 2-5, $4x10^5$ total) were plated onto fibronectin-coated glass coverslips or polyacrylamide gels and grown for approximately 48 hours, at which point a monolayer formed. Cells were treated with control media or 25 ng/mL tumor necrosis factor-α (TNF-α) for the final 24 hours prior to experiments. In

some experiments, HUVECs were transfected with VE-cadherin-GFP (VEcadGFP) using an adenovirus (AdV), which was received as a generous gift from Dr. William Luscinskas (Harvard Medical School). Dr. Luscinskas's lab has previously described the procedure for construction of the VEcadGFP plasmid and transference to an adenovirus expression vector [159]. HUVECs were plated onto fibronectin-coated polyacrylamide gels or glass coverslips and given 1-2 hours to spread, and 3 μL of AdV-VEcadGFP were added to the cells with 2 mL media per substrate. HUVECs were then cultured to monolayer formation as described above. Monolayers were washed with PBS prior to adding additional HUVECs or tumor cells ($1x10^5$ cells total) to the apical surface of the 22x22 mm monolayer. To distinguish between the HUVEC cells within the monolayer and the additional cells added to the monolayer, added HUVECs or MDA-MB-231 cells were stained with the lipophilic $DiIC_{16}$ dye (1 μM) in suspension for 5 minutes at room temperature, followed by centrifugation and a PBS wash.

2.2.3 Live cell imaging and analysis

Live cell microscopy was completed in an enclosed microscope stage incubator at 37°C, 5% CO_2 and 55% humidity using an inverted microscope (Olympus IX71). Images were captured with either a QImaging Retiga-SRV charge-coupled device (CCD) digital camera (QImaging Corporation) using IPLab software (Becton, Dickinson and Company), or with a a QImaging Rolera-MGi CCD digital camera (QImaging Corporation) using Slidebook software (version 4.2.0.9; Intelligent Imaging Innovations). Phase contrast, differential interference contrast (DIC), and/or fluorescence timelapse

images were captured using either a 20x/0.45 NA Ph1 objective or a 60x/1.42 NA oil objective. The fraction of incorporated cells (HUVECs or MDA-MB-231) was calculated by dividing the number of cells that became incorporated at any time during the timelapse sequence by the total number of phase-white cells above the monolayer in the initial frame of the sequence. The time to complete incorporation was calculated using the difference between the time when the cell first began to spread into the monolayer and the time when the cell reached maximum spreading area within the monolayer.

2.2.4 Interference reflection microscopy

Interference reflection microscopy (IRM) was used to detect surface-to-surface interference between light rays reflected from the substrate/medium interface and those from the medium/cell interface, as described in our previous work [160-162]. In this technique, the intensity of the light is a measure of the proximity of the cell to the glass surface, such that areas of the membrane closest to the surface appear dark and those further away appear brighter. Therefore, IRM is an optimal method when evaluating cellular attachment, adhesion, and spreading behavior [160-162]. For spreading experiments, $1x10^5$ MDA-MB-231 cells were plated onto 22x22 mm fibronectin-coated glass coverslips in HUVEC media, resulting in observation of single cells. For these experiments, an inverted microscope (Olympus IX71) with a 60x/1.42 NA oil objective lens and a 100 W mercury lamp (Olympus; used at wavelength 561) was used in combination with a CCD camera (Retiga SRV camera, QImaging) for image capture.

Experiments were performed in an enclosed microscope chamber which maintained culture conditions at 37 °C, 50% humidity, and 5% CO_2. During cell spreading, one frame was recorded every 5 seconds over a period of 1 hour for N=5 independent experiments. For statistical evaluations of spreading areas, images were analyzed using ImageJ (National Institutes of Health) software. The cell-boundaries were traced by hand and area was calculated using ImageJ routines. Areas of MDA-MB-231 cells spreading into a HUVEC monolayer were also traced by hand and compared with single cells spreading onto the endothelium-free coverslip.

2.2.5 Confocal Imaging

A total of $1x10^5$ MDA-MB-231 cells were transfected with 10uL of CellLight Actin-GFP (Life Technologies) according to manufacturer's protocol and allowed to incubate for 24 hours. After 24 hours, infected MDA-MB-231 cells were introduced to a confluent HUVEC monolayer and allowed to incorporate for 15 hours. Following incorporation, cells were fixed in 4% paraformaldehyde and stained using Texas-Red Phalloidin (Invitrogen). Z-stack images were collected using a Zeiss LSM 710 confocal microscope with a 63x oil objective.

2.2.6 Statistical analysis

Statistical analysis was completed by using a Student t-test between pairs of data, or by using ANOVA for groups of data, where $P<0.05$ indicated statistical significance. After ANOVA, multiple comparisons were done using Turkey's honestly significant

difference criterion. All measurements are reported here in the format mean ± standard error.

2.3 Results

2.3.1 Incorporation into the endothelium is the first step in metastatic cancer cell transmigration

MDA-MB-231 metastatic breast cancer cells were introduced onto the apical surface of an EC monolayer and monitored as they interacted with the endothelium (Movie S1). Initially, MDA-MB-231 cells were bright white and spherical in contrast to the underlying phase-darkened and flattened endothelium (Figure 2.1A). Within several hours, the MDA-MB-231 cells began to incorporate into the endothelium, in a process that ranged on average from 40 to 60 minutes (Figure 2.1B) and was visually distinct from neutrophil transmigration through the endothelium (Figure 2.C). Specifically, it appeared that the ECs adjacent to the site of incorporation were physically displaced, creating voids for the MDA-MB-231 cell to spread onto the underlying matrix (Figure 2.1A), whereas neutrophils squeezed through the endothelium without disrupting the monolayer (Figure 2.1C). Some ECs detached from the underlying matrix, rounded up and became spherical following incorporation of MDA-MB-231 cells into the monolayer (Figure 2.2). However, incorporation of MDA-MB-231 cells into the endothelium occurred more slowly, with a smaller slope of "spreading area vs. time", and had a lower final cellular area compared to MDA-MB-231 cells spreading onto an endothelium-free fibronectin-coated substrate (Figure 2.3D), indicating that the endothelium did not favor incorporation of the cancer cell, but rather limited overall spreading area. Furthermore,

MDA-MB-231 cell incorporation into the endothelium occurred more slowly, with a smaller slope of "cumulative incorporation vs. time", in comparison to ECs incorporating into a monolayer of ECs (Figure 2.3A). Thus, it is likely that incorporation of MDA-MB-231 cells into the endothelium occurs by a different mechanism than native ECs spreading into the same endothelium. A375 melanoma cells and SW1990 pancreatic cells were also introduced to the apical surface of the endothelium. Similarly to MDA-MB-231 cells, the melanoma cells and pancreatic cells began to incorporate into the endothelium in a process that lasted approximately 15 minutes and 50 minutes respectively. A375 cancer cells incorporated into the monolayer at a much faster rate compared to metastatic breast cancer cells and their incorporation dynamics closely resembled that of native ECs spreading into the EC monolayer. A375 melanoma cells had a final fraction of incorporation that resembled ECs spreading into ECs, while SW1990 cancer cells had a much lower fraction of incorporation compared to all groups (Fig 2.3C). Furthermore, confocal images (Fig 2.4A) revealed that after 15 hours of incorporation, MDA-MB-231 (green) cells displaced ECs (red) by spreading between adjacent ECs. Orthogonal projections show that MDA-MB-231 cells are in fact spreading between ECs and not migrating underneath them during incorporation (Fig 2.4B).

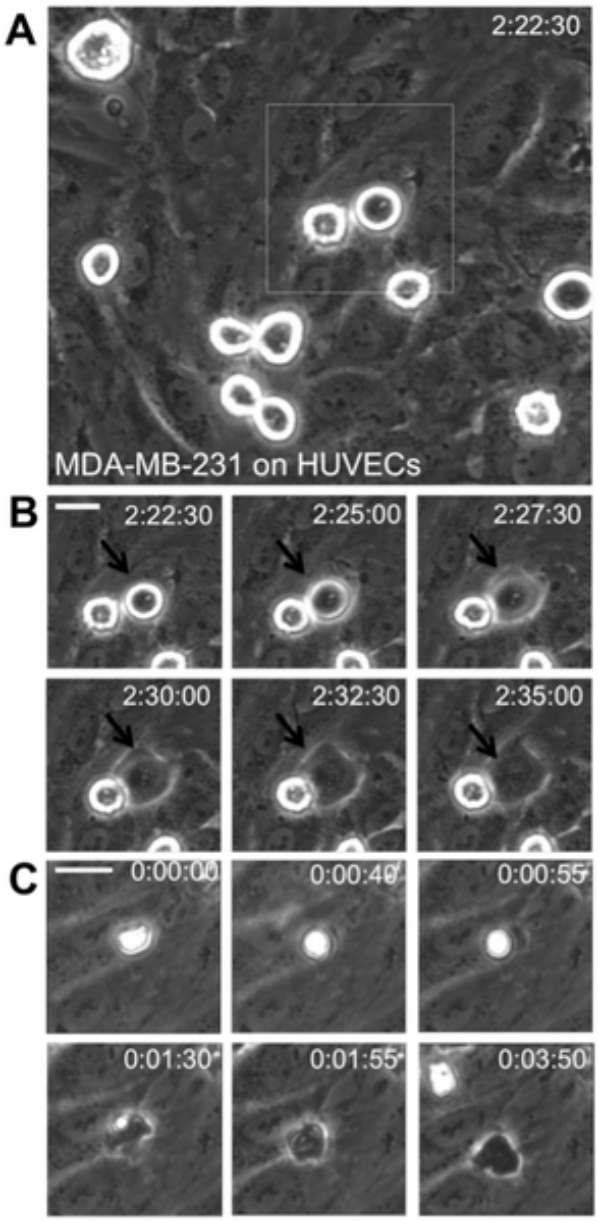

Figure 2.1 (A) Phase contrast image of MDA-MB-231 cells (bright white) atop a human umbilical vein endothelial (HUVEC) monolayer. Scale bar is 20 μm. (B) MDA-MB-231 cell (black arrows) begins to incorporate into the endothelium, as indicated by its change in phase contrast microscopy from bright white to darkened. Scale bar is 20 μm and applies to all images in panel B. Length of time after plating MDA-MB-231 cells on the endothelium is indicated in the upper right corner of each image in hour:minute:second format. The final percentage of incorporation for this experiment was 95%. (C) Phase contrast image sequence of a neutrophil transmigrating through a TNF-α-activated endothelium. Scale bar is 20 μm and applies to all images in panel C. Length of time after plating neutrophils on the endothelium is indicated in the upper right corner of each image in hour:minute:second format.

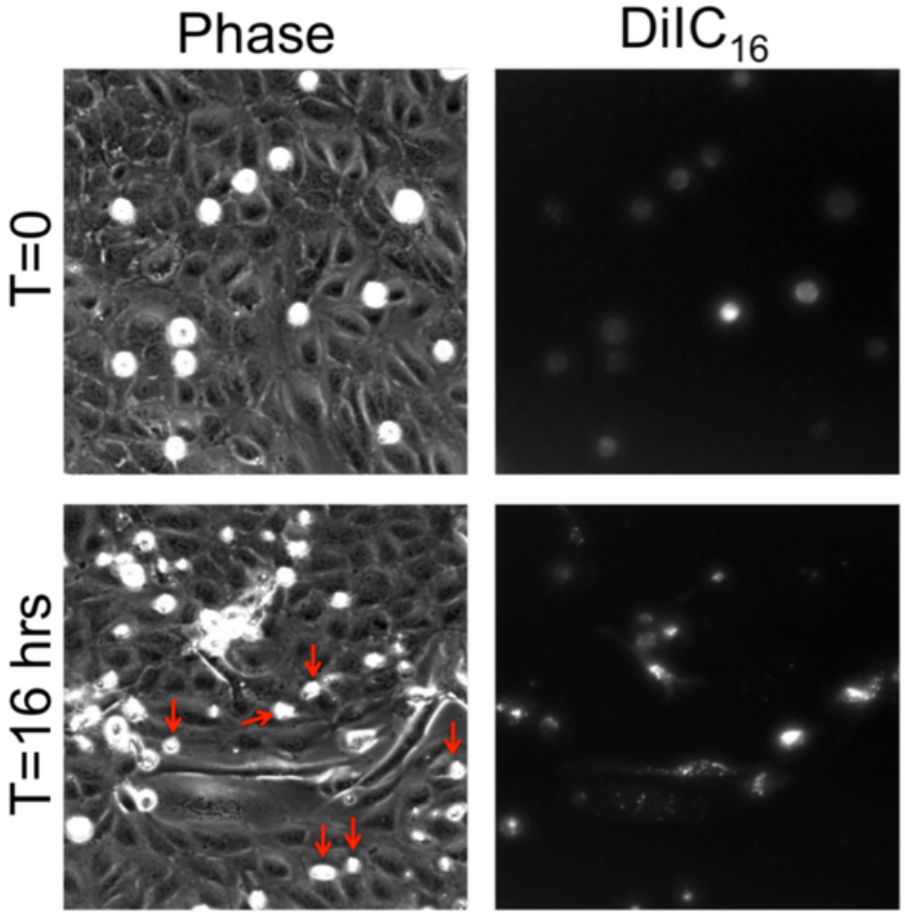

Figure 2.2. MDA-MB-231 incorporation causes detachment and rounding of some endothelial cells. Phase contrast (left) and $DiIC_{16}$ fluorescence (right) images of MDA-MB-231 cells plated onto an untreated HUVEC monolayer, at timepoints immediately after plating (top) and after 16 hours of interaction with the endothelium (bottom). Red arrows point to phase-white cells that do not emit fluorescence; these are endothelial cells that have been forced out of the monolayer and thus have detached and become rounded.

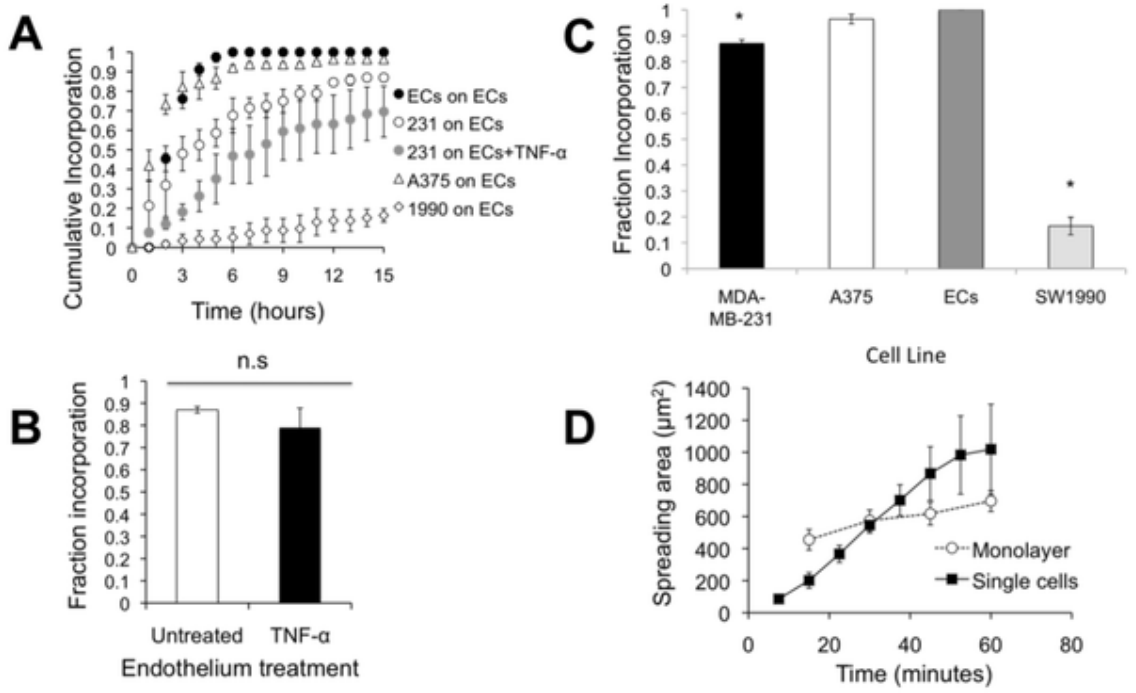

Figure 2.3. Incorporation of MDA-MB-231 does not depend on whether the endothelium is activated by TNF-α. (A) Cumulative fraction of ECs or MDA-MB-231 cells (231), SW1990 (1990), and A375 cells incorporated into the endothelium as a function of time after plating. Data points represent mean ± SEM for at least 3 independent experiments (N>20 cells for each experiment). (B) Final fraction of MDA-MB-231 cells incorporated into the untreated or TNF-α-treated endothelium after 15 hours. Bars represent mean, while error bars represent SEM of at least 3 independent experiments. P>0.05 between these values indicates there is no statistical difference (n.s.). (C) Final fraction of MDA-MB-231 breast cancer cells, ECs, A375 melanoma cells, and SW1990 pancreatic cells incorporated into the endothelium after 15 hours. Bars represent mean, while error bars represent SEM of at least 3 independent experiments. (*) indicates significance (P<.05) when compared to ECs. (D) Plot of spreading area versus time reveals differences in spreading dynamics for MDA-MB-231 cells spreading onto a fibronectin-coated coverslip ("single cells") or into an untreated endothelium ("into monolayer").

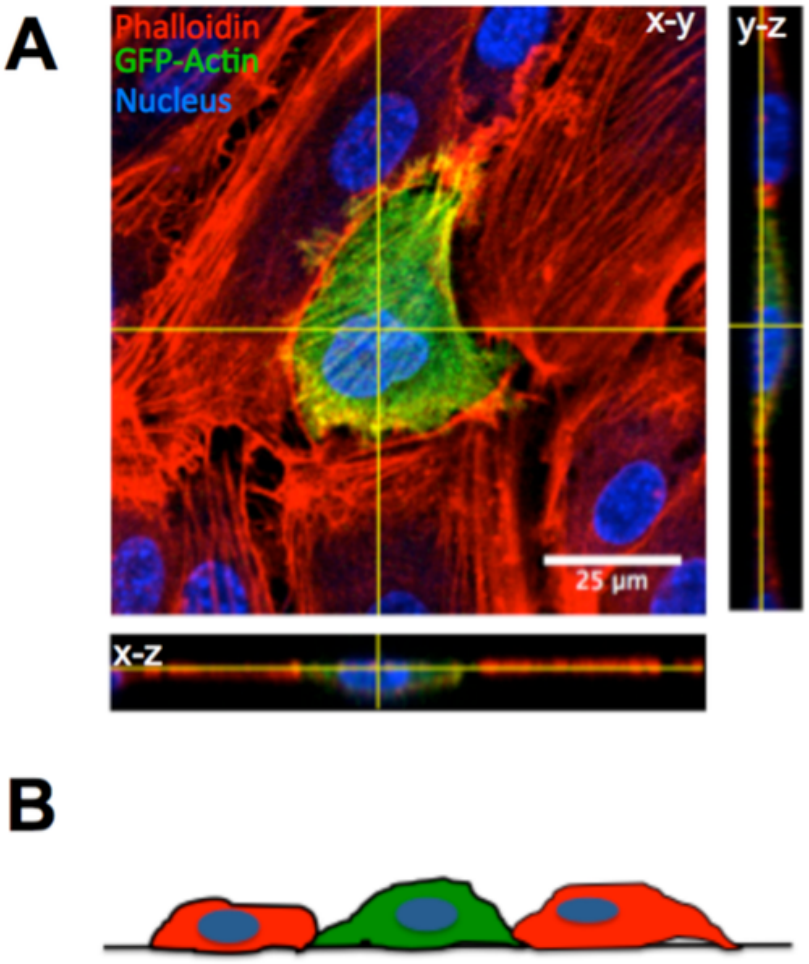

Figure 2.4. Confocal images reveal that MDA-MB-231 cells do not migrate underneath ECs during the incorporation process. (A) A representative MDA-MB-231 (green; Actin-GFP) cell infected with GFP-actin is shown spreading into a HUVEC monolayer (red; Phalloidin). Orthogonal projections are shown. (B) Schematic showing that a cancer cell (green) displaces ECs (red) by spreading between adjacent ECs during incorporation

2.3.2 Activation of the endothelium by TNF-α does not affect incorporation dynamics of breast cancer and melanoma cells

Activation of the endothelium is a key step in the leukocyte adhesion cascade, and our previous work has demonstrated that leukocyte transmigration depends heavily on the activation status of the endothelium [26, 154, 163]. Activation of the endothelium by TNF-α not only upregulates adhesion molecules such as ICAM-1 and vascular cell adhesion molecule-1 (VCAM-1), but also increases EC contractility [155] and reduces EC barrier function [148]. Therefore, our next goal was to determine whether incorporation of metastatic breast cancer cells into the endothelium required the ECs to be activated. Intriguingly, we found that the cumulative fraction of incorporation versus time of MDA-MB-231 cells was similar, regardless of whether the ECs were treated with TNF-α (Figure 2.3A). In addition, the final fraction of cells that incorporated into a TNF-α-activated endothelium after 15 hours was not different from the fraction incorporated into an untreated endothelium (Figure 2.3B). Finally, the time required to complete incorporation (from a rounded sphere to a flattened cell within the endothelium) was not dependent on whether the endothelium was treated with TNF-α (Figure 2.7C). Similar to breast cancer cells, the fraction of incorporation of A375 melanoma cells into ECs was comparable, regardless of whether the ECs were treated with TNF-α (Figure 2.5). These results suggest that some metastatic cancer cells are able to complete the early stages of extravasation, even in the absence of an inflammatory stimulus. However, the fraction of incorporation after 15 hours for SW1990 pancreatic cells was statistically different between untreated ECs and those treated with TNF-α (Figure 2.6). SW1990 cells

incorporated at a much faster rate and higher fraction in TNF-α treated ECs compared to untreated ECs.

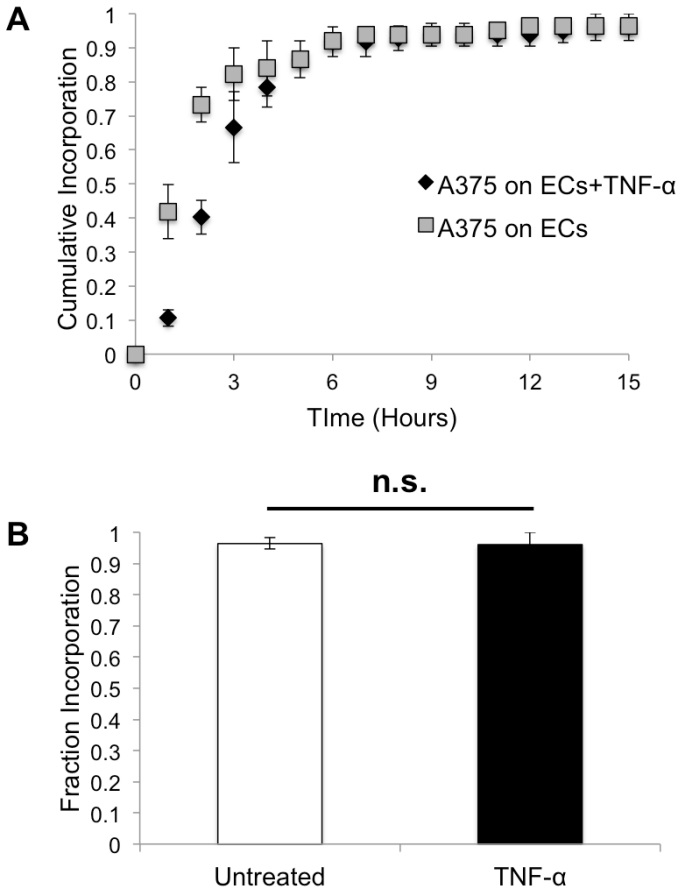

Figure 2.5. (A) Cumulative incorporation of A375 melanoma cells into untreated and TNF-α treated endothelium after 15 hours. Data points represent mean ± SEM for at least 3 independent experiments (N>20 cells for each experiment). (B) Final fraction of incorporation after 15 hours for untreated and TNF-α treated endothelium. Data is not significant (n.s.) (P>0.05).

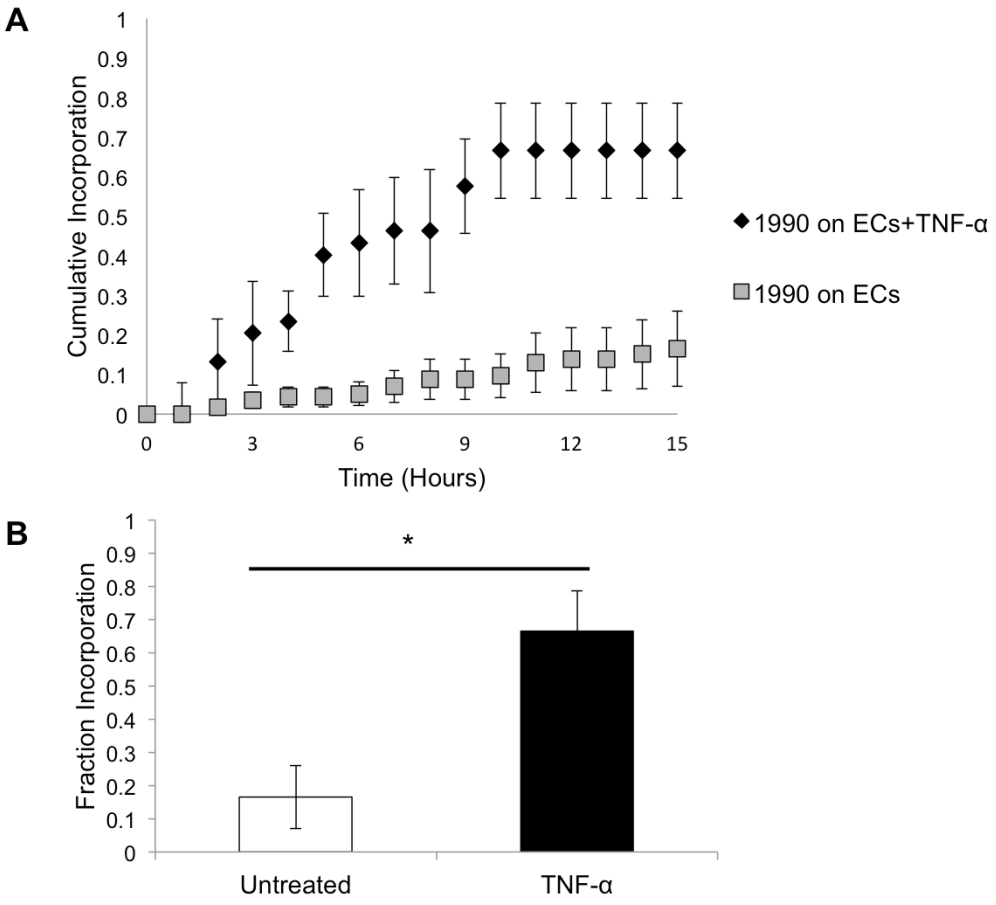

Figure 2.6. (A) Cumulative incorporation of SW1990 cells into untreated and TNF-α treated endothelium after 15 hours. Data points represent mean ± SEM for at least 3 independent experiments (N>20 cells for each experiment). (B) Final fraction of incorporation after 15 hours for untreated and TNF-α treated endothelium. (*) indicates significance when compared to untreated ECs ($P<0.05$).

2.3.3 Incorporation is independent of subendothelial matrix stiffness for breast cancer and melanoma cells

Our previous work has also demonstrated that leukocyte transmigration depends on the mechanical properties of the matrix below the endothelial cells [26, 154]. Stiffer subendothelial matrices promote myosin light chain kinase dependent EC contractility, leading to intercellular gaps and enhanced leukocyte transmigration [26, 154]. Therefore, our next goal was to establish whether metastatic breast cancer cell incorporation into the endothelium was dependent on subendothelial matrix stiffness. Unlike neutrophil transmigration, which increases with subendothelial matrix stiffness, the dynamics of MDA-MB-231 cell incorporation into the endothelium were similar for soft (0.87 kPa), intermediate (280 kPa), and very stiff (glass; 50 GPa) subendothelial substrates (Figure 2. 7A). In addition, the final incorporated fraction of MDA-MB-231 into the endothelium was independent of subendothelial substrate stiffness (Figure 2.7B). and the total time required to complete transmigration was independent of subendothelial substrate stiffness (Figure 2.7C). A375 melanoma cells incorporated into soft, intermediate, and very stiff subendothelial matrices with similar incorporation dynamics and final fraction of incorporation to breast cancer cells (Figure 2.8). SW1990 pancreatic cells displayed a different behavior from the melanoma cells and breast cancer cells. When SW1990 cells were plated on soft and intermediate substrates, they displayed a similar level of incorporation dynamics and final fraction of incorporation after 15 hours (Figure 2.9). However, when allowed to incorporate on very stiff matrices (glass; 50GPa), they displayed a much lower fraction of incorporation and slower incorporation rate. While

subsequent steps of the metastatic cascade may depend on matrix stiffness, our results indicate that the early stages of breast cancer cell extravasation and melanoma extravasation occur irrespective of the mechanical properties of the matrix below the endothelium while pancreatic cell incorporation changes on very stiff substrates.

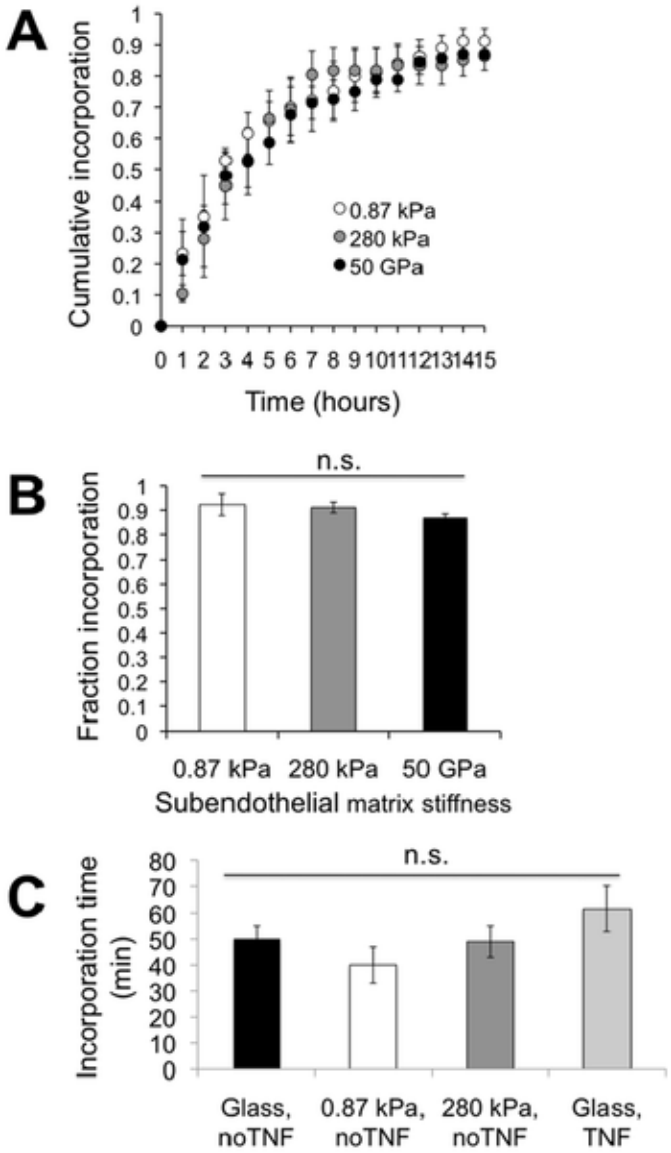

Figure 2.7. Incorporation of MDA-MB-231 does not depend on subendothelial matrix stiffness. (A) Cumulative fraction of MDA-MB-231 cells incorporated into endothelial cells on a fibronectin-coated 0.87 kPa or 280 kPa polyacrylamide gel, or glass (50 GPa). Data points represent mean ± SEM for at least 3 independent experiments (N>20 cells for each experiment). (B) Final fraction of MDA-MB-231 cells incorporated into the (untreated) endothelium as a function of subendothelial matrix stiffness. Bars represent mean, while error bars represent SEM of at least 3 independent experiments. P>0.05 between these values indicates there is no statistical difference (n.s.). (C) Time for MDA-MB-231 cells to complete incorporation is independent of the mechanical properties of the matrix below the endothelial cells. Endothelial cells on fibronectin-coated glass coverslips (50 GPa) or polyacrylamide gels (0.87 kPa or 280 kPa) were left untreated (noTNF) or treated with TNF-α (TNF). No statistical difference in incorporation time was measured as a function of subendothelial matrix stiffness or endothelial cell treatment (P>0.05).

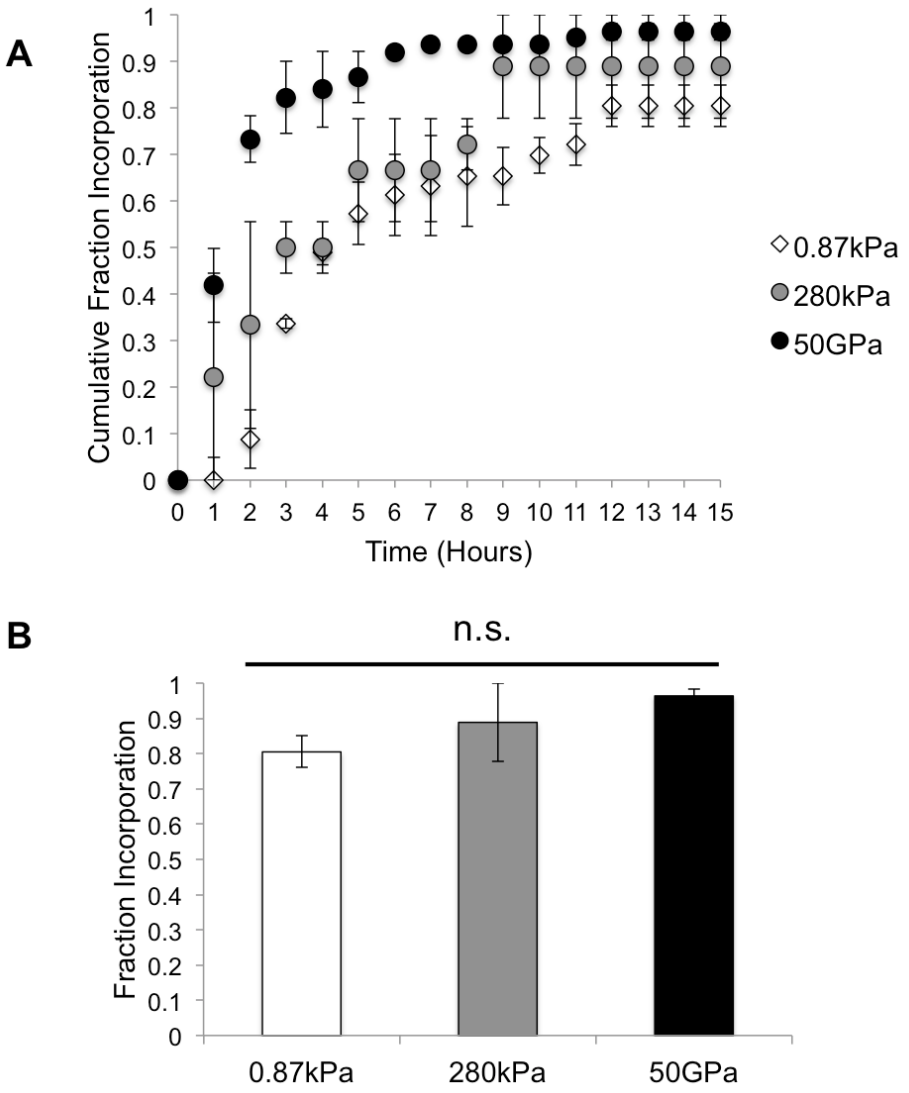

Figure 2.8. (A) Cumulative fraction of A375 cells incorporated into endothelial cells on a fibronectin-coated 0.87 kPa or 280 kPa polyacrylamide gel, or glass (50 GPa). Data points represent mean ± SEM for at least 3 independent experiments (N>20 cells for each experiment). (B) Final fraction of A375 cells incorporated into the (untreated) endothelium as a function of subendothelial substrate stiffness. Bars represent mean, while error bars represent SEM of at least 3 independent experiments. P>0.05 between these values indicates there is no statistical difference (n.s.).

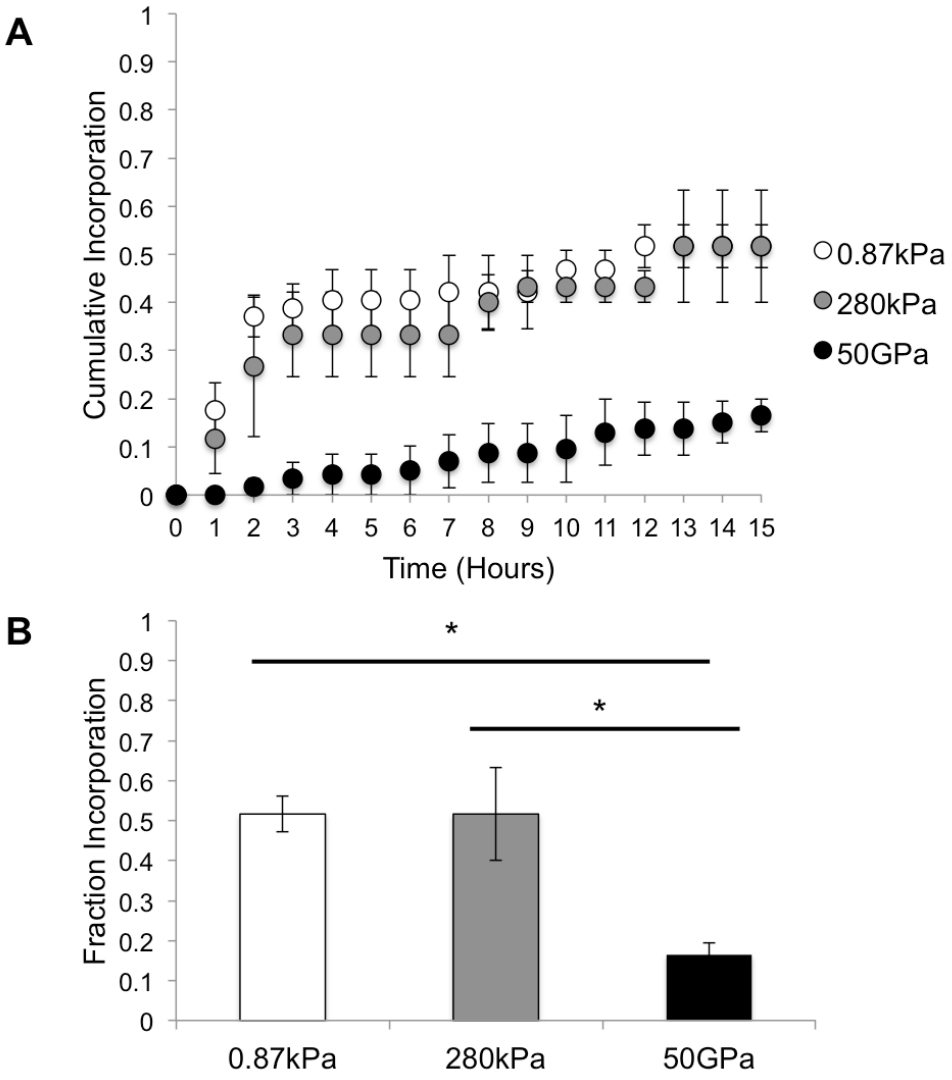

Figure 2.9 (A) Cumulative fraction of SW1990 cells incorporated into endothelial cells on a fibronectin-coated 0.87 kPa or 280 kPa polyacrylamide gel, or glass (50 GPa). Data points represent mean ± SEM for at least 3 independent experiments (N>20 cells for each experiment). (B) Final fraction of SW1990 cells incorporated into the (untreated) endothelium as a function of subendothelial substrate stiffness. Bars represent mean, while error bars represent SEM of at least 3 independent experiments. (*) indicates statistical difference between groups (P<0.05).

2.3.4 Endothelial cells do not express VE-cadherin along borders with incorporated cancer cells

Vascular endothelial cadherin (VE-cadherin) is one of the key homophilic adhesion molecules expressed by ECs at cell-cell borders in a confluent monolayer. The integrity of the endothelium as a vascular barrier is heavily dependent on the proper functioning of VE-cadherin adhesion molecules [164, 165]. As ECs incorporated into a healthy confluent endothelium, GFP-VE-cadherin was expressed by all ECs neighboring the incorporated $DiIC_{16}$-labeled EC (Figure 2.10A), indicating that addition of new ECs onto the monolayer did not disrupt the integrity of the EC junctions. We next sought to identify possible changes in VE-cadherin morphology following incorporation of MDA-MB-231 cells into the endothelium. Strikingly, ECs neighboring incorporated $DiIC_{16}$-labeled MDA-MB-231 cells did not express GFP-VE-cadherin at borderlines with the MDA-MB-231 cells, though they continued to express GFP-VE-cadherin at junctions with other ECs (Figure 2.10B). These results indicate that the early stage of cancer cell extravasation not only affects VE-cadherin-dependent cell-cell adhesion, but may also provide an easily accessible route of extravasation for other circulating tumor cells.

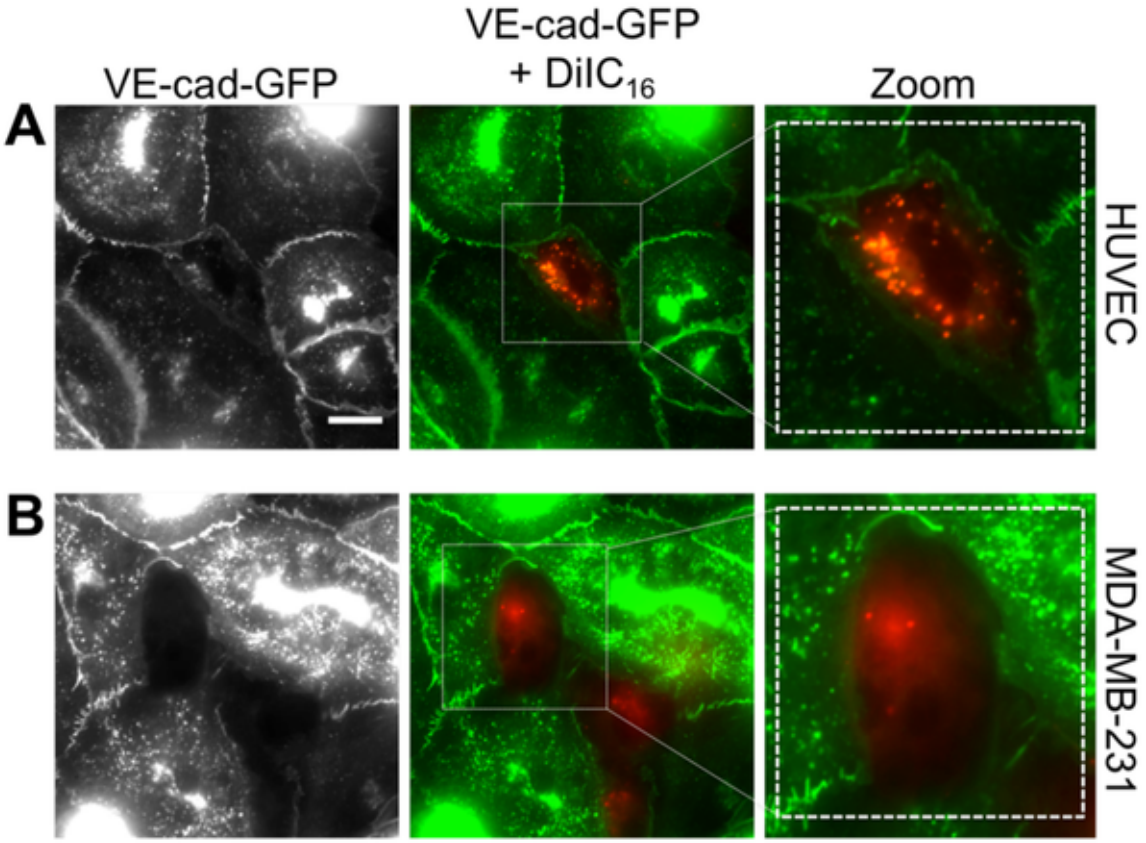

Figure 2.10. Endothelial cells do not express VE-cadherin along borders with incorporated cancer cells. DiIC16-labeled HUVECs (A) or MDA-MB-231 (B) were plated onto endothelial cells expressing VE-cadherin-GFP (VE-cad-GFP). Images were captured following incorporation of each cell type. Scale bar is 10 μm and applies to all images in this figure.

2.3.5 Cancer cell incorporation initiates by dislocating VE-cadherin at endothelial cell junctions

Prior to the onset of MDA-MB-231 incorporation into the endothelium, we observed intact GFP-VE-cadherin at the EC junction directly below the MDA-MB-231 cell (Figure 2.11A; red arrows). This was in direct contrast to the MDA-MB-231 cells that incorporated into the endothelium at earlier timepoints, where GFP-VE-cadherin was not expressed by neighboring ECs (Figure 2.11A; yellow arrows). The first step of incorporation created a disruption in GFP-VE-cadherin at the EC junction directly below the MDA-MB-231 cell, leading to formation of a small (~2 μm^2) hole in the EC junction (Figure 2.11B; red arrow). A second small hole sometimes formed (Figure 2.11B; two red arrows) before the void became significantly larger (~33 μm^2 at T=6:35) and cleared the area of part of the body of the EC. Finally, what began as a small gap in the GFP-VE-cadherin propagated into a huge hole in the endothelium, which became occupied by the MDA-MB-231 cell (Figure 2.11B). We also observed significant displacement and restructuring of GFP-VE-cadherin at nearby EC-EC junctions (Figure 2.11B; yellow arrows).

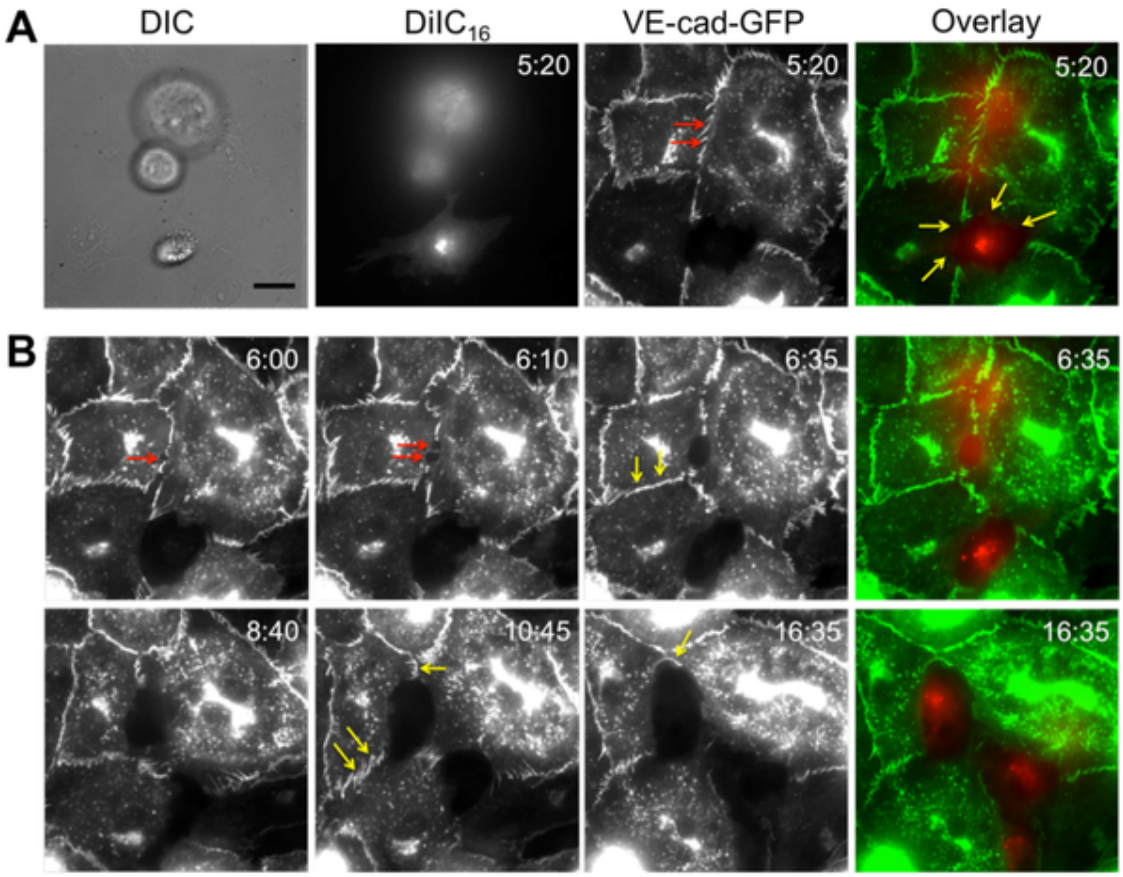

Figure 2.11. Cancer cell incorporation initiates by dislocating VE-cadherin at endothelial cell junctions. $DiIC_{16}$-labeled MDA-MB-231 were plated onto endothelial cells expressing VE-cadherin-GFP (VE-cad-GFP). (A) Shown are differential interference contrast (DIC), $DiIC_{16}$ (red) fluorescence, and VE-cadherin-GFP (green) fluorescence, and overlay images. At this timepoint, one MDA-MB-231 has already incorporated into the endothelium (yellow arrows), and the VE-cadherin-GFP is still intact in the location directly below another MDA-MB-231 cell that has not yet begun to incorporate (red arrows). (B) Fluorescence timelapse sequence of a $DiIC_{16}$-labeled MDA-MB-231 cell (red) incorporating into an endothelium expressing VE-cadherin-GFP (green). Length of time after plating MDA-MB-231 cells on the endothelium is indicated in the upper right corner of each image in hour:minute format. Scale bar in panel A (DIC image) is 10 μm and applies to all images in this figure.

2.4 Discussion

Cancer metastasis continues to be a leading cause of death in cancer patients [130, 131], and one of the critical steps regulating metastasis is extravasation from the vasculature. While the mechanisms regulating this process are unclear, the endothelium is known to play an important role, acting as either a barrier to some cancer cells, or a promoter of invasive capability in other cancer cells including MDA-MB-231 [144, 166]. EC apoptosis and clearance from the basement membrane have previously been reported as side effects during cancer cell extravasation [141, 142]. Similarly, ovarian tumor cell spheroids displace mesothelial cells during intercalation into the submesothelial space [145]. We demonstrate that in our *in vitro* model, most metastatic breast cancer cells clear a space in and appear to become part of the endothelium (without forming VE-cadherin dependent adherens junctions with the ECs), in a process we term "incorporation." We were able to observe this process for multiple metastatic cancer lines, including MDA-MB-231 breast cancer cells, A375 melanoma cells, and SW1990 pancreatic cells. Notably, this process occurs independently of the activation status of the endothelium or subendothelial matrix stiffness for some cell types, even though these are both important regulators of leukocyte transmigration [26, 154].

Our data indicates that incorporation into the endothelium represents the first step in extravasation. Thus, we suggest that cancer cell transmigration is a two-step process in which the cells must first incorporate into the endothelium before completing the second step of migration beneath the endothelium and into the basement membrane or even continuing into the basement membrane without migrating beneath the ECs.

Indeed, partial retraction of the ECs and incorporation of tumor cells has been observed *in vivo* [167, 168] and for mesenchymal stem cells (MSCs) [169, 170]. However, previous studies with MSCs have shown that this step depends heavily on the activation status of the endothelium and the use of VCAM-1 to facilitate transmigration [169-171]. In our work, which is relevant for low-flow conditions such as in the capillaries, we found that incorporation occurs independently of the activation status of the endothelium for breast cancer cells and melanoma cells. In contrast, studies have shown that fibrosarcoma cells displayed increased intravasation rates into an inflamed endothelium [172] and our results indicate that SW1990 pancreatic cells had increased incorporation into the endothelium following endothelial activation. Breast tumor cells lack β2 integrins, which are a ligand for ICAM-1 on the endothelium [173]. Following activation of the endothelium, melanoma cells did not show an increase in incorporation. It has been shown the co-culture of melanoma cells with ECs leads to LFA-1/ICAM-1 receptor couple during transmigration [174]. Therefore, it is likely that there was no difference between activated and untreated ECs because the melanoma cells were increasing ICAM-1 expression even without the presence of TNF-α. These factors may account for the differences observed between leukocytes, MSCs and pancreatic tumor cells. SW1990 cells on the other hand, have been shown to increase adhesion to mesothelial cells following incubation with TNF-α, and that ICAM-1 an important adhesion molecule for pancreatic cancer cells [175]. Further study is necessary to dissect the exact mechanisms of pancreatic cell incorporation. Additionally, tumor cells are capable of attaching to leukocytes by expressing ICAM-1. The leukocytes then act as a linker, connecting the

tumor cells to the endothelium, and enabling firm adhesion and subsequent transmigration [21]. *In vivo*, cancer cells may use this mechanism to localize to sites of inflammation or infection.

Although all the metastatic tumor cells observed in this study incorporated into the endothelium, there was a significant difference between the fractions of incorporation. A375 melanoma cells incorporated into the endothelium significantly more than MDA-MB-231 cells and SW1990 cells and their incorporation dynamics closely resembled that of native ECs spreading into a monolayer. SW1990 tumor cells on the other hand, incorporated at a significantly lower rate. There are multiple factors that can account for these differences. It is likely that the tumor cells each use their own distinct set of adhesion molecules and signaling pathways. Indeed, it has been shown that co-culture of melanoma cells with ECs induces LFA-1/ICAM-1 receptor couple during transmigration [174].

Additionally, we observed that tumor cell incorporation does not depend on the subendothelial matrix stiffness. Subendothelial matrix stiffness varies between homeostasis and pathological disease and likely also depends on vasculature location. When plated on stiffer substrates *in vitro*, the endothelium has a hyper-contractile phenotype that leads to intercellular gap formation [26, 27]. Thus, it would be expected that cancer cells would transmigrate more on stiffer substrates. However, despite these observations, the cumulative fraction of tumor cells that incorporates remains approximately the same independently of subendothelial matrix stiffness and the subsequent hyper-contractility of the EC monolayer for the melanoma cells and breast

cancer cell lines. This indicates that the tumor cells do not take advantage of the hyper-permeability of the endothelium. However, as they migrate beyond the vasculature and into tissues, matrix stiffness may become an important modulator of metastasis; indeed, previous reports have indicated that the matrix stiffness governs 3D cancer cell migration [176]. The pancreatic cells displayed a different behavior when they incorporated in EC monolayers with varied subendothelial matrix stiffness. On soft and intermediate matrices, they displayed similar rates and fraction incorporations. On very stiff 50GPa matrices, incorporation was reduced. Most stiffness' that cells feel are between 10Pa-10000Pa [28]. 50GPa is well outside the physiological range, so it is possible that the cells altered their incorporation behavior based on the very stiff substrate. To dissect the mechanism of why pancreatic cells displayed a decrease of incorporation fraction on very stiff subendothelial matrices would require further study.

Stephan Paget's 'seed and soil hypothesis' has been used to explain the non-random patterns of metastasis formation to visceral organs. Certain tumor cells (the seed) have a propensity to metastasize to particular organs (the soil) in the body. Based on our results, subendothelial matrix stiffness does not play a role in determining where cancer cells initially exit the blood stream. Furthermore, our work suggests that ligands that are upregulated during inflammation do not play a role in determining where cancer cells exit the blood stream, at least in vasculature with low shear stress rates.

During incorporation, ECs do not express VE-cadherin along borders with cancer cells, but continue to express VE-cadherin with neighboring ECs. VE-cadherin was significantly restructured during the incorporation process, indicating that the addition of

tumor cells disrupted the integrity of the monolayer. Additionally, this disruption may provide an easily accessible route for other incorporating cancer cells. Incorporation initiated by creating a small hole in the VE-cadherin between ECs. As incorporation progressed, the hole became much larger, creating a void for the cancer cell to spread onto the underlying fibronectin-coated matrix beneath. These results are consistent with others that have shown that during leukocyte transendothelial migration, a transient gap forms between the ECs, allowing the leukocyte to migrate through, before closing the VE-cadherin junctions [177, 178]. It remains to be seen whether the endothelium would reform junctions as the cancer cell completes extravasation. From our work, it is evident that the incorporation process damages the endothelium since tumor cells physically displace and/or detach ECs during incorporation. Thus, tumor cells damage the endothelium during incorporation, whereas leukocytes and even MSCs appear to leave the endothelium intact in most cases.

Elucidating the mechanistic underpinning for cancer cell diapedesis will be critical in order to understand cancer metastasis and its progression. Significantly, our results show that cancer cell transmigration includes an additional step, incorporation into the endothelium, and that this process occurs independently of inflammation and subendothelial matrix stiffness for some cancer types. Out of the cell lines tested, pancreatic cells displayed differences upon endothelium activation and showed a decreased fraction of incorporation on very stiff substrates. While here we specifically designed our *in vitro* model to focus on the early stages of cancer cell extravasation, future studies could be aimed at investigating subsequent stages of extravasation by

characterizing cancer cell incorporation into an EC monolayer on a 3D matrix through which the tumor cells can penetrate.

2.5 Conclusions

In this Chapter, we explored mechanisms of cancer cell transmigration through the endothelium. This process is intrinsically different from leukocyte transmigration. During leukocyte transmigration, cells squeeze between or through the endothelium and this process is dependent on subendothelial matrix stiffness and activation of the endothelium with TNF-α. During cancer cell extravasation, however, it appears to include an additional step, which we term 'incorporation' into the endothelium. This data suggests that cancer cell transmigration is a two-step process in which cancer cells first incorporate into the monolayer and then migrate under. We also found that cancer cell incorporation occurs independently of matrix stiffness and endothelial activation for melanoma cells and breast cancer cells. However, we found pancreatic cells are sensitive to subendothelial matrix stiffness and endothelial activation. This indicates that homing mechanisms may be cell specific based on adhesion molecules they use and their sensitivity to matrix stiffness. In conclusion, we found that cancer cell extravasation occurs by a very different mechanism from immune cells, and this result could have a significant impact on the cancer field.

A fundamental step during cancer cell extravasation and invasion is the ability to form protrusive processes. There are many proteins and RNAs that localize to protrusions in migrating cells. Localization of RNAs in lamellipodial regions has been

proposed to play an important role during metastatic progression [179], however, the identity and functional significance of these localized mRNAs has been investigated only in few cases [8, 11]. Due to the fact that there is vast heterogeneity in cancer cells, we chose to do the next portion of the work in NIH 3T3 cells as a model system. **In the next two Chapters, we focus on the localization of RNAs at cellular protrusions and their potential significance during cancer metastasis.**

Chapter 3: Effect of Substrate Stiffness and Contractility on APC-dependent mRNA Localization

3.1 Introduction

RNA localization pathways direct RNAs to specific subcellular sites where they can produce proteins locally and affect many physiological functions. Localized RNAs impact many processes such as cellular polarity [180, 181] and migration [11] . Defects in localization have been associated with neurodegenerative disorders and cancer metastasis [108, 179]. Particularly in migrating cells there are at least two pathways that direct RNA localization to the leading edge (reviewed in Chapter 1). In the APC-dependent pathway, numerous RNAs are targeted to cellular protrusions in migrating fibroblasts and their anchoring depends on the tumor suppressor protein Adenomatous Polyposis Coli (APC) [8]. In cellular protrusions, specifically at the plus-ends of detyrosinated microtubules, APC associates with several RNAs such as *Ddr2, Pkp4*, and *Rab13*.

Cellular protrusion extension has been proposed to be a critical step in directional migration [182]. As cells migrate, there are many signaling and cytoskeletal proteins that localize to the leading edge where they play important roles in the regulation of protrusion dynamics [182]. Additionally, at cellular protrusions, RNAs become localized. At the same time, cells sense the extracellular matrix environment as they anchor and pull on their surroundings during migration. Within tissues, cells encounter microenvironments that may range in rigidity from tens of pascals in soft tissue such as the brain, to gigapascals in the stiffest tissues such as bone [30]. When cells encounter

these differences in extracellular matrix stiffness, they alter their behavior, including their modes of migration and forces they exert on the matrix. For example, NIH 3T3 fibroblast cells alter their spreading behavior, exertion of traction forces, as well as their motility on soft flexible polyacrylamide gels compared to stiffer substrates [31, 183]. However, it is currently unknown whether cells alter the localization of RNAs based on the extracellular matrix stiffness. Since APC-dependent RNAs are localized to the protrusions of migrating fibroblasts, and some of the proteins they encode are involved migration, it is likely that their localization is sensitive to substrate stiffness.

Microenvironmental stiffness has also been implicated in breast cancer cell invasion in vitro and metastasis in vivo, both of which may involve defective RNA localization [179]. In fact, in Chapter 1 we found that the effects of microenvironmental stiffness on cancer transmigration are cell-specific [184]. Furthermore, mechanical tension has been shown to influence RNA localization at adhesion sites, which is adjusted by cells based on the mechanical properties of the microenvironment [5]. Additionally, traction force data has indicated that migrating fibroblasts have strong stresses at the leading edge, lateral protrusions and trailing edge [185, 186]. These areas, specifically at the lateral protrusions, are typically where APC-dependent RNAs are localized [8]. Rho/ROCK pseudopodial activation has also been associated with RNA dynamics in tumor cells and Rho regulates β-actin localization through actomyosin interactions [6, 74]. Thus, it is possible that APC-dependent RNA localization can be affected by Rho actomyosin contractility and substrate stiffness. This may have important implications in the context of cancer metastasis.

Our study sought to investigate whether and how substrate stiffness affects APC-dependent RNA localization. We used polyacrylamide gels of physiologically relevant stiffness and combined it with fluorescent in-situ hybridization to visualize RNA distribution. We analyzed RNA distributions from populations of cells and analyzed the effects of substrate stiffness and actomyosin contractility on RNA localization. Our results indicate that stiffness enhances localization and loss of contractility reduces localization. Overall, our analysis of APC-dependent RNA localization under various mechanical and molecular conditions offers new insights into how the mechanical environment and cellular contractility regulates RNA localization.

3.2 Materials and Methods

3.2.1 Polyacrylamide gel preparation

Thin polyacrylamide gels were prepared on glass coverslips according to the method first described by Wang and Pelham [153] and described in detail in previous publications [26, 36, 154-157]. Briefly, 280 kPa (15% acrylamide + 1.2% bis acrylamide), 5 kPa (5% acrylamide + 0.05% bis acrylamide) and 1 kPa (3% acrylamide + 0.2% bis acrylamide) gels were created and coated with 0.1mg/mL fibronectin (Sigma-Aldrich) as previously described [26]. Characterization of the Young's modulus of the gels was accomplished by atomic force microscopy and dynamic mechanical analysis, while analysis of surface-bound fibronectin was accomplished by immunofluorescence [36, 156].

3.2.2 Cell Culture and Fluorescent In Situ Hybridization (FISH)

NIH/3T3 cells were grown in DMEM supplemented with 10% calf serum, and penicillin, and streptomycin (Invitrogen), and sodium pyruvate. Cells were plated on fibronectin-coated polyacrylamide gels for two hours and subsequently fixed in 4% paraformaldehyde for ten minutes. Fluorescence in situ hybridizations (FISH) was performed using the Affymetrix QuantiGene ViewRNA assay according to manufacturer's instructions.

mRNA in situ hybridization allows for fluorescent detection of localized RNAs in cells. The Affymetrix assay, in particular, is a non-radioactive method that allows for single molecule sensitivity. A specific probe set, containing 40 oligo probes, hybridizes to the target mRNA as 20 oligo pairs. Each oligo pair forms a platform for the formation of a signal amplification tree through a series of sequential hybridization steps. Once the structure is assembled, it has the capacity to generate 400-fold signal amplification.

Three RNAs were simultaneously visualized in these experiments: localized mRNA, non-localized mRNA, and 18S rRNA. 18S ribosomal RNA is the structural RNA for the small subunit of the eukaryotic cytoplasmic ribosomes, and thus is abundant throughout the cell. Because of its abundance, the 18S probe is used to obtain the cell mask. The non-localized mRNA probe acts as an internal control, and is a disperse RNA that is found throughout the cells. In 3T3 cells, a probe against PolyA was used to detect poly-adenylated RNAs. In this way, the general population of RNA distribution can be observed. The 'localized' RNA probe used was against the APC-dependent *Ddr2* RNA.

In some cases, the cell masks obtained through the 18S RNA fluorescent staining

were used to measure cell areas using Imagej.

3.2.3 Image Acquisition

FISH images were obtained using a Leica SP8 confocal microscope (equipped with a HC PL APO 63x oil CS2 objective). Maximum-intensity projections of Z-stacks were obtained; background subtracted, and analyzed using Image J. In the case of PolyA staining, the nuclear mask was subtracted from the images because it has a high background signal in the nucleus. In the case of soft substrates (1 kPa), the nuclear signal was subtracted from the PolyA channel and the RNA channel to take into account the rounded morphology of the cells. When comparing soft (1 kPa) versus stiff substrates (5 kPa, 280 kPa), the nuclear signal was also subtracted from the RNA channel and PolyA channel.

The channel detecting the 18S probe was used to obtain a binary cell mask of the whole cell area. Similarly, the channel detecting the nuclei was used to obtain a binary mask of the nuclear area. The quantification was performed using a method developed called the Peripheral Distribution Index (PDI) that we adapted from Park et al. [187]. Using the PDI, the distance is calculated from the centroid of the nucleus to each RNA pixel, weighted for intensity, and divided by a hypothetical uniform distribution to normalize for cell morphology. The second moment (μ_2) of RNA pixels is calculated using the formula below where r^2 is the distance from centroid of the nucleus to each RNA pixel (i,j) and I_{ij} is the intensity value of the pixel.

$$\mu_2 = \Sigma_{ij} r^2 \frac{I_{ij}}{\Sigma_{ij} I_{ij}}$$

To generate the hypothetical uniform distribution (μ_2'), a binary cell mask image is generated and the second moment is calculated from each pixels coordinated within the mask. The PDI is then calculated:

$$PDI = \frac{\mu_2}{\mu_2'}$$

Values of 1 mean that the RNAs are uniformly distributed; values less than 1 mean the RNAs are more centrally located, and values greater than 1 mean the RNAs are more peripherally distributed (see Figure 3.1).

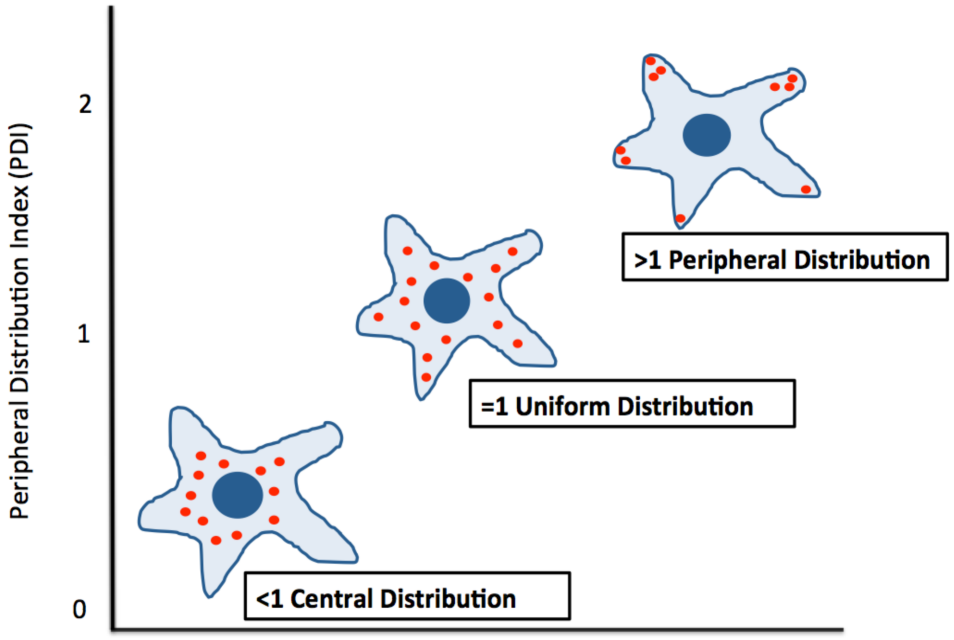

Figure 3.1 The peripheral distribution index (PDI) is a way to quantify mRNA localization from a population of cells. The distance is measured from the centroid of the nucleus to the RNA molecules (depicted in red) and divided by a hypothetical uniform distribution. Values <1 have a central distribution; values =1 have a uniform distribution; and values >1 have a peripheral distribution.

3.2.4 Drug Treatments

Cells were treated with 50uM Blebbistatin (Sigma) for two hours or 10uM Y27632 (Sigma). Control cells were treated with vehicle (DMSO). In the case of LPA, cells were serum starved overnight and allowed to attach to gels for two hours before 10uM lysophosphatidic acid (LPA) was added for two hours.

3.2.5 siRNA Transfection

NIH/3T3 cells were transfected with siRNA to a 40pmol final concentration with Lipofectamine RNAiMAX (Thermo Fisher Scientific, cat# 13778-150) according to the manufacturer's instructions. Cells were incubated for three days before being analyzed siRNAs used were as follows (Qiagen):

siRNA	Target Sequence	Catalog Number
Myh9a#1	5'-CAGGGCTTATCTACACCTATT-3'	SI01321411
Negative Control	Proprietary	1027281

Table 3.1. siRNAs used to perform knock-down experiments.

3.2.6 Traction Force Microscopy

Cell traction forces were measured by embedding 0.2um fluorescent beads in the upper surface of polyacrylamide gels. Images were taken in the 'stressed' state with the cell attached to the substrate. The cell was subsequently detached using trypsin and another image was taken in the 'null' state. To correct for experimental drift, the imagej

plugin “align slices in stack” was used. The displacement field was subsequently calculated using the particle image velicometry as previously described (PIV) [188]. With the displacement field obtained through the PIV analysis, the traction force field was reconstructed by Fourier traction cytometry (FITC). The PIV and traction force microscopy macros are available online and can be implemented in imagej.

3.2.7 Statistical Analysis

To establish significance between the internal control mRNA and the localized/experimental mRNA, the Wilcoxon signed-rank test was used with a p value < 0.05. To compare values between two groups, the Student’s t-test was performed with a p value < 0.05.

3.3 Results

3.3.1 Substrate stiffness enhances Ddr2 mRNA localization

When NIH 3T3 mouse fibroblasts are plated on soft, fibronectin-coated 1 kPa gels, the cells remain round and not well spread out (Figure 3.2A). On stiffer 5 kPa and 280 kPa substrates, cells spread out more and form long protrusions (Figure 3.2A). These observations are consistent with previous results that observed cell spreading is increased on stiffer substrates [31, 183]. Using traction force microscopy, we measured cell traction forces on the substrates of varying stiffness. Cells on stiffer substrates (5 kPa and 280 kPa) had increased traction forces compared to soft 1 kPa gels. To observe

RNA localization, FISH was performed. *Ddr2* was used as a representative APC-dependent RNA. On soft, 1 kPa gels, *Ddr2* mRNA is diffuse throughout the cytoplasm. On 5 kPa gels, *Ddr2* mRNA becomes more peripherally localized (Figure 3.2A; white arrows). On stiff 280 kPa substrates, *Ddr2* RNA is also localized to the periphery. PDI analysis showed that on 1 kPa gels, there was no significant difference between PolyA and *Ddr2* RNA distribution (Figure 3.2B). On 5 kPa and 280 kPa gels, *Ddr2* RNA is localized compared to the internal control. These results indicate that *Ddr2* RNA localization is mechanosensitive. We hypothesized that the effects of RNA localization on stiffer substrates was due to increased cell contractility. mRNA localization at adhesion sites is influenced by mechanical tension [5], which is adjusted by cells as a function of the mechanical properties of the cell environment. Furthermore, several studies have shown that cytoskeletal tension is influenced by ECM stiffness [189-191]. Thus it is possible that actomyosin contractility could account for the increased localization on stiffer substrates.

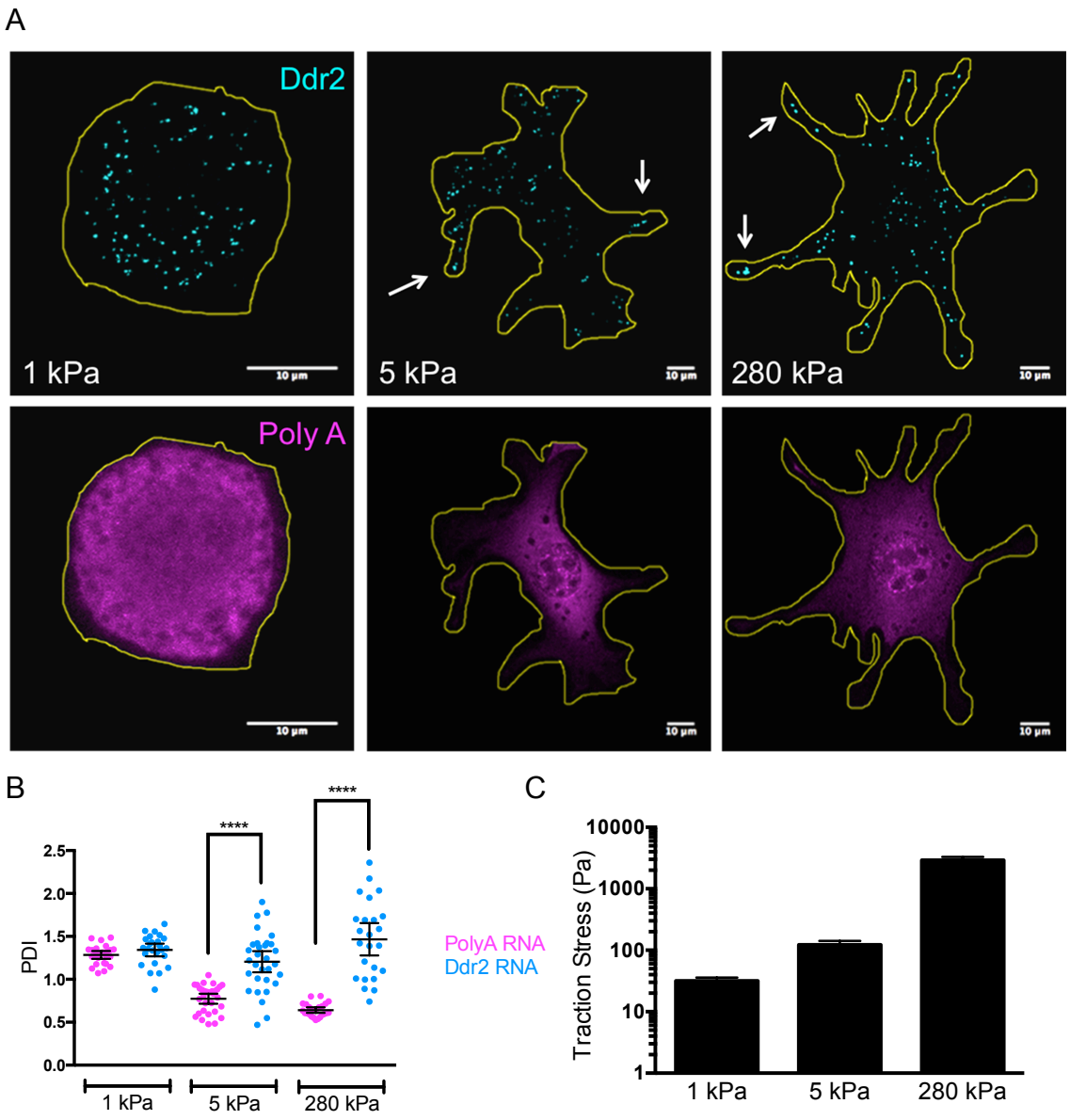

Figure 3.2. (A) Representative images depicting FISH staining on polyacrylamide gels. Arrows point to areas where *Ddr2* mRNAs (cyan) are peripherally localized on 5 kPa and 280 kPa gels compared to PolyA staining (magenta). (B) Peripheral distribution index analysis shows that on 5 kPa and 280kpa *Ddr2* mRNA is more localized compared to control PolyA staining ($P<0.0001$). Error bars represent the mean with 95% confidence interval. (C) Traction stress measurements indicate that cells exert more traction stress on stiffer substrates. Error bars represent SEM.

3.3.2 Myosin II inhibition reduces Ddr2 RNA localization on stiff substrates

To test our hypothesis that increased contractility accounts for increased localization on stiff substrates, we wanted to see if we could reduce RNA localization by inhibiting actomyosin contractility. One of the main regulators of cytoskeletal tension is the Rho family of GTPases. Rho functions via Rho kinase (ROCK) to regulate myosin-II light chain phosphorylation through inhibitory phosphorylation of myosin phosphatase. Contractile tension within the actin cytoskeleton is generated by myosin II. We used Y27632 and blebbistatin to reduce cell contractility. Blebbistatin inhibits myosin II by blocking myosin in the actin-detached state and prevents rigid actomyosin cross-linking, thus reducing cell contractility [192]. Y27632 is a specific ROCK inhibitor that competes with ATP for binding to the catalytic site [193]. Traction force measurements indicated that Y27632 and blebbistatin reduced traction stresses, verifying the treatments reduced cell contractility (Figure 3.3C). When FISH was performed, it was observed that both Y27632 and blebbistatin reduced *Ddr2* RNA localization compared to vehicle (DMSO) treated cells on 5 kPa gels (Figure 3.3B). Most of the *Ddr2* RNAs were located towards the center of the cell and many cellular protrusions were devoid of *Ddr2* staining (Figure 3.3A) that was observed in control (DMSO-treated) cells (Figure 3.3A). However, inhibiting actomyosin contractility did not completely abolish RNA localization when compared to PolyA RNA.

To further confirm the effects of contractility on RNA localization, we knocked down myosin II using siRNA against myh9a (non-muscle myosin heavy chain) (Figure 3.4B). In si-control cells, RNAs were localized to the periphery. In myosin II

knockdown cells, RNAs were more diffuse throughout the cytoplasm. PDI analysis showed that *Ddr2* localization was reduced in knockdown cells compared to control siRNA (Figure 3.4C). To confirm that this knockdown also reduced cellular contractility, traction force measurements were performed on 5 kPa gels. Indeed, traction forces were reduced in myosin II knockdown cells compared to si-control cells. These results indicate that actomyosin contractility plays a role in regulating *Ddr2* RNA localization to cellular protrusions.

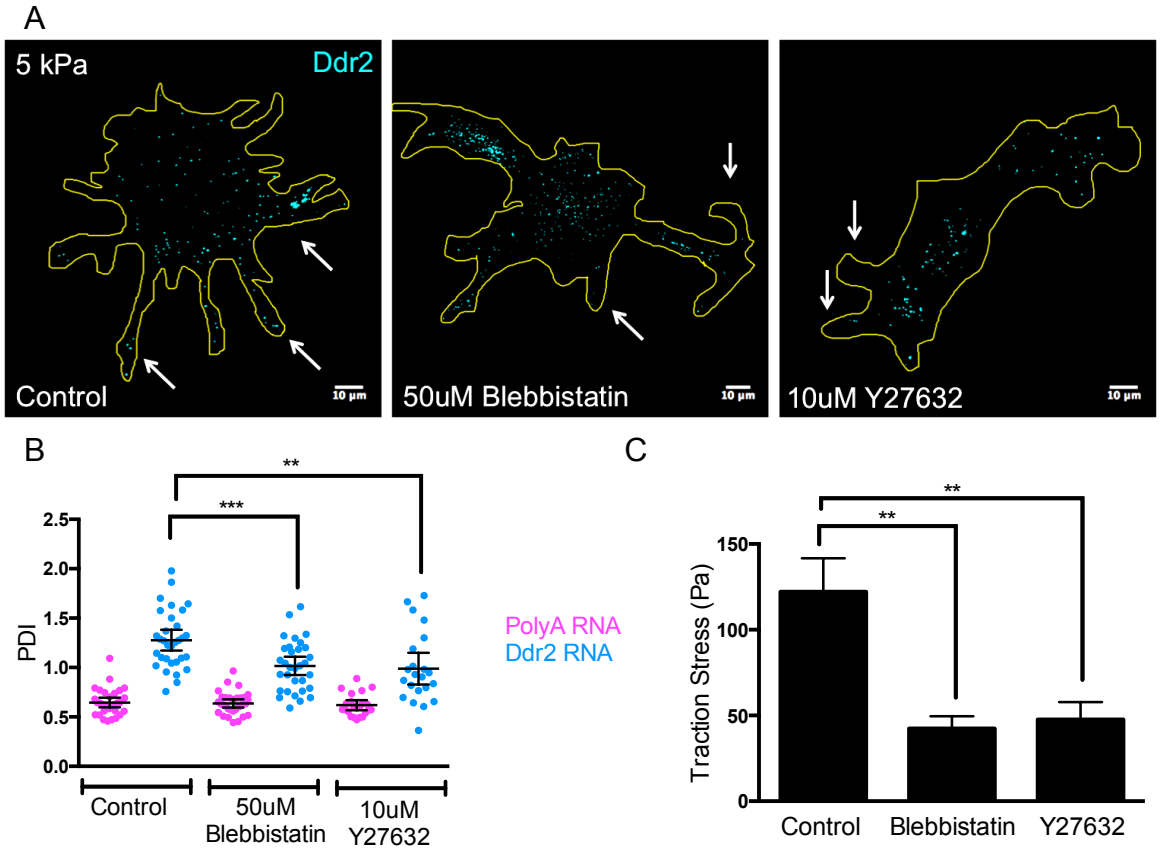

Figure 3.3. (A) Representative images showing control treated cells show Ddr2 localization at protrusions (white arrows) in control cells. Blebbistatin and Y27632 treated cells show more Ddr2 staining in the perinuclear regions and many protrusions are absent of Ddr2 RNAs (white arrows). (B) PDI analysis shows blebbistatin treatment reduces Ddr2 localization ($P<0.001$) and Y27632 also reduces localization ($P<0.01$) (C) Traction force measurements indicate blebbistatin and Y27632 lower cellular contractility compared to vehicle (control) treated cells ($P<0.01$). Error bars represent SEM.

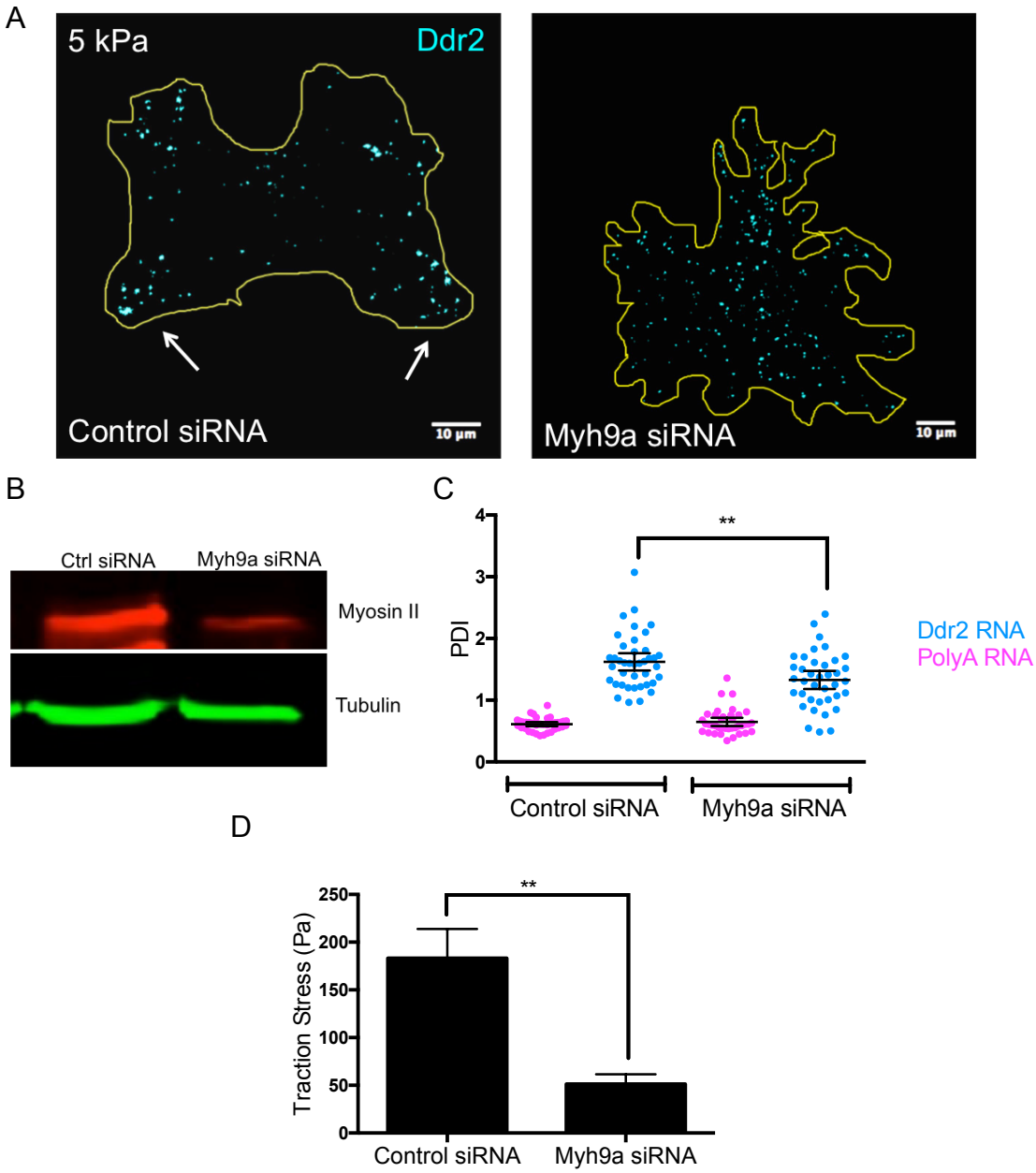

Figure 3.4. (A) Representative images of control siRNA and myh9a siRNA treated cells. White arrows point to peripheral *Ddr2* mRNAs. (B) Western blot shows reduction in myosin II with myh9a siRNA. Tubulin content remains the same in control and myosin knockdown cells. (C) Myh9a siRNA treated cell show a reduction in *Ddr2* RNA localization ($P<0.01$). (D) Cell average traction force measurements show that myosin II knockdown cells have reduced traction forces ($P<.01$, $N=8$) Error bars are SEM .

3.3.3 LPA increases contractility and induces RNA localization on soft substrates

To further test the role of contractility in *Ddr2* RNA localization, we treated cells on soft 1 kPa substrates with lysophosphatidic acid (LPA). LPA is known to activate Rho and stimulates contraction of the actomyosin skeleton [37]. When cells were treated with LPA, they became more elongated (Figure 3.5A) and increased their spreading area (Figure 3.5D). Traction force measurements also indicated that cells treated with LPA exerted more traction stress on average (70 Pa) compared to control (30 Pa) (Figure 3.5 C). To test the role of actomyosin contractility on *Ddr2* RNA localization, we performed FISH on LPA treated cells. Indeed, LPA treated cells showed peripheral distribution of RNAs compared to PolyA staining (Figure 3.5B). Control cells showed diffuse staining and no localization. These results indicate that it is possible to promote localization on soft substrates by increasing cellular contractility with LPA stimulation.

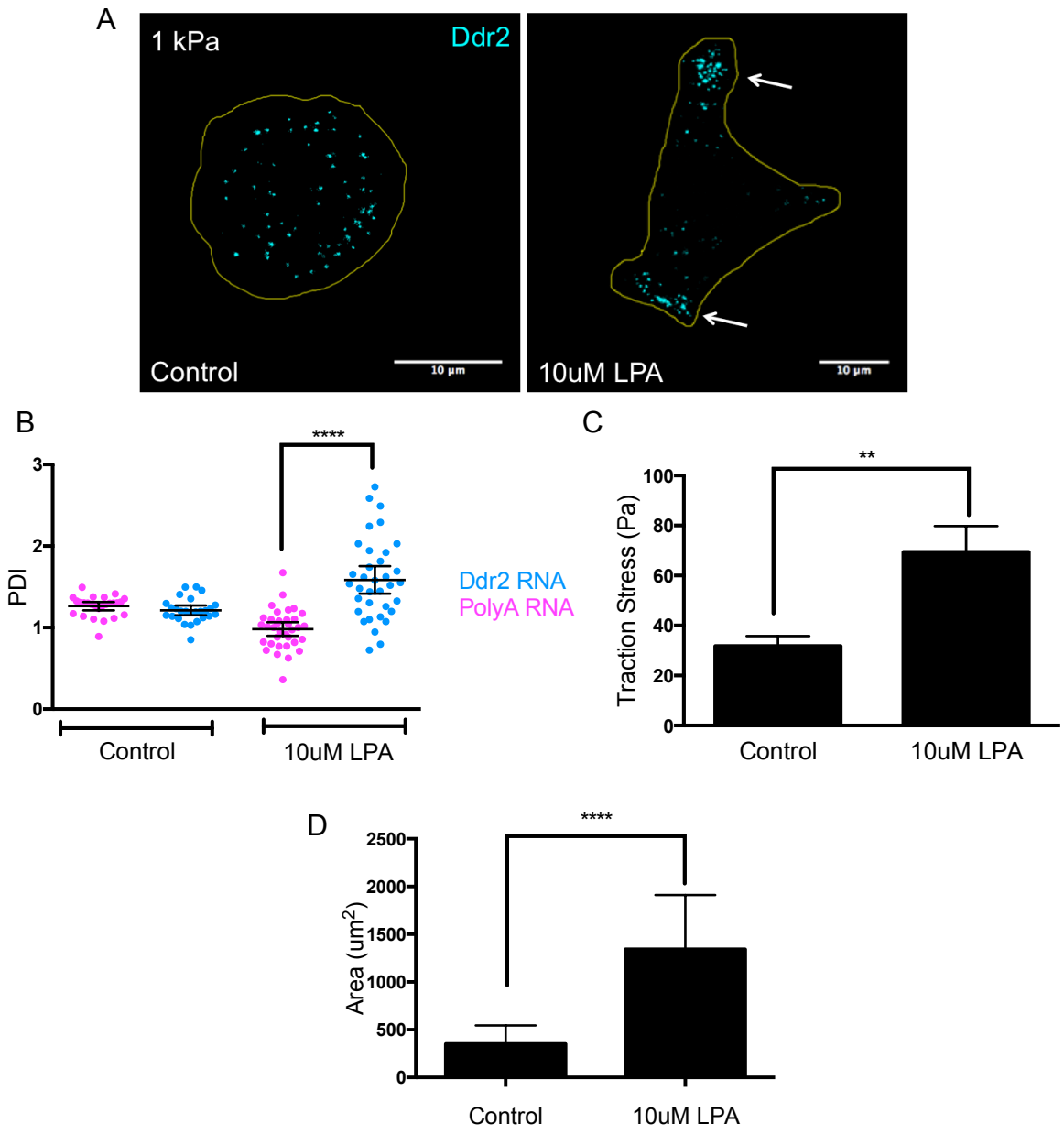

Figure 3.5 (A) Representative images showing cells on 1 kPa gels in control and LPA treated groups. LPA treated cells become larger and more elongated with peripheral *Ddr2* localization. White arrows point to peripheral *Ddr2* RNA localization. (B) PDI analysis shows *Ddr2* RNA is localized compared to PolyA control (P<0.0001). Bars represent the mean with 95% confidence interval. (C) Traction force measurements show that cells exert higher traction on 1 kPa substrates when treated with LPA (P<0.01, N=20). Error bars represent SEM (D) Cell area measurements indicate that LPA-treated cells have a higher spreading area compared to control cells on 1 kPa substrates (P<0.0001, N=30). Error bars are standard deviation.

3.4 Discussion

RNA localization is a tightly regulated event that is critical for many cellular functions. A subset of RNAs, including *Ddr2*, is localized to the protrusions in migrating fibroblasts and is dependent on APC for anchoring at the ends of detyrosinated microtubules [8]. During migration, cells sense and respond to the mechanical properties of their environment and modulate their contractility accordingly. The stiffness that cells feel *in vivo* situations, however, is much less than glass substrates. However, little is known how mRNAs respond to substrate stiffness and cellular contractility. In the current work, we hypothesized that increasing substrate stiffness and enhanced cellular contractility would play a role in *Ddr2* RNA localization.

We chose to use polyacrylamide gels of different stiffness to see how cells alter RNA localization in response to the mechanical environment. The use of this system offers many advantages including the ability to tailor the stiffness easily by changing the concentration of cross-linker, control the stiffness of gel independent of extracellular protein amount, and create gels of physiologically relevant stiffness. In this work, we chose to vary the range of stiffness from 1-280 kPa in order to mimic the changes of tissue stiffness that occur throughout the body and during disease pathologies such as cancer. For example, the stiffness of brain (0.1-1 kPa) is much less than that of bone (~2-4 GPa) [194]. Furthermore, the stiffness of the primary tumor has been shown in many cases to be stiffer than normal tissue [189].

On stiffer substrates, we saw an increase in *Ddr2* RNA localization to the periphery. We hypothesized that the increased actomyosin contractility on the stiff

substrates could account for this. To verify this, we performed traction force microscopy to measure cellular traction forces on the different substrates. Indeed, we observed higher traction forces on 5 kPa and 280 kPa substrates compared to the soft, 1 kPa substrates. These findings and the values we obtained are in accordance with previous studies done with fibroblasts [183, 186]. It would be interesting in future studies to observe the distribution of traction forces with the localization of RNAs concurrently. Furthermore, it would also be interesting to see whether *Ddr2* RNAs localize to the front or trailing edge of the cell during migration. In migrating fibroblasts, the leading edge and sometimes the trailing edge have the highest localization of traction forces [183, 186]. Additionally, since APC-dependent RNAs associate with Glu-MT that tend to orient themselves toward the leading edge of the cell, it is likely that APC-dependent RNAs localize to the leading edge during migration [195].

In this work, we addressed the role of contractility and substrate stiffness in migrating cells. However, this system may be relevant to other systems such as collective migration and tissue formation. On stiff substrates, cells migrate away from one another whereas on soft substrates they merge together to form tissue-like structures [196]. While in this dissertation, we have mainly focused on the localization of *Ddr2* RNA that is involved in cell-substrate adhesion and migration; there are other APC-dependent RNAs that may play a role in cell-cell junctions. *Pkp4* mRNA which encodes for the protein Plakophilin 4 is thought to be a component of desmosomes and adherens junctions [94]. Furthermore, myosin II contractility plays a role in tissue-like cell compaction. It is likely to be responsible for the contraction of cell-processes during

tissue-like cell compaction and the formation of cell-cell adhesions [196]. In breast cancer cells, ZBP1/IMP1 targets RNAs not only to the leading edge, but also to cell-cell junctions (E-cadherin and β-actin) [197]. Taken together, it is possible that the same factors can target RNAs to different places depending on specific conditions or cell type.

To address our hypothesis and evaluate the role of contractility in RNA localization, we performed a series of assays in which cells were plated on substrates of varying stiffness and treated with pharmacological drugs to target specific biophysical machinery. On 1 kPa gels, LPA was used to activate RhoA. However, LPA has multiple downstream effectors and it is possible that it could have other non-specific effects. To further test the role of RhoA in the localization of RNAs a Rho activator could be used.

It is interesting to note that inhibiting actomyosin contractility with blebbistatin, Y27632 and myosin knockdown did not completely abolish RNA localization. Thus it is likely that RNA localization is mediated through interplay between the actin and microtubule cytoskeleton. Microtubules have been shown to regulate cell spreading based on substrate stiffness and cell contractility. On soft matrices, microtubules are necessary to form dendritic extensions and on stiff substrates microtubules are necessary for polarization but not spreading [198]. *Ddr2* RNA is known to associate specifically with detyrosinated microtubules and not with the actin cytoskeleton [8]. The actin and microtubule cytoskeleton coordinate in various physiological events and a dynamic balance between them is necessary for cell contractility, polarization and migration. Cells in culture normally maintain high contractility and exert forces on rigid substrates using myosin II to contract actin fibers. F-actin, myosin II, microtubules and

focal adhesions interact to mediate efficient cell migration [71, 199]. During migration the microtubule cytoskeleton becomes polarized with many of them detyrosinated with their plus ends preferentially facing the leading edge [195]. RhoA has also been shown to regulate microtubule activity. In fibroblasts, the formation of stable, non-dynamic detyrosinated microtubules is induced by activation of RhoA and is mediated by its downstream effector mDia [200]. Thus it is likely that detyrosinated microtubules are involved in the localization of RNAs on stiffer substrates and their disruption might account for a reduction in localization upon actomyosin inhibition. This might be a reason why inhibiting actomyosin contractility did not completely abolish RNA localization. To completely abolish localization, it might be necessary to more directly reduce the amount of detyrosinated microtubules in the cell. Based on this, we hypothesized that contractility influences RNA localization by affecting the detyrosinated microtubule network.

Previous research has indicated that integrin binding and mechanical tension induce movement of RNAs and ribosomes to focal adhesions, but the identity of these RNAs was unknown. It was also unknown how the microenvironment might influence RNA localization. We show here for the first time that *Ddr2* RNA localization is mechanosensensitive, and that substrate stiffness and contractility play a role in its localization to cellular protrusions.

3.5 Conclusions

In this Chapter, we focused on the localization of *Ddr2* mRNA to cellular protrusions in fibroblasts. We were interested in how RNA localization changes in response to the stiffness of the mechanical environment. We saw that on stiffer substrates, *Ddr2* RNA is localized to the protrusions and is diffuse in the cytoplasm on soft substrates. We hypothesized the increased localization on stiffer substrates was due to the increased actomyosin contractility. We saw that contractility plays a role in RNA localization, but inhibiting contractility does not completely abolish localization. **In the next Chapter, we specifically explore the effects of substrate stiffness on microtubule detyrosination, as well as the effects of contractility on detyrosinated microtubule structure. Furthermore, we explore the connection between contractility and detyrosinated microtubule structure and molecular players that might be involved.**

Chapter 4: Role of Microtubule Detyrosination on mRNA Localization and Effect of Contractility on Microtubule Detyrosination

4.1 Introduction

Microtubules contribute to the font-back polarity that is essential for directional migration in a variety of environments. One way this is achieved is through the selective stabilization of microtubules towards the leading edge [195]. Because of their longevity, this subset of microtubules can be post-translationally modified by detyrosination or acetylation of tubulin. These subsets of microtubules are longer-lived than their dynamic counterparts [201]. Specifically, APC-dependent RNAs associate with detyrosinated microtubules (Glu-microtubules (Glu-MT)) [8]. In Chapter 3, it was shown that substrate stiffness enhances *Ddr2* localization and that modulating contractility through LPA or blebbistatin/Y27632 can enhance/reduce localization respectively. It was hypothesized that contractility through the modulation of the detyrosinated microtubule network affects *Ddr2* RNA localization. Furthermore, another question we had was whether detyrosinated microtubules were sufficient themselves to induce localization.

Detyrosinated microtubules occur when they are post-translationally modified by a tubulin carboxypeptidase (TCP) that removes the terminal tyrosine and exposes a glutamate (Figure 4.5). The tyrosine is then replaced by tubulin tyrosine ligase (TTL). By knocking down TTL levels within the cell, the amount of detyrosinated microtubules

can be increased. While the specific TCP is unknown for the removal of the terminal tyrosine, a chemical compound called parthenolide inhibits TCP and prevents formation of detyrosinated microtubules in cells [202].

Factors have been identified that contribute to the detyrosination of microtubules. Rho GTPase and its downstream effector the formin mDia are key factors in a microtubule stabilization pathway [200]. However, Rho only stimulates mDia in the presence of integrin and FAK signaling [203]. Extracellular matrix rigidity positively regulates Rho activity and FAK autophosphorylation [189]. It is likely that microtubule detyrosination may change with substrate stiffness and that this may affect RNA localization. Thus, this may lead to increased microtubule stabilization on stiff substrates and relate to increased RNA localization.

This Chapter explores the changes of the detyrosinated microtubule network in response to substrate stiffness and contractility. It also explores whether directly modulating the detyrosinated microtubule content is sufficient to affect localization.

4.2 Methods

4.2.1 Immunostaining

For immunofluorescence, cells were plated onto gels and were fixed with 4%PFA in PBS for 15 minutes, permeabilized with 0.2% Triton X-100 in PBS for 5 minutes, blocked with 3% BSA for 1 hour and incubated with primary antibodies (anti-Glu tubulin) overnight at 4˚C. Coverslips were incubated with anti-α-tubulin for 1 hour. Primary antibodies used were anti-Glu-tubulin (Abcam, cat# ab48389; 1/250 dilution for

IF) and anti-α-tubulin (Sigma-Aldrich, cat# T6199; 1/1000 dilution). Secondary antibodies were conjugated with Alexa 488, 546 or 647 (Alexa Fluora series from Thermo Fisher Scientific, 1/200 dilution each). Nuclei or whole cell area were stained with DAPI or cell mask blue stain, respectively.

4.2.2 Western Blot

To analyze drug treatment effects on microtubule detyrosination, cells were plated on cell culture plates and treated with 50uM blebbistatin, 10uM Y27632 or 5uM parthenolide before being lysed in 0.5% triton-x in RSB buffer and measured for protein concentration using the BCA assay. The primary antibodies uses were anti-Glu-tubulin (Abcam, cat# ab48389, 1:2000 dilution) and anti-acetylated tubulin (Sigma, cat #T7451, 1:20,000 dilution). For western blot, the following secondary antibodies were used: anti-rabbit (conjugated with IRDye 800CW, Li-cor, cat# 926-32213, 1/15000 dilution), anti-mouse (conjugated with IRDye 680RD, Li-cor, cat# 926-68072, 1/15000 dilution). Western blot membranes were scanned with Odyssey (Li-Cor) and signal intensity was measured on image studio lite software.

4.2.3 Drug Treatments

Cells were allowed to spread for two hours before being treated with 5 uM parthenolide for two hours (Sigma-Aldrich, cat# P0667-5MG). Cells were treated with LPA, Blebbistatin and Y27632 as described in Chapter 3.

4.2.4 siRNA transfection

NIH/3T3 cells were transfected with siRNA to a 40 pmol final concentration with Lipofectamine RNAiMAX (Thermo Fisher Scientific, cat# 13778-150) according to the manufacturer's instructions. Cells were incubated for three days before being analyzed siRNAs used are listed in Table 4.1:

siRNA	Target Sequence	Catalog Number
TTL #3	5' CACCGCAAGTTTGACATTCGA-3'	SI01458331
Negative Control	Proprietary	1027281

Table 4.1. siRNAs used to perform knock-down experiments.

4.2.5 Statistical Analysis

To establish significance between the internal control mRNA and the localized/experimental mRNA, the Wilcoxon signed-rank test was used with a p value < 0.05. To compare values between two groups, the Student's t-test was performed with a p value < 0.05.

4.3 Results

4.3.1 Substrate Stiffness Enhances microtubule detyrosination

Our first question was to understand how substrate stiffness affects the Glu-MT network because APC-dependent RNAs are anchored at the plus-ends of detyrosinated microtubules [8]. Therefore, we examined the Glu-MT network on polyacrylamide gels of different stiffness. Cells on soft, 1 kPA gels showed no defined detyrosinated microtubule network and mostly had diffuse staining present (Figure 4.1A). However, on

1 kPa gels, the overall microtubule network appeared intact as stained with α-tubulin antibody. On intermediate 5 kPa, and 280 kPa, about 70-80% of the cells showed a well-defined Glu-MT network with several fibers immunostained with Glu-MT antibody (Figure 4.1B). On soft substrates, *Ddr2* mRNA is diffuse throughout the cytoplasm and this is accompanied by an absence of detyrosinated microtubules. Similarly, on stiffer substrates, the higher percentage of cells showing an intact Glu-MT network is accompanied by *Ddr2* localization. These results indicate the substrate stiffness affects the microtubule network by increasing the amount of stable microtubules, specifically Glu-MTs.

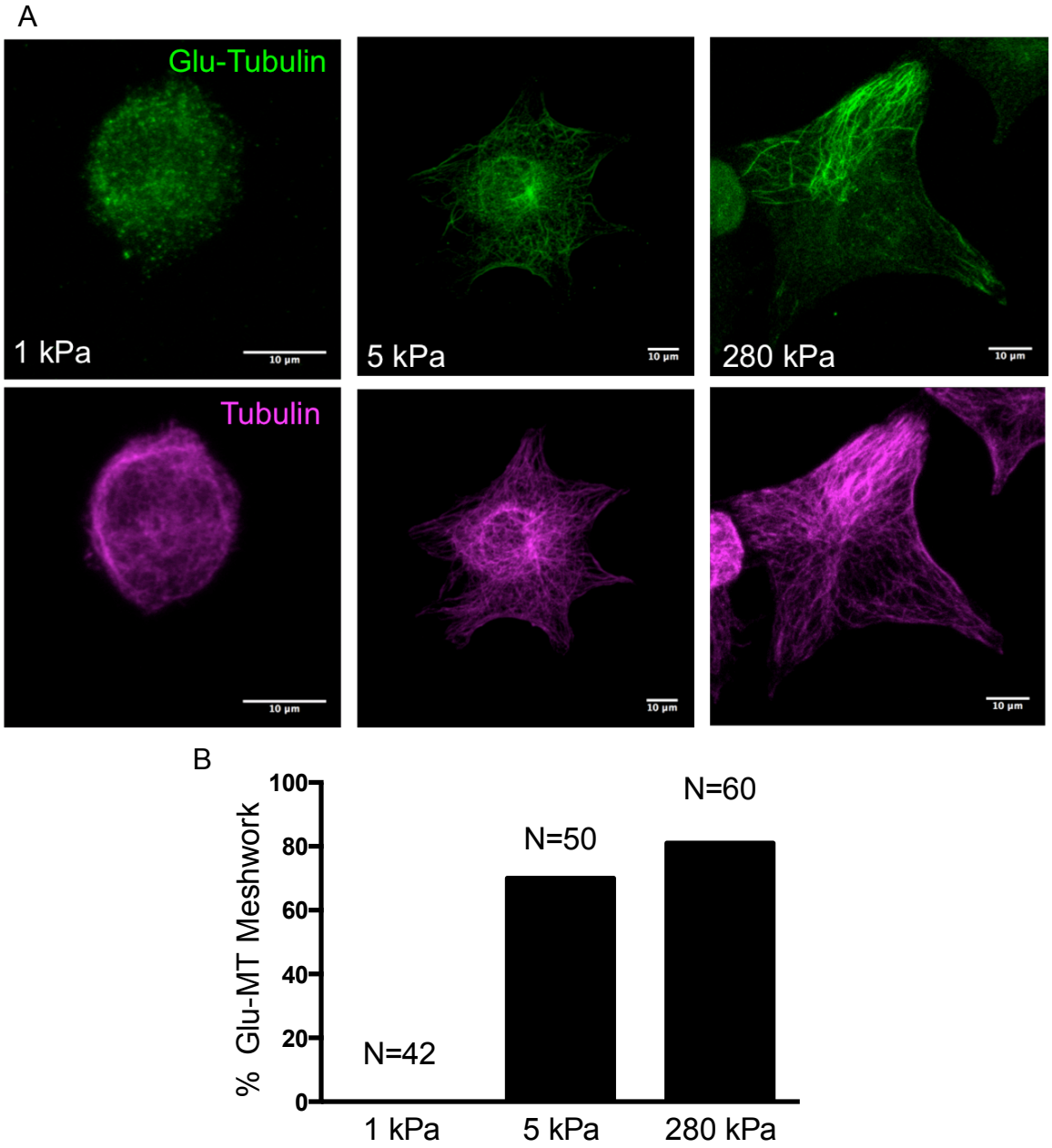

Figure 4.1. (A) On soft 1 kPa substrates, Glu-MT staining is diffuse and there are no Glu-MT fibers stained with antibody while the overall tubulin network looks intact. On 5 kPa and 280 kPa substrates, there are an increasing number of fibers stained with Glu-MT antibody and they appear to have a 'meshwork' structure. (B) On 1 kPa gels, no cells observed appeared to have a Glu-MT meshwork structure. On 5 kPa and 280 kPa there was an increase in the number of cells (60-80%) that had a Glu-MT structure. The number of cells is indicated by 'N=' above the bars.

4.3.2 Cell Contractility is required for the formation of a detyrosinated microtubule network

Our next objective was to measure the effects of contractility on Glu-MT structure. We showed that on soft 1 kPa substrates, cells increased peripheral localization of RNAs and tension upon treatment with LPA, thus we stained Glu-MT to examine the effect of LPA on the microtubules. In control cells, none of the cells observed showed a defined meshwork structure, but in LPA treated cells approximately 30% of cells showed defined Glu-MT fibers.

We also showed that treatment with myosin II inhibitor blebbistatin or ROCK inhibitor Y27632 led to a decrease in RNA localization. When detyrosinated microtubules were immunostained, we observed a decrease in the number of cells that showed a fibrous meshwork structure when treated with blebbistatin or Y27632. Less than 30-40% of cells on 5 kPa and 280 kPa substrates showed stained Glu-MT fibers when treated with blebbistatin or Y27632 (Figure 4.3B). Most of the stained Glu-MT in blebbistatin treated cells appeared to be localized in very thin protrusions far from the center of the cell (Figure 4.3A). Blebbistatin treated cells showed an absence of Glu-MT in the perinuclear region whereas control cells had detyrosinated microtubules located in areas throughout the cell. However, in blebbistatin treated cells the overall α-tubulin structure appeared intact, especially in the perinuclear region where there was Glu-MT staining absent (Figure 4.3A). Similarly, Y27632 cells showed disruptions in Glu-MT structure. There were many cells where there were very few (<5) fibers stained (Figure 4.3A). These results indicate that contractility is necessary for formation of a

detyrosinated microtubule meshwork.

To test whether there was a decrease in detyrosinated microtubule protein levels, western blot was performed. Previous reports have shown an increase in microtubule stability, specifically with acetylated microtubules (AC-MT), following actomyosin inhibition [204]. Acetylated microtubules are generated through post-translational modifications of a-tubulin and are also found on a more stable population of microtubules. We examined both AC-MT levels and Glu-MT protein levels. There was a decrease in the ratio of Glu-MT:tubulin levels in blebbistatin and Y27632 treated cells, even though its small magnitude did not reach statistical significance compared to control (Figure 4.4B). Consistent with prior reports, there was also a small increase in AC tubulin:tubulin ratio, again though without reaching statistical significance against the control (Figure 4.4C). Taken together, these results indicate that an intact Glu-MT network is necessary for RNA localization and that when it becomes disrupted (i.e. by reducing cell tension) RNA localization becomes disturbed.

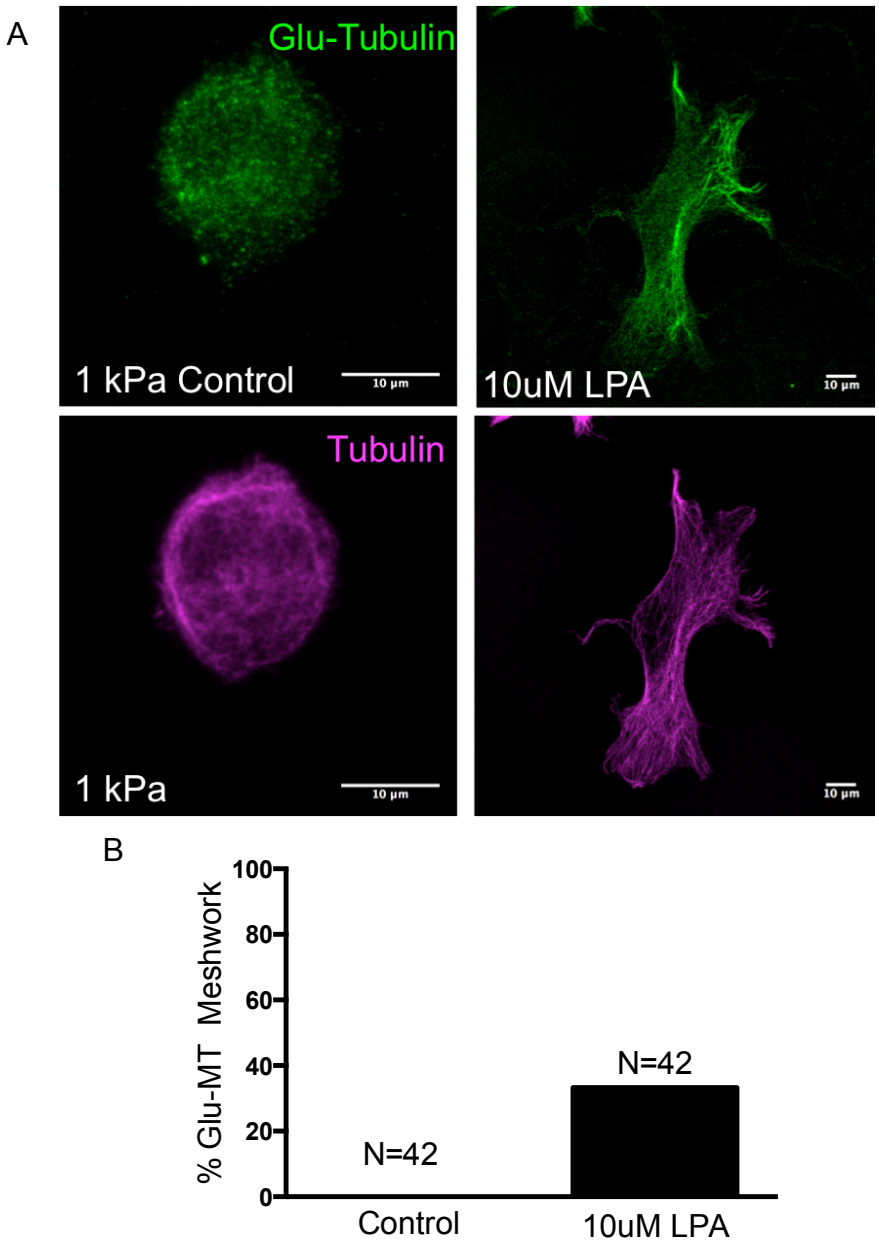

Figure 4.2. (A) Representative images showing Glu-MT staining of LPA treated cells on soft substrates. Control cells do not show a meshwork structure and LPA treated cells show several fibers stained with Glu-MT antibody. (B) LPA increases the percent of cells that have a meshwork structure on 1 kPa substrates.

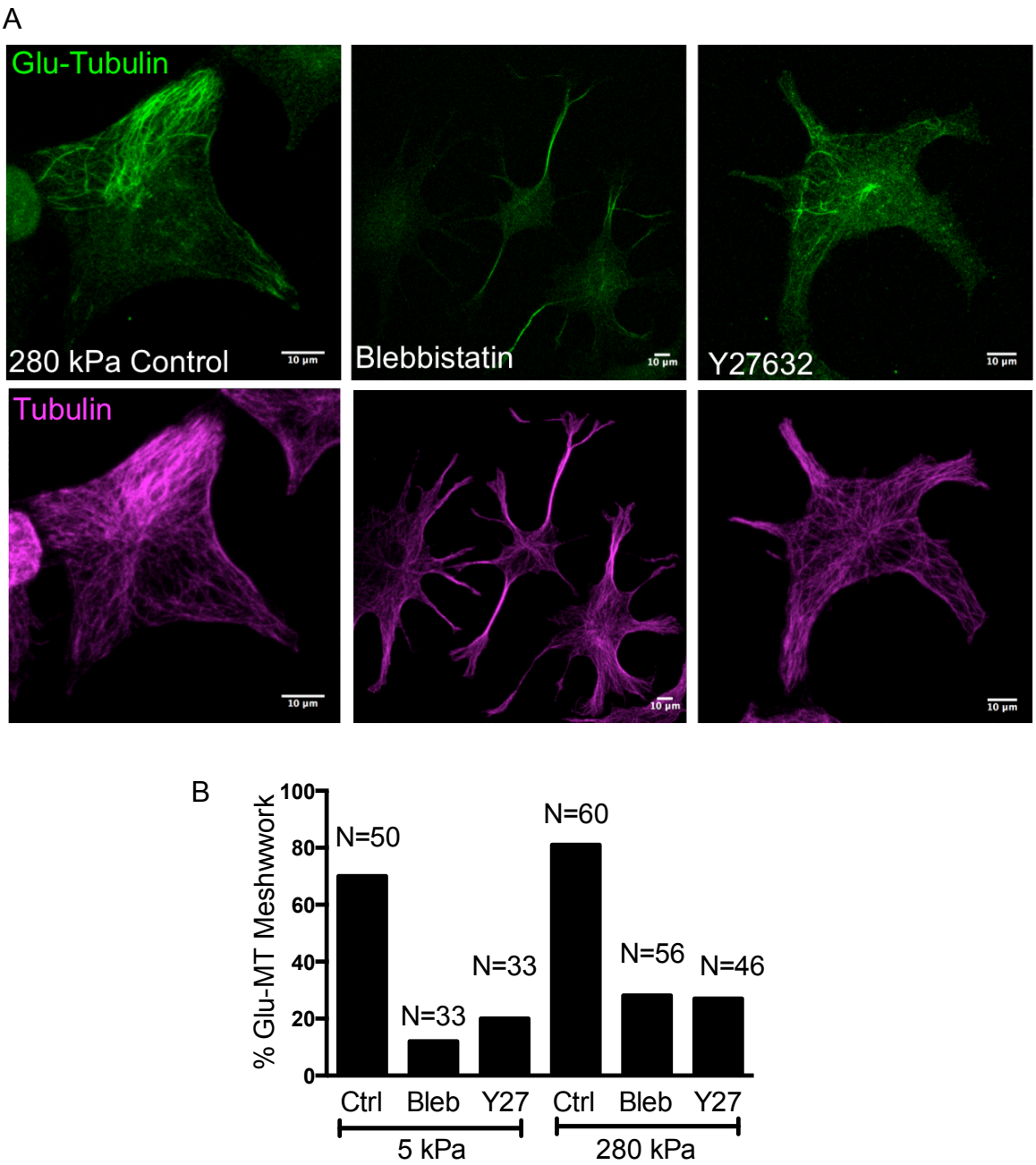

Figure 4.3. (A) Representative images showing Glu-MT staining of control, blebbistatin and Y27632 treated cells on 280 kPa substrates. Control cells show several fibers stained with Glu-MT and blebbistatin and Y27632 show very few fibers stained. (B) Blebbistatin and Y27632 treatments reduce the percent of cells that show a Glu-MT meshwork structure on 5 kPa and 280 kPa substrates.

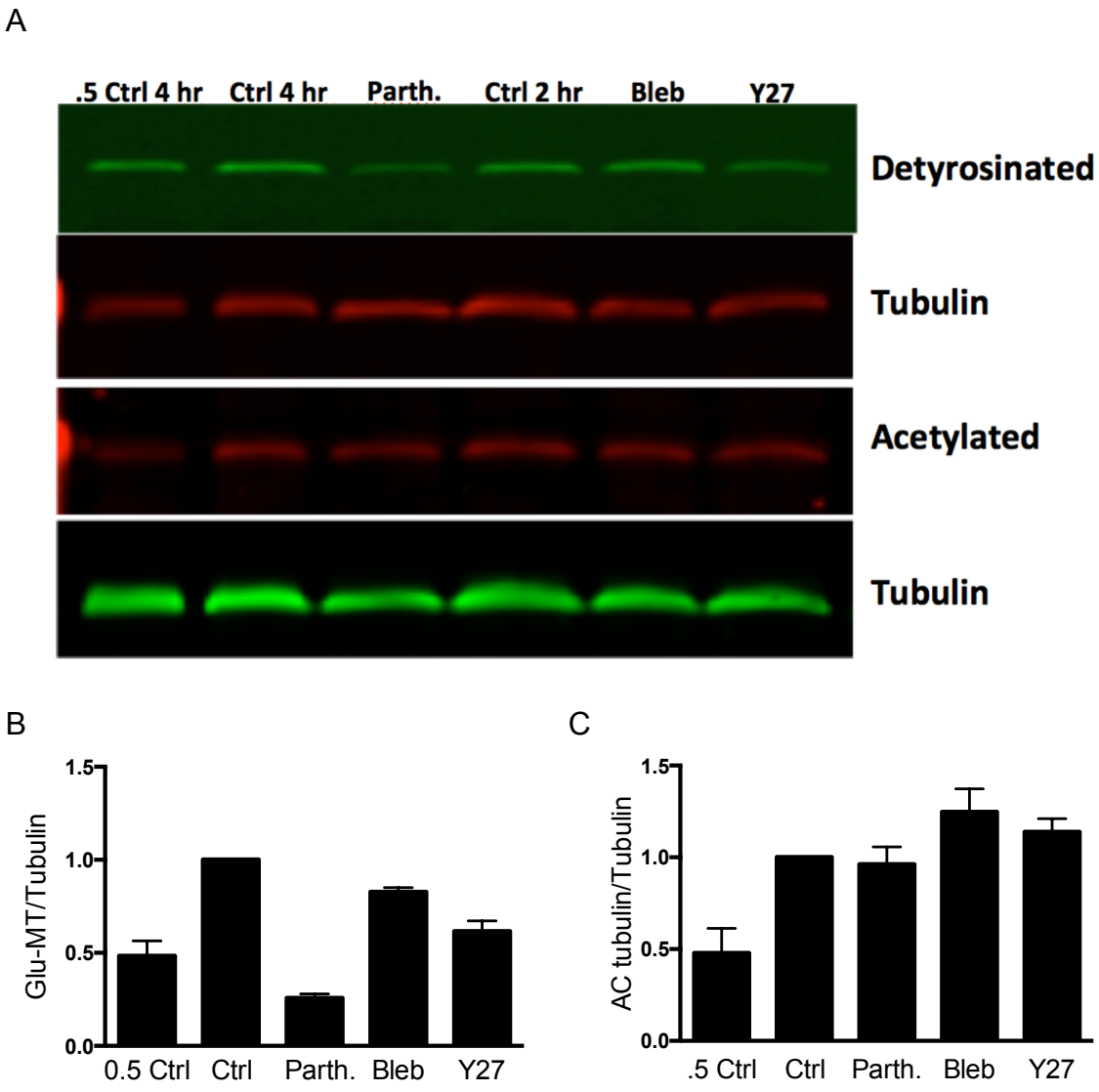

Figure 4.4. (A) Representative western blots showing acetylated tubulin and detyrosinated tubulin concentrations with drug treatments. Loading half of the control amount served as a loading control. Cells were plated for 4 hours to serve as a control for parthenolide treated cells or two hours as a control for blebbistatin and Y27632 treated cells. (B) The ratio of detyrosinated/tubulin signal intensity. Parthenolide (Parth.) treated cells showed a decrease in the ration and blebbistatin (Bleb) and Y27632 (Y27) also showed a slight decrease (N=4). Data was normalized to control. (C) The ratio of acetylated (AC) tubulin/tubulin signal intensity. Blebbistatin and Y27632 treated cells showed a slight increase. Data was normalized to control. (N=4 western blots).

4.3.3 Detyrosinated microtubules are required for RNA localization at cell protrusions

We have showed that contractility reduces RNA localization, and that changes in contractility correlate with changes in the Glu-MT structure. Another question we wanted to address was whether Glu-MTs were sufficient themselves to affect RNA localization or if contractility was also necessary to drive localization. To do this, we modulated the Glu-MT amount within the cells

Since *Ddr2* RNA localization is mislocalized on soft substrates, a question we had was whether increasing the amount of detyrosinated microtubules was sufficient to recover RNA localization. TTL was knocked down using siRNA, thus increasing the amount of Glu-MTs within the cell (Figure 4.5). PDI analysis was then used to assess the effect of Glu-tubulin levels on APC-dependent RNA localization. Even though the cells retained similar morphology between control siRNA and TTL siRNA treated cells, PDI analysis showed an increase in peripheral RNA amounts (Figure 4.6A). These results show that by increasing Glu-MT levels in cells, it is sufficient to recover RNA localization on soft substrates.

Our next question was whether reduction of detyrosinated microtubules on stiff substrates was sufficient to mislocalize RNAs. To test this, parthenolide was used to block TCP and reduce Glu-MTs within the cell (Figure 4.5). In cells that were treated with parthenolide, the *Ddr2* RNA distribution became more centralized compared to control cells (Figure 4.7). Indeed, PDI analysis showed a reduction in peripheral RNA localization on both 5 kPa and 280 kPa substrates with parthenolide treatment. These results indicate that detyrosinated microtubules are required and sufficient for localization

of APC-dependent RNAs to cellular protrusions.

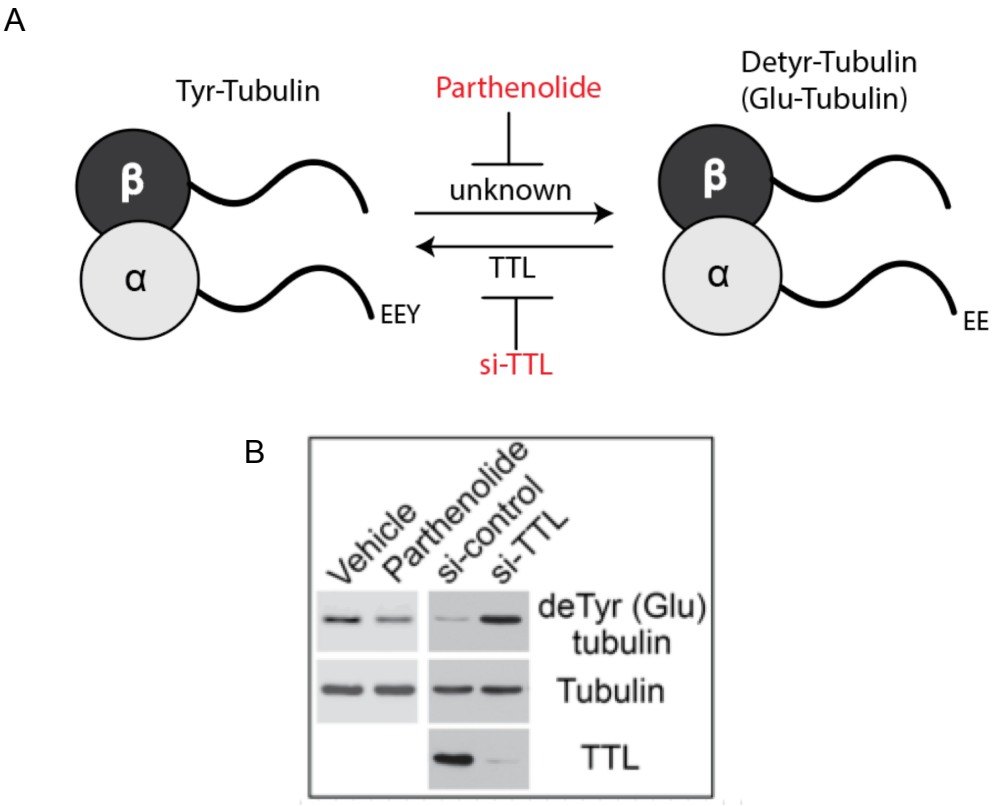

Figure 4.5. (A) An unknown tubulin carboxy peptidase (TCP) removes the terminal tyrosine from the alpha subunit to form stable detyrosinated microtubules. TCP activity can be blocked with a drug called parthenolide. Tubulin tyrosine ligase (TTL) adds the tyrosine back onto alpha subunit to create zmore dynamic, tyrosinated microtubules. TTL levels can be reduced using siRNA. (B) Western blot showing how parthenolide and si-TTL modulate the detyrosinated microtubule levels. Parthenolide decreases the amount of Glu-MTs and si-TTL knocks down TTL levels and increases the amount of Glu-MTs. These treatments do not affect the overall amount of microtubules.

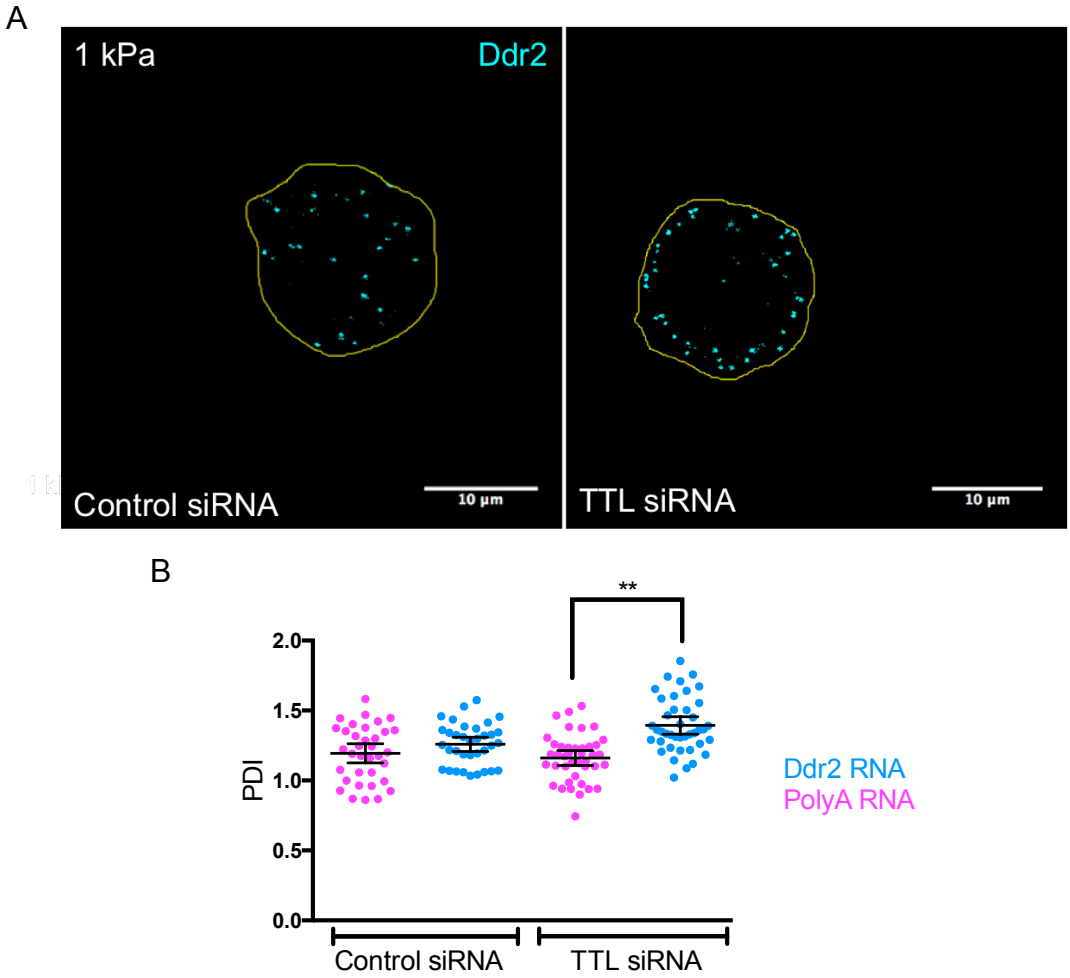

Figure 4.6 (A) Representative images showing si-control and si-TTL treated cells on soft 1 kPa substrates. Cells retained a round morphology, but si-TTL cells showed peripheral distribution of *Ddr2* RNA. (B) PDI analysis indicates that si-TTL cells have *Ddr2* localization compared to PolyA RNA ($P<0.01$). Error bars represent mean with 95% confidence interval.

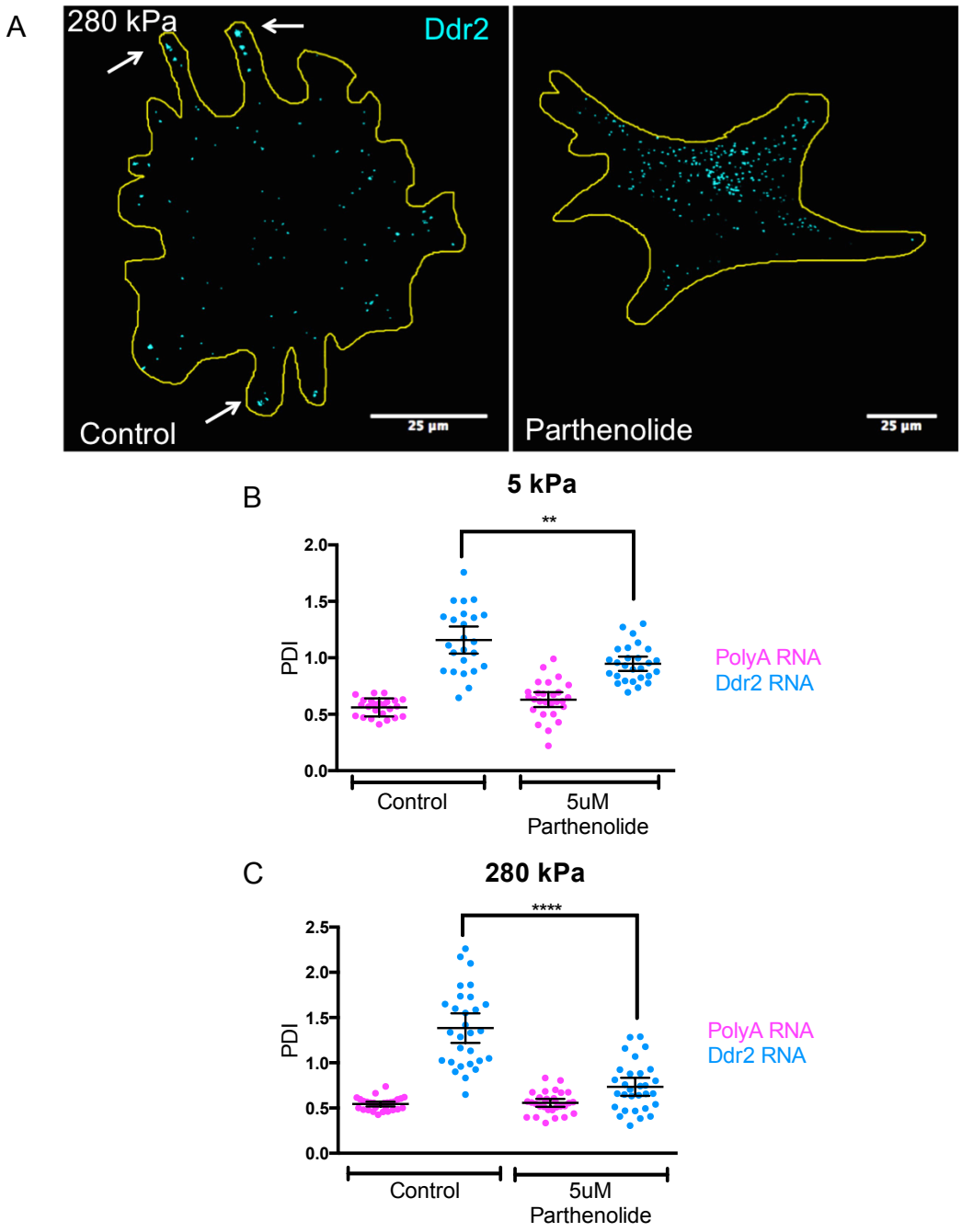

Figure 4.7. (A) Representative images showing *Ddr2* RNA localization in control and parthenolide treated cells on 280 kPa gels. Parthenolide treated cells have many protrusions that are absent of *Ddr2* RNAs (white arrows) while control cells show *Ddr2* RNAs localized to the protrusions (white arrows). (B) and (C) Parthenolide treatment reduces *Ddr2* RNA localization compared to control ($P<0.0001$) on 5 kPa (B) and 280 kPa substrates (C). Error bars represent mean and 95% confidence interval.

4.3.4 The effect of contractility on localization is mediated through microtubule detyrosination

Our next question was to address the relationship between contractility and microtubule detyrosination on RNA localization. In Chapter 3, we showed contractility can both enhance and reduce RNA localization, but not does completely abolish localization. In an effort to understand this relationship, we pre-treated cells with LPA and then blocked detyrosinated microtubules with parthenolide on soft substrates. When cells were pre-treated with LPA and then parthenolide (Figure 4.8A), they maintained a similar morphology to LPA treated cells. However, the RNAs were located towards the perinuclear region in the center of the cell. PDI analysis showed that there was no longer a significant difference between PolyA control RNA and *Ddr2* RNA in LPA+parthenolide treated cells. In control cells, RNAs were non-localized, and LPA induced localization.

In order to further test the relationship between actomysoin contractility and detyrosinated microtubule structure, we knocked down TTL and treated cells with blebbistatin. In si-TTL cells treated with blebbistatin, we observed less long and thin protrusions compared to blebbistatin treated cells alone (Figure 4.9A). In si-control blebbistatin treated cells, many of the protrusions were devoid of RNAs compared to the control siRNA cells as observed in Chapter 3. However, the si-TTL cells that were treated with blebbistatin still had *Ddr2* RNA present in the protrusions (Figure 4.9A). They also showed a recovery in localization. There was no significant difference between si-control and si-TTL cells treated with blebbistatin on 5 kPa and 280 kPa

substrates (Figure 4.9B,C). This indicates that by increasing the amount of Glu-MT within the cell, the effects of reduced actomyosin contractility on RNA localization were recovered. Thus, actoymosin contractility through modulation of the detyrosinated microtubule network regulates *Ddr2* RNA localization to protrusions.

To observe changes in the cytoskeletal network, detyrosinated microtubules were immunostained on 5 kPa and 280 kPa substrates. In si-control cells, cells showed a meshwork structure of detyrosinated microtubules with several fibers stained with the antibody. When si-control cells were treated with blebbistatin, there were many fibers that were absent from the perinuclear region and the overall meshwork structure appeared disrupted. In Figure 4.10A, the zoom panel shows an area where the meshwork structure is absent when si-control cells are treated with blebbistatin. The same area shows that the meshwork structure is still intact for the overall α-tubulin structure indicating that blebbistatin disrupted the Glu-MT network and not the overall microtubule network. In si-TTL cells, there appeared to be more fibers stained with antibody compared to si-control cells. When si-TTL cells were treated with blebbistatin, there appeared to be a recovery in meshwork structure, with a higher percentage of cells (~70-80%) having a meshwork structure. In Figure 4.10A, the zoom panel shows that si-TTL cells treated with blebbistatin still had a meshwork structure present in the perinuclear region unlike si-control cells treated with blebbistatin. By increasing the amount of detyrosinated microtubules within the cell, the effect of blebbistatin on Glu-MT disruption was eliminated.

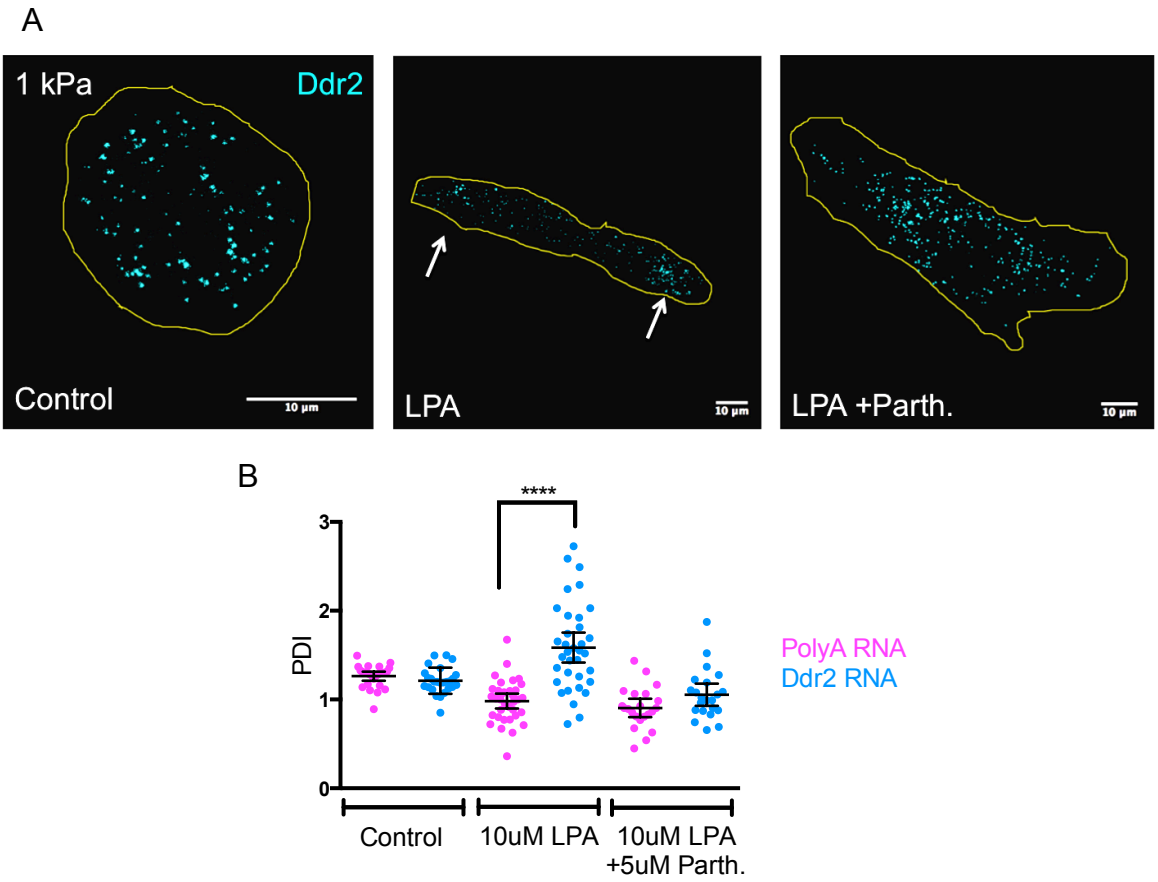

Figure 4.8. (A) Representative images show *Ddr2* RNA FISH staining on 1 kPa gels. White arrows point to where RNAs are peripherally localized in LPA treated cells. (B) PDI analysis of RNA localization shows that LPA induces localization ($P<0.0001$) and that LPA+parthenolide treatment showed no localization compared to PolyA control.

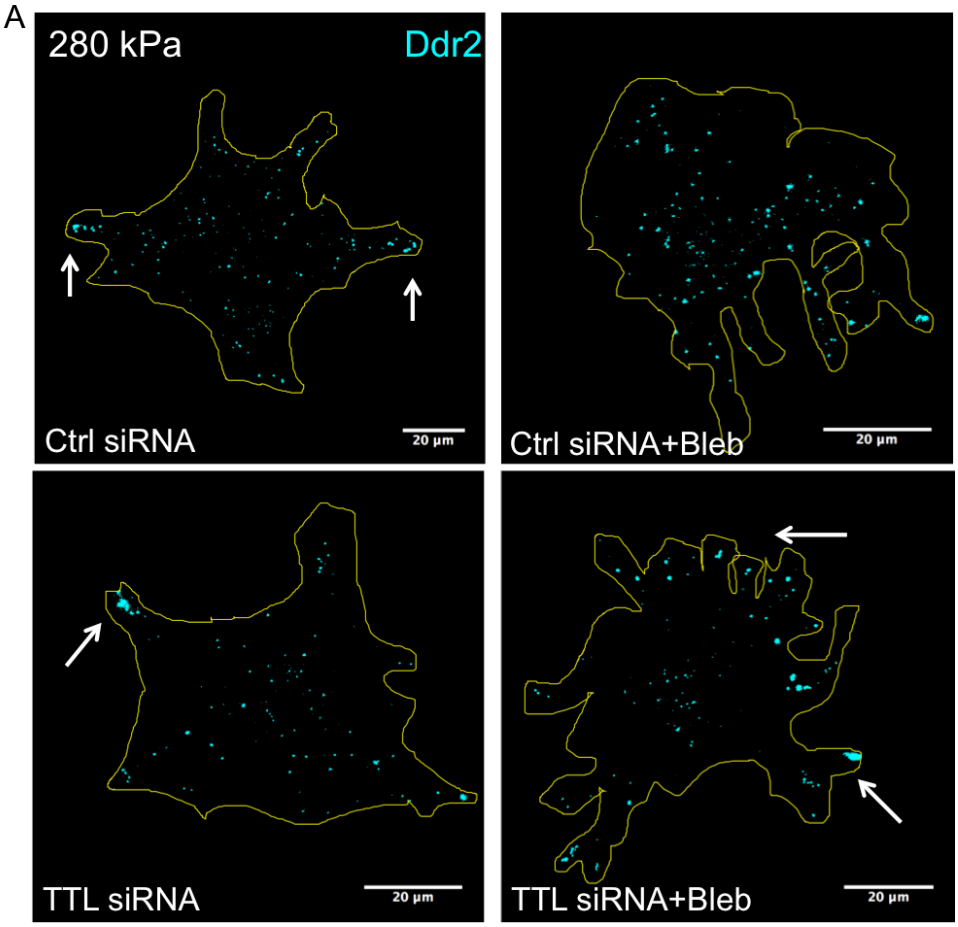
A
280 kPa
Ddr2
Ctrl siRNA
20 μm
Ctrl siRNA+Bleb
20 μm
TTL siRNA
20 μm
TTL siRNA+Bleb
20 μm

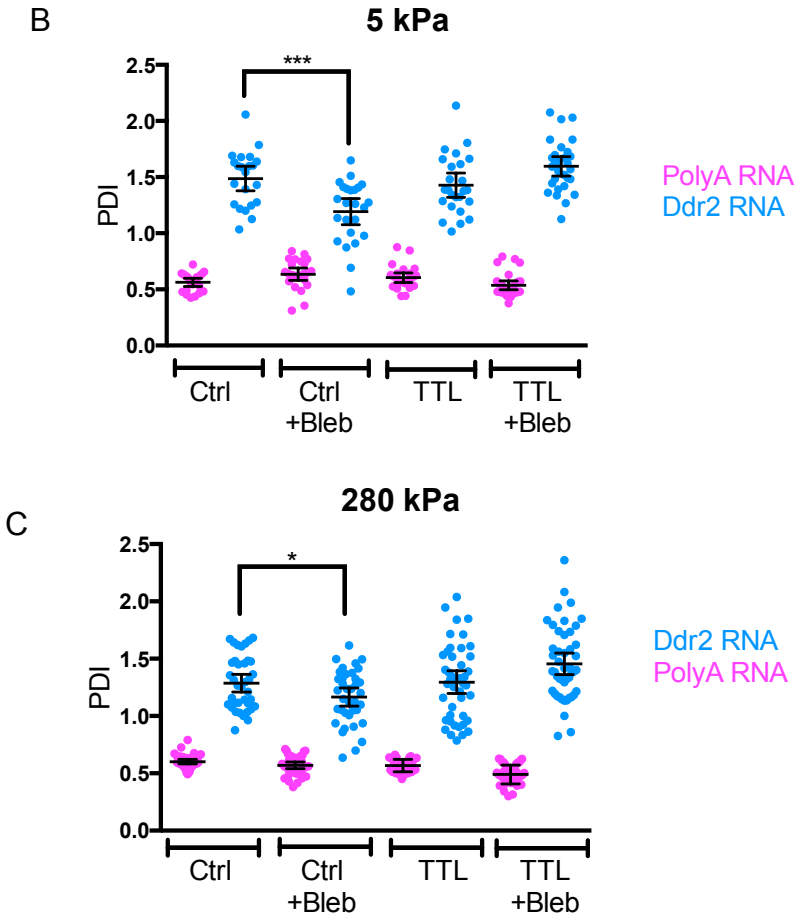

Figure 4.9. (A) Representative FISH images showing *Ddr2* RNA staining in control siRNA, control siRNA + blebbistatin, TTL siRNA, and TTL siRNA + blebbistatin treated cells on 280 kPa gels. In si-control and si-TTL treated cells, white arrows point to peripheral *Ddr2* localization. In si-control + blebbistatin treated cells, most of the RNA staining is located in the perinuclear region. (B) On 5 kPa gels, si-control + blebbistatin treated cells show a reduction in RNA localization ($P<0.001$). Si-TTL cells treated with blebbistatin did not show a reduction in RNA localization. (C) On 280 kPa gels, si-control + blebbistatin treated cells show a reduction in RNA localization ($P<0.05$). Si-TTL cells treated with blebbistatin did not show a reduction in RNA localization. Error bars represent mean with 95% confidence interval.

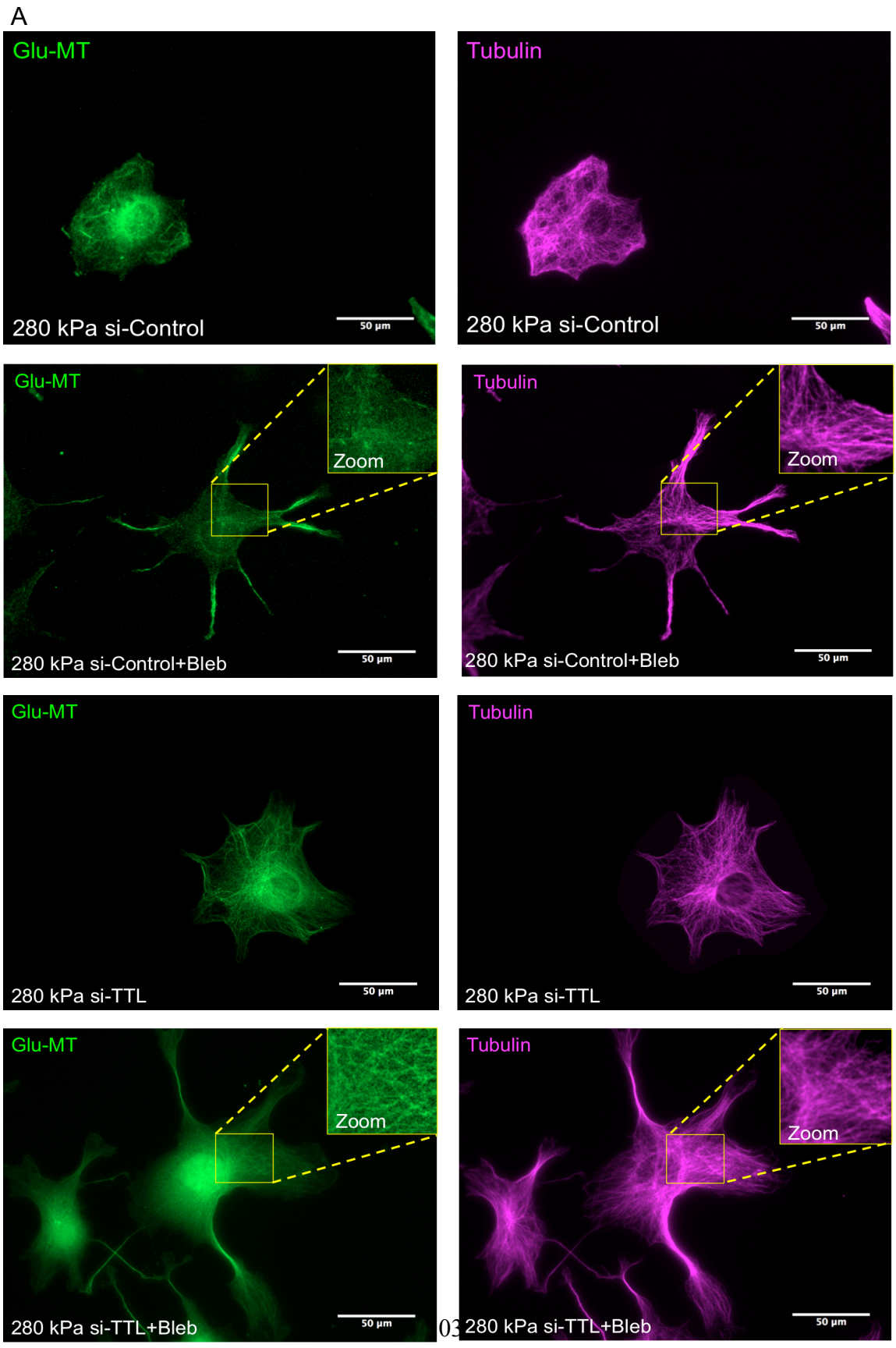
A
Glu-MT
280 kPa si-Control
50 μm
Tubulin
280 kPa si-Control
50 μm
Glu-MT
Zoom
280 kPa si-Control+Bleb
50 μm
Tubulin
Zoom
280 kPa si-Control+Bleb
50 μm
Glu-MT
280 kPa si-TTL
50 μm
Tubulin
280 kPa si-TTL
50 μm
Glu-MT
Zoom
280 kPa si-TTL+Bleb
50 μm
Tubulin
Zoom
280 kPa si-TTL+Bleb
50 μm

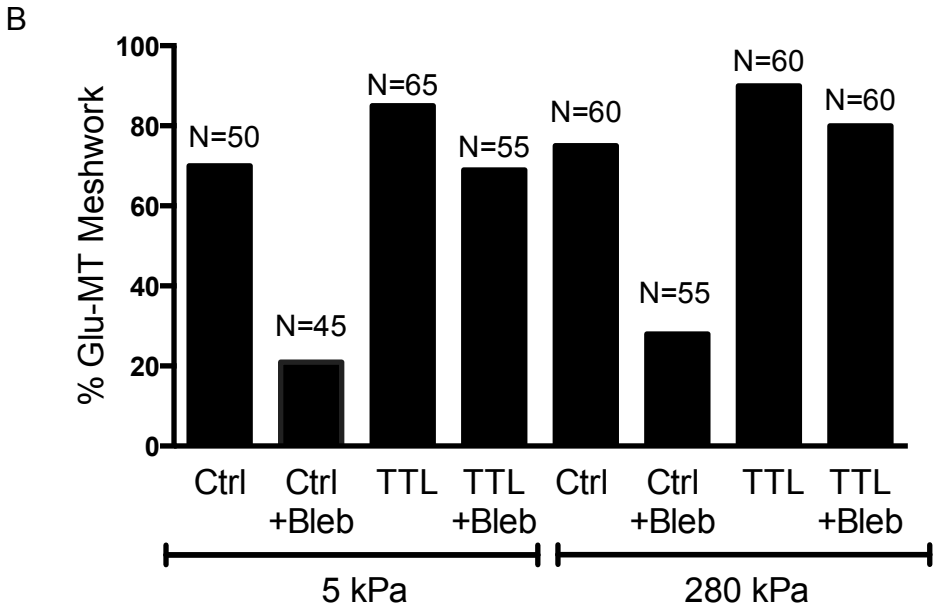

Figure 4.10. (A) Representative images of Glu-MT and α-tubulin and in si-control, si-control+blebbistatin, si-TTL and si-TTL+blebbistatin on 280 kPa gels. The 'Zoom' panel in si-control+blebbistatin and si-TTL+blebbistatin represents a perinuclear area stained with Glu-MT or tubulin. Si-control cells treated with blebbistatin showed an absence of a Glu-MT network in the perinuclear region, while the overall tubulin structure appeared intact. Si-TTL cells treated with blebbistatin displayed a Glu-MT meshwork structure in the perinuclear region. (B) The graph depicts the percent of cells with a Glu-MT network for si-control (ctrl), si-control+blebbistatin (ctrl+bleb), si-TTL (TTL) and si-TTL+blebbistatin (TTL+bleb) for 5 kPa and 280 kPa substrates. The N at the top of the graph represents the total number of cells analyzed for each sample.

4.4 Discussion

In this work, we investigated the connections between cell tension, substrate stiffness and the microtubule network and how these factors might regulate RNA localization. Our results indicate that the effects of contractility on RNA localization are mediated through the detyrosinated microtubule network. On stiff substrates, cells have increased actomyosin contractility and this is regulated through the Rho/ROCK pathway. The increase in tension leads to the formation of a Glu-MT network that results in RNA localization to the protrusions. It has been shown that Rho-GTPase is necessary for selective stabilization of microtubules, but that it does not bind directly to the microtubules [124]. Palazzo et al. showed that mDia is a downstream Rho effector implicated in regulating the microtubule stability in cells [200]. mDia interacts with three MT +TIP proteins, EB1, APC, and CLIP170, and EB1 and APC have been implicated in microtubule stability [203, 205, 206]. Thus, we suggest a working model for RNA localization in which RhoA activates the Rho/ROCK pathway and the formation of stable microtubules through mDia (Figure 4.11). Based on this, future studies could focus on expressing a constitutively active form of mDia in cells and seeing if a recovery of RNA localization is observed after inhibiting contractility. Additionally, experiments could see if on soft substrates, expressing an active form of mDia induces RNA localization.

A negative feedback loop also exists between cytoskeletal tension and Rho. Inhibition of cell contraction has also been shown to lead to down regulated Rho levels [207]. We had shown that inhibiting actomyosin contractility on stiff substrates led to a

decrease in RNA localization. This feedback signaling could account for the decrease in Glu-MT meshwork structure that was seen in blebbistatin and Y27632 treated cells and also for the decrease in RNA localization we saw in Chapter 3. By reducing cell tension with blebbistatin or ROCK inhibitor, it led to a down regulation of Rho signaling and potentially mDia, thus affect detyrosinated microtubules and RNA localization.

These results are interesting because previous reports have shown an increase in stable microtubule formation upon blebbistatin treatment [204]. However, they specifically showed an increase in acetylated tubulin, another post-translational modification of tubulin that exhibits stability [204]. Our western blots showed small decreases in Glu-MT levels within the cells and small increases in acetylated tubulin upon blebbistatin and Y27632 treatment. However, our western blots were performed on rigid plastic cell culture plates. It is possible that on softer substrates, we would observe a larger decrease in Glu-MT protein levels upon blebbistatin treatment. Another possibility for the different results observed could be that we used a different concentration and treatment time of blebbistatin than in previous studies.

Our work also has relevance in cancer metastasis. During cancer progression, the tumor microenvironment becomes stiffer. This biomechanical property is due to the largely cross-linked and oriented collagenous matrix [1]. The increased stiffness promotes invadapodia formation and enhances tumor cell invasion by driving focal adhesion assembly [208]. Increased tumor cell migration is highly driven by Rho-GTPase activity that stimulates actin assembly and actomyosin contractility [209]. It is

possible that the localization of RNAs in the stiff microenvironment could be a promoter in metastatic cancer cell invasion.

The regulation of *Ddr2* RNA at cellular protrusions could also be a promoter in metastatic cancer cell invasion. *Ddr2* is a collagen receptor tyrosine kinase receptor that has been implicated in several cancer cell behaviors. It has been observed to play a role in tumor angiogenesis, invasion and metastasis [104, 210, 211]. Additionally, it has been reported that *Ddr2* is a critical regulator of the cancer cell epithelial to mesenchymal transition [212].

In this work, we showed that matrix stiffness increases microtubule detyrosination. Glu-MTs are also involved in cancer progression. For instance, loss of TTL induces mesenchymal transition of breast cancer cells, which may contribute to metastatic potential and altered cell response [213]. Additionally, Glu-MTs have been found to be associated with dynamic membrane protrusions (termed microtentacles) that occur in detached metastatic cell lines and facilitate tumor cell reattachment and cell-cell adhesion [213, 214]. It is possible that there are localized RNAs at the ends of the microtentacles to help facilitate attachment and adhesion during processes such as transmigration.

Before this work, the effects of the mechanical environment on RNA localization and microtubule stability were unknown. It was also unknown how contractility and detyrosinated microtubules coordinate in regulating RNA localization to protrusions. We show here that cell tension promotes a detyrosinated microtubule network which then results in peripheral RNA localization. While we used fibroblasts as a model system to study the effects of the microenvironment on RNA localization, this work has

significance in cancer metastasis. We envision a scenario where as tumor stiffness increases; it increases cell contractility and microtubule detyrosination and ultimately drives the localization of *Ddr2* RNA to cellular protrusions where it then promotes a more metastatic phenotype.

4.5 Conclusions

In summary, contractility influences RNA localization through modulation of the detyrosinated microtubule network. In cells plated on increasingly rigid substrates, we observe an increase in the percentage of cells with an intact Glu-MT meshwork. Further we see that increasing contractility through LPA induces Glu-MT meshwork formation and inhibiting contractility reduces the percent of cells with a Glu-MT network. When we inhibit the formation Glu-MT through the use of parthenolide that blocks the TCP, we observe a decrease in RNA localization on stiff substrates. By increasing the amount of detyrosinated microtubules on soft substrates by using TTL siRNA, we observe an increase in RNA localization. These results indicate that detyrosinated microtubules are necessary and sufficient for *Ddr2* RNA localization. Our results together suggest that cell-substrate interactions play an important role in the localization of *Ddr2* RNA to cellular protrusions. These biophysical interactions may play an important role during disease pathologies such as cancer metastasis where the tissue microenvironment becomes stiffer during disease progression.

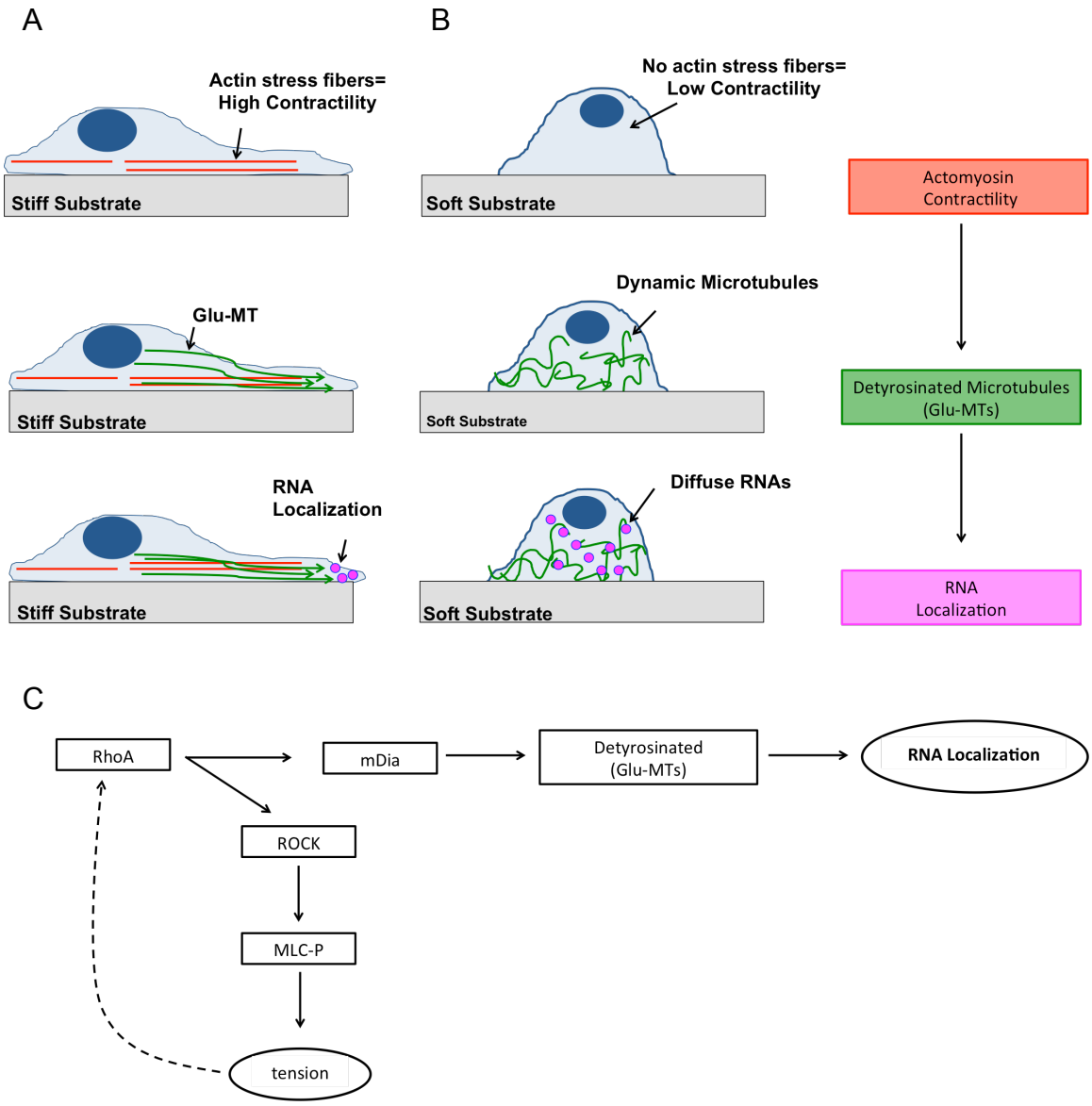

Figure 4.11. (A). On stiff substrates, cells exhibit high contractility as depicted with actin stress fibers (red). This leads to the formation of polarized, stable, detyrosinated microtubules (green arrows) and localization of APC-dependent RNAs (magenta) at cell protrusions. (B) On soft substrates, cells exhibit low contractility and have dynamic microtubules (green) causing RNAs to be diffuse. (C) Proposed signaling cascade showing RhoA and its downstream effectors and their effects on localization. RhoA activates both ROCK and mDia leading to cell tension (through myosin light chain phosphorylation (MLC-P) and myosin movement along actin cytoskeleton) and detyrosinated microtubule formation respectively. This in turn leads to RNA localization. A feedback loop exists between cell tension and Rho such that a decrease in contractility causes Rho down regulation and subsequent disruption in detyrosinated microtubules and RNA localization.

Chapter 5: Summary and Future Directions

5.1 Summary

Overall, in the work generated from this thesis project we have examined biophysical properties of cancer cell transmigration and mRNA localization. We believe that these results can translate to further understanding cancer progression and cancer metastasis. The main principles learned from this work are the following:

Chapter 2: Mechanisms of Cancer Cell Transmigration

1. Cancer cell transmigration may be a two-step process in which cancer cells first 'incorporate' into the endothelium before subsequent invasion into the subendothelial matrix.
2. Incorporation occurs independently of matrix stiffness and endothelial activation for melanoma cells and breast cancer cells. Pancreatic cells transmigrate more with endothelial activation and on softer substrates. Likely, the biophysical principles (i.e. subendothelial matrix stiffness) governing incorporation are cell-specific.
3. Incorporation initiates by dislocating VE-Cadherin at endothelial cell-cell junctions and disrupts it during incorporation.
4. The endothelial monolayer becomes damaged during cancer cell incorporation.

Chapter 3: Effect of Substrate Stiffness and Contractility on APC-dependent mRNA Localization

1. Matrix stiffness enhances APC-dependent RNA localization.
2. Inhibiting actomyosin contractility reduces RNA localization on stiff substrates.
3. Enhancing actomyosin contractility increases RNA localization on soft substrates.

Chapter 4: Role of Microtubule Detyrosination on mRNA Localization and Effect of Contractility on Microtubule Detyrosination

1. Detyrosinated microtubules are required and sufficient for RNA localization at cell protrusions.
2. Substrate stiffness increases microtubule detyrosination.
3. Contractility increases microtubule detyrosination.
4. The effect of contractility on localization is mediated through microtubule detyrosination.

In the first part of this work we examined mechanisms of cancer cell transmigration through the endothelium. Leukocytes routinely transmigrate through the endothelium to sites of inflammation or injury. However, we found that cancer cell transmigration is very different from this process. In our previous work we found that this process was dependent on subendothelial matrix stiffness and endothelial activation with TNF-α and that leukocytes directly transmigrate through the endothelium [26, 27]. Cancer cells appear to have an additional step, namely incorporation into the endothelium. Metastatic

cells may first incorporate into the endothelial monolayer and then migrate under the monolayer. Additionally, this step occurs independent of matrix stiffness and endothelial activation for melanoma and breast cancer cells. However, pancreatic cells incorporated more into softer subendothelial matrices and incorporated more under endothelial activation. These data suggest that the incorporation into the endothelium is cell-specific. The mechanism of cancer cell extravasation is quite different from immune cells, and this result could have impact on the cancer field.

In the next part of our work, we wanted to examine molecular mechanisms that might be involved in cancer metastasis. We decided to focus on the localization of RNAs. Deregulation of localization pathways has been proposed to play an important part in cancer metastasis. Furthermore, matrix stiffness increases as tumors progress and promotes a more metastatic phenotype. Thus, we focused on the localization of RNAs on substrates of varying stiffness. We focused on APC-dependent localization pathway in which RNAs are localized to protrusions in migrating fibroblasts at the ends of detyrosinated microtubules [8]. Since the APC-dependent pathway is well characterized in fibroblasts, we looked at RNA localization in this cell type. Interestingly, we found that on soft 1 kPa substrates, *Ddr2* RNA is diffuse throughout the cytoplasm and is localized to the periphery on stiffer 5 kPa and 280 kPa substrates. Since the localization of these RNAs to the cell periphery corresponds with areas of higher traction forces in cells, we hypothesized that cellular contractility influences RNA localization. To test this hypothesis, we used inhibitors of the Rho/ROCK pathway, one of the main regulators of cytoskeletal tension. We found that inhibiting contractility reduced RNA localization

and enhancing contractility induced RNA localization. These results indicate that actomyosin contractility through the Rho GTPase may regulate *Ddr2* RNA localization.

To further understand the mechanism of *Ddr2* RNA localization to cellular protrusions, we investigated the relationship between contractility and detyrosinated microtubules. *Ddr2* RNA is likely associated with detyrosinated microtubules in protrusions [8]. We found that microtubule detyrosination increases with substrate stiffness. Additionally, we found that inhibiting contractility reduces microtubule detyrosination and enhancing contractility induces microtubule detyrosination. Furthermore, we found that detyrosinated microtubules are required and sufficient for *Ddr2* RNA localization. We also found that when enhancing contractility with LPA and inhibiting Glu-MTs with parthenolide, that RNAs became mislocalized on soft substrates. When contractility was inhibited using blebbistatin, and cells were treated with TTL siRNA, we observed a recovery in RNA localization. These results indicated that contractility through modulation of the detyrosinated microtubule network affect RNA localization. Cell-substrate interactions are an important parameter to take into consideration. We saw here that it influences microtubule detyrosination and RNA localization, which may ultimately impact cell behavior. This work has relevance during disease pathologies such as cancer metastasis. As the microenvironment becomes stiffer, it may induce localization of these RNAs to cellular protrusions and promote a more metastatic phenotype.

5.2 Future Directions

In the scope of this work we have investigated two aspects of cancer metastasis: cancer cell incorporation/transmigration and localization of RNAs to cellular protrusions. There are many future studies that could be done to further understand the role of localized RNAs in cancer metastasis as well as the mechanisms of cancer cell transmigration. Below we have outlined some areas of future work that could build upon the data presented in this dissertation.

5.2.1 RNA localization in metastatic cells

In this dissertation, we have studied the role of RNA localization in NIH 3T3 cells as a model system to see how matrix stiffness influences localization. Future studies could use a breast cancer progression model to study RNA localization as a function of metastasis. The MCF10A cell series is a breast cancer progression model composed of four different cell lines representing different stages of pre-malignant to invasive transformation [215-217]. The series was established from the immortalized mammary epithelial cell line MCF10A, which were derived from a patient with fibrocystic disease [218]. The MCF10A cells were transformed with Ras to generate the pre-malignant MCF10At.1k that forms benign hyperplastic lesions after introduction into immune compromised mice. Passage of the MCF10At.1k through mice led to the isolation of the tumorigenic MCF10CA1h cells and the invasive, lung-colony forming MCF10CA1a cells. Both of these cell lines give rise to tumors within days of introduction into mice [217, 219, 220]. These two tumorigenic cell lines, CA1a and CA1h have an activating

mutation in *PIK3CA*, which is mutated in approximately 30% of human breast cancer cases [221, 222]. Thus, the MCF10A series represents an advantageous model for assessing how intrinsic mutations associated with breast cancer progression alter RNA localization in cells with a similar genetic background. Similarly, this model would allow for identification of RNA altercations during metastatic progression from normal breast epithelium (MCF10A) to invasive, lung colony forming MCF10CA1.

5.2.2 Mechanical stretching to induce localization

In this dissertation we have tested the role of actomyosin contractility on the localization of RNAs to cellular protrusions by using siRNA, pharmacological treatments, and by plating cells on substrates of varying stiffness. To more directly test the role of contractility and mechanical tension on RNA localization, cells could be mechanically stretched. For example, on soft substrates where RNAs are mislocalized, it would be interesting to see if mechanical tension is sufficient to induce localization. Likely, this would be accompanied by an increase in detyrosinated microtubules as well. When randomly oriented cells become exposed to cyclic uniaxial stretch, they respond by aligning with their long axis in the direction of minimum strain [223, 224]. The microtubule and actin cytoskeleton also both realign significantly during stretch. More specifically, detyrosinated microtubules form on the onset of cell polarization and are aligned with the axis of polarity in many cells types [225]. Thus, it is a reasonable hypothesis that mechanical stretching could induce localization on soft substrates through the formation of a polarized detyrosinated microtubule network.

5.2.3 RNA localization during transmigration and invasion

During transmigration, cells adhere to the endothelium, and protrusion formation through the endothelium and into the basement membrane drives cellular migration from the blood stream into the underlying tissue. Since protrusion formation is a fundamental step in transmigration, we believe localized mRNAs may be playing an intrinsic role in this process. There have been genome wide screens that have identified protrusion localized RNAs in metastatic cancer cells [75]. It would be interesting to test whether these localized RNAs change when migrating through the endothelium or through different types of endothelium. Additionally, it would also be interesting to observe RNAs during processes such as invadapodia formation and subsequent migration through the extracellular matrix. Furthermore, studies have shown that cancer cells are able to switch between forms of migration depending on their environmental conditions [226]. Mesenchymal type movement is characterized by elongated cellular morphology and requires extracellular proteolysis. In amoeboid movement, the cells undergo active blebbing driven by actomyosin contractility consistent with a mechanism of cells squeezing through voids to deform the matrix. Future studies could also investigate under which forms of migration RNAs localize and dissect their function.

5.2.4 Cancer cell migration below the endothelium

In Chapter 2, we showed that cancer cells incorporate into the endothelium. We hypothesize that this is a two-step process in which cancer cells first incorporate into the

endothelial monolayer before subsequent migration underneath the endothelium and into the basement membrane. These assays were performed on rigid glass substrates or on polyacrylamide gels to allow manipulation of the mechanical properties of the microenvironment. By using a collagen gel, it would allow subsequent migration underneath the monolayer. By doing this, it would allow us to observe if cancer cell do in fact incorporate into the monolayer first before transmigration. Another aspect that this might allow us to observe is whether the endothelium still becomes damaged during this process. We observed that cancer cell incorporation appeared to damage the endothelial monolayer, probably due to loss of cell-cell contacts. Perhaps because the tumor cells may rely more on proteases to break down the collagen gel during the incorporation process on a collagen gel, this would present less damage to the endothelial monolayer.

5.4 Significance and Conclusion

In most cases, the primary tumor is not dangerous unless it is localized in a compromising site, such as the brain. The major problem of cancer is its capability to spread to other sites. In fact, the vast majority of cancer mortality is due to cancer metastasis. A mechanistic understanding of the different stages of metastasis is necessary to improve current therapies or create new ones. In this dissertation we have studied mechanisms of cancer metastasis: transmigration and RNA localization. We found that cancer cell transmigration is inherently different from immune cell transmigration. It includes an additional step, which we call ‘incorporation’ into the endothelium. This step

in the transmigration process has not been observed before and is a novel finding that could have a significant impact on the cancer field. By finding out the specific mechanisms of cancer incorporation and transmigration, it may be possible to develop treatments to prevent these steps and inhibit the formation of secondary tumors.

On a more molecular level, we focused on the localization of RNAs to cellular protrusions and their potential implications during the early stages of metastatic transformation using fibroblasts as a model. Identifying factors that associate with either promoting cancer aggressiveness or suppressing it have the potential to serve as novel molecular targets for cancer therapy. RNA binding proteins and their subsequent RNA localization targets have been implicated in metastasis. In this dissertation we discovered important links between substrate stiffness, detyrosinated microtubules and RNA localization. The effect of the mechanical properties of the matrix on the localization of RNAs is an aspect that had not been studied. We found that matrix stiffness promotes the localization of RNAs. It is possible that by identifying RNAs and RNA binding proteins that correlate with cancer aggressiveness, that they can serve as new targets for cancer therapy. The field will benefit from further exploration on the mechanical properties of the matrix and how it affects RNA localization and it's relationship to cellular behavior and its relevance to cancer metastasis.

5.5 Author Contributions to Work

Chapter 2: Conceived and designed the experiments: Kimberly Strokam Susan Hamilla, and Helim Aranda-Espinioza. Performed the experiments: Kimberly Stroka and Susan

Hamilla Analyzed the data: Kimberly Stroka and Susan Hamilla. Contributed reagents/materials/analysis tools: Kimberly Stroka and Susan Hamilla. Wrote the paper: Kimberly Stroka, Susan Hamilla, and Helim Aranda-Espinoza

Chapter 3 and 4: Conceived and designed the experiments: Susan Hamilla, Helim Aranda-Espinoza and Voula Mili. Performed the experiments: Susan Hamilla. Analyzed the data: Susan Hamilla. Contributed reagents/materials/analysis tools: Susan Hamilla and Voula Mili.

Bibliography

1. Levental KR, Yu H, Kass L, Lakins JN, Egeblad M, Erler JT, et al. Matrix crosslinking forces tumor progression by enhancing integrin signaling. Cell. 2009;139(5):891-906. doi: 10.1016/j.cell.2009.10.027. PubMed PMID: 19931152; PubMed Central PMCID: PMCPMC2788004.

2. Lopez JI, Kang I, You WK, McDonald DM, Weaver VM. In situ force mapping of mammary gland transformation. Integr Biol (Camb). 2011;3(9):910-21. doi: 10.1039/c1ib00043h. PubMed PMID: 21842067; PubMed Central PMCID: PMCPMC3564969.

3. Parekh A, Ruppender NS, Branch KM, Sewell-Loftin MK, Lin J, Boyer PD, et al. Sensing and modulation of invadopodia across a wide range of rigidities. Biophys J. 2011;100(3):573-82. doi: 10.1016/j.bpj.2010.12.3733. PubMed PMID: 21281571; PubMed Central PMCID: PMCPMC3030182.

4. Ridley AJ, Schwartz MA, Burridge K, Firtel RA, Ginsberg MH, Borisy G, et al. Cell migration: integrating signals from front to back. Science. 2003;302(5651):1704-9. Epub 2003/12/06. doi: 10.1126/science.1092053
302/5651/1704 [pii]. PubMed PMID: 14657486.

5. Chicurel ME, Singer RH, Meyer CJ, Ingber DE. Integrin binding and mechanical tension induce movement of mRNA and ribosomes to focal adhesions. Nature. 1998;392(6677):730-3. doi: 10.1038/33719. PubMed PMID: 9565036.

6. Latham VM, Yu EH, Tullio AN, Adelstein RS, Singer RH. A Rho-dependent signaling pathway operating through myosin localizes beta-actin mRNA in fibroblasts. Current biology : CB. 2001;11(13):1010-6. PubMed PMID: 11470405.

7. Mingle LA, Okuhama NN, Shi J, Singer RH, Condeelis J, Liu G. Localization of all seven messenger RNAs for the actin-polymerization nucleator Arp2/3 complex in the protrusions of fibroblasts. J Cell Sci. 2005;118(Pt 11):2425-33. doi: 10.1242/jcs.02371. PubMed PMID: 15923655; PubMed Central PMCID: PMCPMC1283079.

8. Mili S, Moissoglu K, Macara IG. Genome-wide screen reveals APC-associated RNAs enriched in cell protrusions. Nature. 2008;453(7191):115-9. doi: 10.1038/nature06888. PubMed PMID: 18451862; PubMed Central PMCID: PMCPMC2782773.

9. de Hoog CL, Foster LJ, Mann M. RNA and RNA binding proteins participate in early stages of cell spreading through spreading initiation centers. Cell. 2004;117(5):649-62. PubMed PMID: 15163412.

10. Natkunam Y, Vainer G, Chen J, Zhao S, Marinelli RJ, Hammer AS, et al. Expression of the RNA-binding protein VICKZ in normal hematopoietic tissues and neoplasms. Haematologica. 2007;92(2):176-83. PubMed PMID: 17296566.

11. Shestakova EA, Singer RH, Condeelis J. The physiological significance of beta -actin mRNA localization in determining cell polarity and directional motility. Proc Natl Acad Sci U S A. 2001;98(13):7045-50. doi: 10.1073/pnas.121146098. PubMed PMID: 11416185; PubMed Central PMCID: PMCPMC34620.

12. Jemal A, Siegel R, Ward E, Hao Y, Xu J, Thun MJ. Cancer statistics, 2009. CA: a cancer journal for clinicians. 2009;59(4):225-49. doi: 10.3322/caac.20006. PubMed PMID: 19474385.

13. Weinberg RA. Cancer Biology and Therapy: the road ahead. Cancer biology & therapy. 2002;1(1):3. PubMed PMID: 12170761.

14. Muller WA. Mechanisms of leukocyte transendothelial migration. Annu Rev Pathol. 2011;6:323-44. doi: 10.1146/annurev-pathol-011110-130224. PubMed PMID: 21073340; PubMed Central PMCID: PMCPMC3628537.

15. Voura EB, Ramjeesingh RA, Montgomery AM, Siu CH. Involvement of integrin alpha(v)beta(3) and cell adhesion molecule L1 in transendothelial migration of melanoma cells. Mol Biol Cell. 2001;12(9):2699-710. PubMed PMID: 11553709; PubMed Central PMCID: PMCPMC59705.

16. Sandig M, Voura EB, Kalnins VI, Siu CH. Role of cadherins in the transendothelial migration of melanoma cells in culture. Cell Motil Cytoskeleton. 1997;38(4):351-64. doi: 10.1002/(SICI)1097-0169(1997)38:4<351::AID-CM5>3.0.CO;2-6. PubMed PMID: 9415377.

17. Tremblay PL, Auger FA, Huot J. Regulation of transendothelial migration of colon cancer cells by E-selectin-mediated activation of p38 and ERK MAP kinases. Oncogene. 2006;25(50):6563-73. doi: 10.1038/sj.onc.1209664. PubMed PMID: 16715142.

18. Burdick MM, Chu JT, Godar S, Sackstein R. HCELL is the major E- and L-selectin ligand expressed on LS174T colon carcinoma cells. The Journal of biological chemistry. 2006;281(20):13899-905. doi: 10.1074/jbc.M513617200. PubMed PMID: 16565092.

19. Hanley WD, Napier SL, Burdick MM, Schnaar RL, Sackstein R, Konstantopoulos K. Variant isoforms of CD44 are P- and L-selectin ligands on colon carcinoma cells. FASEB journal : official publication of the Federation of American Societies for Experimental Biology. 2006;20(2):337-9. doi: 10.1096/fj.05-4574fje. PubMed PMID: 16352650.

20. Napier SL, Healy ZR, Schnaar RL, Konstantopoulos K. Selectin ligand expression regulates the initial vascular interactions of colon carcinoma cells: the roles of CD44v and alternative sialofucosylated selectin ligands. The Journal of biological chemistry. 2007;282(6):3433-41. doi: 10.1074/jbc.M607219200. PubMed PMID: 17135256.

21. Strell C, Lang K, Niggemann B, Zaenker KS, Entschladen F. Surface molecules regulating rolling and adhesion to endothelium of neutrophil granulocytes and MDA-MB-468 breast carcinoma cells and their interaction. Cellular and molecular life sciences : CMLS. 2007;64(24):3306-16. doi: 10.1007/s00018-007-7402-6. PubMed PMID: 17994288.

22. Garofalo A, Chirivi RG, Foglieni C, Pigott R, Mortarini R, Martin-Padura I, et al. Involvement of the very late antigen 4 integrin on melanoma in interleukin 1-augmented experimental metastases. Cancer research. 1995;55(2):414-9. PubMed PMID: 7529137.

23. Okahara H, Yagita H, Miyake K, Okumura K. Involvement of very late activation antigen 4 (VLA-4) and vascular cell adhesion molecule 1 (VCAM-1) in tumor necrosis factor alpha enhancement of experimental metastasis. Cancer research. 1994;54(12):3233-6. PubMed PMID: 7515767.

24. Glinsky VV, Glinsky GV, Rittenhouse-Olson K, Huflejt ME, Glinskii OV, Deutscher SL, et al. The role of Thomsen-Friedenreich antigen in adhesion of human breast and prostate cancer cells to the endothelium. Cancer research. 2001;61(12):4851-7. PubMed PMID: 11406562.

25. Glinsky VV, Huflejt ME, Glinsky GV, Deutscher SL, Quinn TP. Effects of Thomsen-Friedenreich antigen-specific peptide P-30 on beta-galactoside-mediated homotypic aggregation and adhesion to the endothelium of MDA-MB-435 human breast carcinoma cells. Cancer research. 2000;60(10):2584-8. PubMed PMID: 10825125.

26. Stroka KM, Aranda-Espinoza H. Endothelial cell substrate stiffness influences neutrophil transmigration via myosin light chain kinase-dependent cell contraction. Blood. 2011;118(6):1632-40. doi: 10.1182/blood-2010-11-321125. PubMed PMID: 21652678; PubMed Central PMCID: PMCPMC3156049.

27. Stroka KM, Levitan I, Aranda-Espinoza H. OxLDL and substrate stiffness promote neutrophil transmigration by enhanced endothelial cell contractility and ICAM-1. J Biomech. 2012;45(10):1828-34. doi: 10.1016/j.jbiomech.2012.04.011. PubMed PMID: 22560286; PubMed Central PMCID: PMCPMC3376185.

28. Bao G, Suresh S. Cell and molecular mechanics of biological materials. Nature materials. 2003;2(11):715-25. doi: 10.1038/nmat1001. PubMed PMID: 14593396.

29. Wakatsuki T, Kolodney MS, Zahalak GI, Elson EL. Cell mechanics studied by a reconstituted model tissue. Biophys J. 2000;79(5):2353-68. doi: 10.1016/S0006-3495(00)76481-2. PubMed PMID: 11053115; PubMed Central PMCID: PMC1301123.

30. Discher DE, Janmey P, Wang YL. Tissue cells feel and respond to the stiffness of their substrate. Science. 2005;310(5751):1139-43. doi: 10.1126/science.1116995. PubMed PMID: 16293750.

31. Pelham RJ, Jr., Wang Y. Cell locomotion and focal adhesions are regulated by substrate flexibility. Proc Natl Acad Sci U S A. 1997;94(25):13661-5. PubMed PMID: 9391082; PubMed Central PMCID: PMCPMC28362.

32. Lo CM, Wang HB, Dembo M, Wang YL. Cell movement is guided by the rigidity of the substrate. Biophys J. 2000;79(1):144-52. PubMed PMID: WOS:000088048500011.

33. Peyton SR, Putnam AJ. Extracellular matrix rigidity governs smooth muscle cell motility in a biphasic fashion. Journal of cellular physiology. 2005;204(1):198-209. doi: 10.1002/jcp.20274. PubMed PMID: 15669099.

34. Harley BA, Kim HD, Zaman MH, Yannas IV, Lauffenburger DA, Gibson LJ. Microarchitecture of three-dimensional scaffolds influences cell migration behavior via junction interactions. Biophys J. 2008;95(8):4013-24. doi: 10.1529/biophysj.107.122598. PubMed PMID: 18621811; PubMed Central PMCID: PMC2553126.

35. Stroka KM, Aranda-Espinoza H. Effects of Morphology vs. Cell-Cell Interactions on Endothelial Cell Stiffness. Cell Mol Bioeng. 2011;4(1):9-27. doi: 10.1007/s12195-010-0142-y. PubMed PMID: 21359128; PubMed Central PMCID: PMCPMC3044329.

36. Stroka KM, Aranda-Espinoza H. Neutrophils display biphasic relationship between migration and substrate stiffness. Cell Motil Cytoskeleton. 2009;66(6):328-41. doi: 10.1002/cm.20363. PubMed PMID: 19373775.

37. Chrzanowska-Wodnicka M, Burridge K. Rho-stimulated contractility drives the formation of stress fibers and focal adhesions. J Cell Biol. 1996;133(6):1403-15. PubMed PMID: 8682874; PubMed Central PMCID: PMCPMC2120895.

38. Griffin MA, Sen S, Sweeney HL, Discher DE. Adhesion-contractile balance in myocyte differentiation. J Cell Sci. 2004;117(Pt 24):5855-63. doi: 10.1242/jcs.01496. PubMed PMID: 15522893.

39. Riveline D, Zamir E, Balaban NQ, Schwarz US, Ishizaki T, Narumiya S, et al. Focal contacts as mechanosensors: externally applied local mechanical force induces growth of focal contacts by an mDia1-dependent and ROCK-independent mechanism. The Journal of cell biology. 2001;153(6):1175-86. PubMed PMID: 11402062; PubMed Central PMCID: PMC2192034.

40. Alenghat FJ, Ingber DE. Mechanotransduction: all signals point to cytoskeleton, matrix, and integrins. Science's STKE : signal transduction knowledge environment. 2002;2002(119):pe6. doi: 10.1126/stke.2002.119.pe6. PubMed PMID: 11842240.

41. Hinz B, Celetta G, Tomasek JJ, Gabbiani G, Chaponnier C. Alpha-smooth muscle actin expression upregulates fibroblast contractile activity. Molecular biology of the cell. 2001;12(9):2730-41. PubMed PMID: 11553712; PubMed Central PMCID: PMC59708.

42. Friedl P, Alexander S. Cancer invasion and the microenvironment: plasticity and reciprocity. Cell. 2011;147(5):992-1009. doi: 10.1016/j.cell.2011.11.016. PubMed PMID: 22118458.

43. Kostic A, Lynch CD, Sheetz MP. Differential matrix rigidity response in breast cancer cell lines correlates with the tissue tropism. PloS one. 2009;4(7):e6361. doi: 10.1371/journal.pone.0006361. PubMed PMID: 19626122; PubMed Central PMCID: PMC2709918.

44. Tilghman RW, Blais EM, Cowan CR, Sherman NE, Grigera PR, Jeffery ED, et al. Matrix rigidity regulates cancer cell growth by modulating cellular metabolism and protein synthesis. PloS one. 2012;7(5):e37231. doi: 10.1371/journal.pone.0037231. PubMed PMID: 22623999; PubMed Central PMCID: PMC3356407.

45. Tilghman RW, Cowan CR, Mih JD, Koryakina Y, Gioeli D, Slack-Davis JK, et al. Matrix rigidity regulates cancer cell growth and cellular phenotype. PloS one. 2010;5(9):e12905. doi: 10.1371/journal.pone.0012905. PubMed PMID: 20886123; PubMed Central PMCID: PMC2944843.

46. Mardakheh FK, Paul A, Kumper S, Sadok A, Paterson H, McCarthy A, et al. Global Analysis of mRNA, Translation, and Protein Localization: Local Translation Is a Key Regulator of Cell Protrusions. Developmental cell. 2015;35(3):344-57. doi: 10.1016/j.devcel.2015.10.005. PubMed PMID: 26555054; PubMed Central PMCID: PMC4643311.

47. Liao G, Simone B, Liu G. Mis-localization of Arp2 mRNA impairs persistence of directional cell migration. Exp Cell Res. 2011;317(6):812-22. doi: 10.1016/j.yexcr.2010.12.002. PubMed PMID: 21146522; PubMed Central PMCID: PMCPMC3057629.

48. Wang G, Huang Z, Liu X, Huang W, Chen S, Zhou Y, et al. IMP1 suppresses breast tumor growth and metastasis through the regulation of its target mRNAs. Oncotarget. 2016. doi: 10.18632/oncotarget.7464. PubMed PMID: 26910917.

49. Gu W, Pan F, Singer RH. Blocking beta-catenin binding to the ZBP1 promoter represses ZBP1 expression, leading to increased proliferation and migration of metastatic breast-cancer cells. J Cell Sci. 2009;122(Pt 11):1895-905. doi: 10.1242/jcs.045278. PubMed PMID: 19461076; PubMed Central PMCID: PMCPMC2684840.

50. Jeffery WR, Tomlinson CR, Brodeur RD. Localization of actin messenger RNA during early ascidian development. Dev Biol. 1983;99(2):408-17. PubMed PMID: 6194032.

51. Lecuyer E, Yoshida H, Parthasarathy N, Alm C, Babak T, Cerovina T, et al. Global analysis of mRNA localization reveals a prominent role in organizing cellular architecture and function. Cell. 2007;131(1):174-87. doi: 10.1016/j.cell.2007.08.003. PubMed PMID: 17923096.

52. Eberwine J, Belt B, Kacharmina JE, Miyashiro K. Analysis of subcellularly localized mRNAs using in situ hybridization, mRNA amplification, and expression profiling. Neurochem Res. 2002;27(10):1065-77. PubMed PMID: 12462405.

53. Martin KC, Zukin RS. RNA trafficking and local protein synthesis in dendrites: an overview. J Neurosci. 2006;26(27):7131-4. doi: 10.1523/JNEUROSCI.1801-06.2006. PubMed PMID: 16822966.

54. Blower MD, Feric E, Weis K, Heald R. Genome-wide analysis demonstrates conserved localization of messenger RNAs to mitotic microtubules. J Cell Biol. 2007;179(7):1365-73. doi: 10.1083/jcb.200705163. PubMed PMID: 18166649; PubMed Central PMCID: PMCPMC2373496.

55. Besse F, Ephrussi A. Translational control of localized mRNAs: restricting protein synthesis in space and time. Nat Rev Mol Cell Biol. 2008;9(12):971-80. doi: 10.1038/nrm2548. PubMed PMID: 19023284.

56. Jambhekar A, Derisi JL. Cis-acting determinants of asymmetric, cytoplasmic RNA transport. RNA. 2007;13(5):625-42. doi: 10.1261/rna.262607. PubMed PMID: 17449729; PubMed Central PMCID: PMCPMC1852811.

57. Chao JA, Patskovsky Y, Patel V, Levy M, Almo SC, Singer RH. ZBP1 recognition of beta-actin zipcode induces RNA looping. Genes Dev. 2010;24(2):148-58. doi: 10.1101/gad.1862910. PubMed PMID: 20080952; PubMed Central PMCID: PMCPMC2807350.

58. Patel VL, Mitra S, Harris R, Buxbaum AR, Lionnet T, Brenowitz M, et al. Spatial arrangement of an RNA zipcode identifies mRNAs under post-transcriptional control. Genes Dev. 2012;26(1):43-53. doi: 10.1101/gad.177428.111. PubMed PMID: 22215810; PubMed Central PMCID: PMCPMC3258965.

59. Ding D, Lipshitz HD. Localized RNAs and their functions. Bioessays. 1993;15(10):651-8. doi: 10.1002/bies.950151004. PubMed PMID: 7506023.

60. Forrest KM, Gavis ER. Live imaging of endogenous RNA reveals a diffusion and entrapment mechanism for nanos mRNA localization in Drosophila. Curr Biol. 2003;13(14):1159-68. PubMed PMID: 12867026.

61. Carson JH, Cui H, Barbarese E. The balance of power in RNA trafficking. Curr Opin Neurobiol. 2001;11(5):558-63. PubMed PMID: 11595488.

62. Bullock SL, Nicol A, Gross SP, Zicha D. Guidance of bidirectional motor complexes by mRNA cargoes through control of dynein number and activity. Curr Biol. 2006;16(14):1447-52. doi: 10.1016/j.cub.2006.05.055. PubMed PMID: 16860745.

63. Dynes JL, Steward O. Dynamics of bidirectional transport of Arc mRNA in neuronal dendrites. J Comp Neurol. 2007;500(3):433-47. doi: 10.1002/cne.21189. PubMed PMID: 17120280.

64. Krauss J, Lopez de Quinto S, Nusslein-Volhard C, Ephrussi A. Myosin-V regulates oskar mRNA localization in the Drosophila oocyte. Curr Biol. 2009;19(12):1058-63. doi: 10.1016/j.cub.2009.04.062. PubMed PMID: 19481457.

65. King ML, Messitt TJ, Mowry KL. Putting RNAs in the right place at the right time: RNA localization in the frog oocyte. Biol Cell. 2005;97(1):19-33. doi: 10.1042/BC20040067. PubMed PMID: 15601255.

66. Becalska AN, Gavis ER. Lighting up mRNA localization in Drosophila oogenesis. Development. 2009;136(15):2493-503. doi: 10.1242/dev.032391. PubMed PMID: 19592573; PubMed Central PMCID: PMCPMC2709059.

67. Heym RG, Niessing D. Principles of mRNA transport in yeast. Cell Mol Life Sci. 2012;69(11):1843-53. doi: 10.1007/s00018-011-0902-4. PubMed PMID: 22159587; PubMed Central PMCID: PMCPMC3350770.

68. Weil TT, Forrest KM, Gavis ER. Localization of bicoid mRNA in late oocytes is maintained by continual active transport. Dev Cell. 2006;11(2):251-62. doi: 10.1016/j.devcel.2006.06.006. PubMed PMID: 16890164.

69. Huttelmaier S, Zenklusen D, Lederer M, Dictenberg J, Lorenz M, Meng X, et al. Spatial regulation of beta-actin translation by Src-dependent phosphorylation of ZBP1. Nature. 2005;438(7067):512-5. doi: 10.1038/nature04115. PubMed PMID: 16306994.

70. Medioni C, Mowry K, Besse F. Principles and roles of mRNA localization in animal development. Development. 2012;139(18):3263-76. doi: 10.1242/dev.078626. PubMed PMID: 22912410; PubMed Central PMCID: PMCPMC3424039.

71. Small JV, Resch GP. The comings and goings of actin: coupling protrusion and retraction in cell motility. Curr Opin Cell Biol. 2005;17(5):517-23. doi: 10.1016/j.ceb.2005.08.004. PubMed PMID: 16099152.

72. Condeelis J, Singer RH. How and why does beta-actin mRNA target? Biol Cell. 2005;97(1):97-110. doi: 10.1042/BC20040063. PubMed PMID: 15601261.

73. Poon MM, Choi SH, Jamieson CA, Geschwind DH, Martin KC. Identification of process-localized mRNAs from cultured rodent hippocampal neurons. J Neurosci. 2006;26(51):13390-9. doi: 10.1523/JNEUROSCI.3432-06.2006. PubMed PMID: 17182790.

74. Stuart HC, Jia Z, Messenberg A, Joshi B, Underhill TM, Moukhles H, et al. Localized Rho GTPase activation regulates RNA dynamics and compartmentalization in tumor cell protrusions. J Biol Chem. 2008;283(50):34785-95. doi:

10.1074/jbc.M804014200. PubMed PMID: 18845542; PubMed Central PMCID: PMCPMC3259890.

75. Jakobsen KR, Sorensen E, Brondum KK, Daugaard TF, Thomsen R, Nielsen AL. Direct RNA sequencing mediated identification of mRNA localized in protrusions of human MDA-MB-231 metastatic breast cancer cells. J Mol Signal. 2013;8(1):9. doi: 10.1186/1750-2187-8-9. PubMed PMID: 24004954; PubMed Central PMCID: PMCPMC3844448.

76. Thomsen R, Lade Nielsen A. A Boyden chamber-based method for characterization of astrocyte protrusion localized RNA and protein. Glia. 2011;59(11):1782-92. doi: 10.1002/glia.21223. PubMed PMID: 21858875.

77. Kislauskis EH, Zhu X, Singer RH. Sequences responsible for intracellular localization of beta-actin messenger RNA also affect cell phenotype. J Cell Biol. 1994;127(2):441-51. PubMed PMID: 7929587; PubMed Central PMCID: PMCPMC2120214.

78. Lawrence JB, Singer RH. Intracellular localization of messenger RNAs for cytoskeletal proteins. Cell. 1986;45(3):407-15. PubMed PMID: 3698103.

79. Bassell GJ, Singer RH. Neuronal RNA localization and the cytoskeleton. Results Probl Cell Differ. 2001;34:41-56. PubMed PMID: 11288678.

80. Latham VM, Jr., Kislauskis EH, Singer RH, Ross AF. Beta-actin mRNA localization is regulated by signal transduction mechanisms. J Cell Biol. 1994;126(5):1211-9. PubMed PMID: 8063858; PubMed Central PMCID: PMCPMC2120163.

81. Gu W, Pan F, Zhang H, Bassell GJ, Singer RH. A predominantly nuclear protein affecting cytoplasmic localization of beta-actin mRNA in fibroblasts and neurons. J Cell Biol. 2002;156(1):41-51. doi: 10.1083/jcb.200105133. PubMed PMID: 11781334; PubMed Central PMCID: PMCPMC2173579.

82. Oleynikov Y, Singer RH. Real-time visualization of ZBP1 association with beta-actin mRNA during transcription and localization. Curr Biol. 2003;13(3):199-207. PubMed PMID: 12573215.

83. Song T, Zheng Y, Wang Y, Katz Z, Liu X, Chen S, et al. Specific interaction of KIF11 with ZBP1 regulates the transport of beta-actin mRNA and cell motility. J Cell Sci. 2015;128(5):1001-10. doi: 10.1242/jcs.161679. PubMed PMID: 25588836; PubMed Central PMCID: PMCPMC4342582.

84. Ma B, Savas JN, Yu MS, Culver BP, Chao MV, Tanese N. Huntingtin mediates dendritic transport of beta-actin mRNA in rat neurons. Sci Rep. 2011;1:140. doi: 10.1038/srep00140. PubMed PMID: 22355657; PubMed Central PMCID: PMCPMC3216621.

85. Liu G, Grant WM, Persky D, Latham VM, Jr., Singer RH, Condeelis J. Interactions of elongation factor 1alpha with F-actin and beta-actin mRNA: implications for anchoring mRNA in cell protrusions. Molecular biology of the cell. 2002;13(2):579-92. doi: 10.1091/mbc.01-03-0140. PubMed PMID: 11854414; PubMed Central PMCID: PMC65651.

86. Welch MD, DePace AH, Verma S, Iwamatsu A, Mitchison TJ. The human Arp2/3 complex is composed of evolutionarily conserved subunits and is localized to cellular regions of dynamic actin filament assembly. The Journal of cell biology. 1997;138(2):375-84. PubMed PMID: 9230079; PubMed Central PMCID: PMC2138188.

87. Mingle LA, Bonamy G, Barroso M, Liao G, Liu G. LPA-induced mutually exclusive subcellular localization of active RhoA and Arp2 mRNA revealed by sequential FRET and FISH. Histochemistry and cell biology. 2009;132(1):47-58. doi: 10.1007/s00418-009-0589-x. PubMed PMID: 19365637; PubMed Central PMCID: PMC2753266.

88. Yasuda K, Zhang H, Loiselle D, Haystead T, Macara IG, Mili S. The RNA-binding protein Fus directs translation of localized mRNAs in APC-RNP granules. J Cell Biol. 2013;203(5):737-46. doi: 10.1083/jcb.201306058. PubMed PMID: 24297750; PubMed Central PMCID: PMCPMC3857475.

89. Weber E, Berta G, Tousson A, St John P, Green MW, Gopalokrishnan U, et al. Expression and polarized targeting of a rab3 isoform in epithelial cells. The Journal of cell biology. 1994;125(3):583-94. PubMed PMID: 8175882; PubMed Central PMCID: PMC2119989.

90. Zahraoui A, Joberty G, Arpin M, Fontaine JJ, Hellio R, Tavitian A, et al. A small rab GTPase is distributed in cytoplasmic vesicles in non polarized cells but colocalizes with the tight junction marker ZO-1 in polarized epithelial cells. The Journal of cell biology. 1994;124(1-2):101-15. PubMed PMID: 8294494; PubMed Central PMCID: PMC2119893.

91. Marzesco AM, Dunia I, Pandjaitan R, Recouvreur M, Dauzonne D, Benedetti EL, et al. The small GTPase Rab13 regulates assembly of functional tight junctions in epithelial cells. Molecular biology of the cell. 2002;13(6):1819-31. doi: 02-02-0029. PubMed PMID: 12058051; PubMed Central PMCID: PMC117606.

92. Kanda I, Nishimura N, Nakatsuji H, Yamamura R, Nakanishi H, Sasaki T. Involvement of Rab13 and JRAB/MICAL-L2 in epithelial cell scattering. Oncogene. 2008;27(12):1687-95. doi: 10.1038/sj.onc.1210812. PubMed PMID: 17891173.

93. Ioannou MS, Bell ES, Girard M, Chaineau M, Hamlin JN, Daubaras M, et al. DENND2B activates Rab13 at the leading edge of migrating cells and promotes metastatic behavior. J Cell Biol. 2015;208(5):629-48. doi: 10.1083/jcb.201407068. PubMed PMID: 25713415; PubMed Central PMCID: PMCPMC4347646.

94. Setzer SV, Calkins CC, Garner J, Summers S, Green KJ, Kowalczyk AP. Comparative analysis of armadillo family proteins in the regulation of a431 epithelial cell junction assembly, adhesion and migration. The Journal of investigative dermatology. 2004;123(3):426-33. doi: 10.1111/j.0022-202X.2004.23319.x. PubMed PMID: 15304078.

95. Wolf A, Keil R, Gotzl O, Mun A, Schwarze K, Lederer M, et al. The armadillo protein p0071 regulates Rho signalling during cytokinesis. Nature cell biology. 2006;8(12):1432-40. doi: 10.1038/ncb1504. PubMed PMID: 17115030.

96. Hatzfeld M. Plakophilins: Multifunctional proteins or just regulators of desmosomal adhesion? Bba-Mol Cell Res. 2007;1773(1):69-77. doi: Doi 10.1016/J.Bbamcr.2006.04.009. PubMed PMID: WOS:000243733900008.

97. Papagerakis S, Shabana AH, Depondt J, Gehanno P, Forest N. Immunohistochemical localization of plakophilins (PKP1, PKP2, PKP3, and p0071) in primary oropharyngeal tumors: correlation with clinical parameters. Human pathology. 2003;34(6):565-72. PubMed PMID: 12827610.

98. Dusek RL, Attardi LD. Desmosomes: new perpetrators in tumour suppression. Nature reviews Cancer. 2011;11(5):317-23. doi: 10.1038/nrc3051. PubMed PMID: 21508970; PubMed Central PMCID: PMC3799918.

99. Lemeer S, Bluwstein A, Wu Z, Leberfinger J, Muller K, Kramer K, et al. Phosphotyrosine mediated protein interactions of the discoidin domain receptor 1. Journal of proteomics. 2012;75(12):3465-77. doi: 10.1016/j.jprot.2011.10.007. PubMed PMID: 22057045.

100. Vogel WF, Abdulhussein R, Ford CE. Sensing extracellular matrix: an update on discoidin domain receptor function. Cellular signalling. 2006;18(8):1108-16. doi: 10.1016/j.cellsig.2006.02.012. PubMed PMID: 16626936.

101. Su J, Yu JT, Ren TT, Zhang W, Zhang YQ, Liu XP, et al. Discoidin domain receptor 2 is associated with the increased expression of matrix metalloproteinase-13 in synovial fibroblasts of rheumatoid arthritis. Mol Cell Biochem. 2009;330(1-2):141-52. doi: Doi 10.1007/S11010-009-0127-0. PubMed PMID: WOS:000270687500015.

102. Ruiz PA, Jarai G. Collagen I Induces Discoidin Domain Receptor (DDR) 1 Expression through DDR2 and a JAK2-ERK1/2-mediated Mechanism in Primary Human Lung Fibroblasts. Journal of Biological Chemistry. 2011;286(15):12912-23. doi: Doi 10.1074/Jbc.M110.143693. PubMed PMID: WOS:000289282200011.

103. Vonk LA, Doulabi BZ, Huang CL, Helder MN, Everts V, Bank RA. Collagen-induced expression of collagenase-3 by primary chondrocytes is mediated by integrin alpha 1 and discoidin domain receptor 2: a protein kinase C-dependent pathway. Rheumatology. 2011;50(3):463-72. doi: Doi 10.1093/Rheumatology/Keq305. PubMed PMID: WOS:000287745600006.

104. Zhang K, Corsa CA, Ponik SM, Prior JL, Piwnica-Worms D, Eliceiri KW, et al. The collagen receptor discoidin domain receptor 2 stabilizes SNAIL1 to facilitate breast cancer metastasis. Nature cell biology. 2013;15(6):677-87. doi: 10.1038/ncb2743. PubMed PMID: 23644467; PubMed Central PMCID: PMC3794710.

105. Afonso PV, McCann CP, Kapnick SM, Parent CA. Discoidin domain receptor 2 regulates neutrophil chemotaxis in 3D collagen matrices. Blood. 2013;121(9):1644-50. doi: 10.1182/blood-2012-08-451575. PubMed PMID: 23233663; PubMed Central PMCID: PMC3587327.

106. Fallini C, Zhang H, Su Y, Silani V, Singer RH, Rossoll W, et al. The survival of motor neuron (SMN) protein interacts with the mRNA-binding protein HuD and regulates localization of poly(A) mRNA in primary motor neuron axons. The Journal of neuroscience : the official journal of the Society for Neuroscience. 2011;31(10):3914-25. doi: 10.1523/JNEUROSCI.3631-10.2011. PubMed PMID: 21389246; PubMed Central PMCID: PMC3070748.

107. Rossoll W, Jablonka S, Andreassi C, Kroning AK, Karle K, Monani UR, et al. Smn, the spinal muscular atrophy-determining gene product, modulates axon growth and localization of beta-actin mRNA in growth cones of motoneurons. The Journal of cell biology. 2003;163(4):801-12. doi: 10.1083/jcb.200304128. PubMed PMID: 14623865; PubMed Central PMCID: PMC2173668.

108. Bassell GJ, Warren ST. Fragile X syndrome: loss of local mRNA regulation alters synaptic development and function. Neuron. 2008;60(2):201-14. doi: 10.1016/j.neuron.2008.10.004. PubMed PMID: 18957214; PubMed Central PMCID: PMCPMC3691995.

109. Dictenberg JB, Swanger SA, Antar LN, Singer RH, Bassell GJ. A direct role for FMRP in activity-dependent dendritic mRNA transport links filopodial-spine morphogenesis to fragile X syndrome. Developmental cell. 2008;14(6):926-39. doi: 10.1016/j.devcel.2008.04.003. PubMed PMID: 18539120; PubMed Central PMCID: PMC2453222.

110. Kao DI, Aldridge GM, Weiler IJ, Greenough WT. Altered mRNA transport, docking, and protein translation in neurons lacking fragile X mental retardation protein. Proceedings of the National Academy of Sciences of the United States of America. 2010;107(35):15601-6. doi: 10.1073/pnas.1010564107. PubMed PMID: 20713728; PubMed Central PMCID: PMC2932564.

111. Nagaoka K, Udagawa T, Richter JD. CPEB-mediated ZO-1 mRNA localization is required for epithelial tight-junction assembly and cell polarity. Nat Commun. 2012;3. doi: Artn 675
Doi 10.1038/Ncomms1678. PubMed PMID: WOS:000302060100016.

112. Martin TA, Watkins G, Mansel RE, Jiang WG. Loss of tight junction plaque molecules in breast cancer tissues is associated with a poor prognosis in patients with breast cancer. Eur J Cancer. 2004;40(18):2717-25. doi: Doi 10.1016/J.Ejca.2004.08.008. PubMed PMID: WOS:000225993400018.

113. Ioannidis P, Mahaira L, Papadopoulou A, Teixeira MR, Heim S, Andersen JA, et al. CRD-BP: a c-Myc mRNA stabilizing protein with an oncofetal pattern of expression. Anticancer research. 2003;23(3A):2179-83. PubMed PMID: 12894594.

114. Tessier CR, Doyle GA, Clark BA, Pitot HC, Ross J. Mammary tumor induction in transgenic mice expressing an RNA-binding protein. Cancer research. 2004;64(1):209-14. PubMed PMID: 14729626.

115. Wang T, Hopkins D, Schmidt C, Silva S, Houghton R, Takita H, et al. Identification of genes differentially over-expressed in lung squamous cell carcinoma using combination of cDNA subtraction and microarray analysis. Oncogene. 2000;19(12):1519-28. doi: 10.1038/sj.onc.1203457. PubMed PMID: 10734311.

116. Hwang YS, Xianglan Z, Park KK, Chung WY. Functional invadopodia formation through stabilization of the PDPN transcript by IMP-3 and cancer-stromal crosstalk for PDPN expression. Carcinogenesis. 2012;33(11):2135-46. doi: 10.1093/carcin/bgs258. PubMed PMID: 22859271.

117. Vikesaa J, Hansen TV, Jonson L, Borup R, Wewer UM, Christiansen J, et al. RNA-binding IMPs promote cell adhesion and invadopodia formation. The EMBO journal. 2006;25(7):1456-68. doi: 10.1038/sj.emboj.7601039. PubMed PMID: 16541107; PubMed Central PMCID: PMC1440323.

118. Magiera MM, Janke C. Post-translational modifications of tubulin. Curr Biol. 2014;24(9):R351-4. doi: 10.1016/j.cub.2014.03.032. PubMed PMID: 24801181.

119. Janke C. The tubulin code: molecular components, readout mechanisms, and functions. J Cell Biol. 2014;206(4):461-72. doi: 10.1083/jcb.201406055. PubMed PMID: 25135932; PubMed Central PMCID: PMCPMC4137062.

120. Szyk A, Piszczek G, Roll-Mecak A. Tubulin tyrosine ligase and stathmin compete for tubulin binding in vitro. J Mol Biol. 2013;425(14):2412-4. doi: 10.1016/j.jmb.2013.04.017. PubMed PMID: 23624152; PubMed Central PMCID: PMCPMC4201589.

121. Prota AE, Magiera MM, Kuijpers M, Bargsten K, Frey D, Wieser M, et al. Structural basis of tubulin tyrosination by tubulin tyrosine ligase. J Cell Biol. 2013;200(3):259-70. doi: 10.1083/jcb.201211017. PubMed PMID: 23358242; PubMed Central PMCID: PMCPMC3563685.

122. Khawaja S, Gundersen GG, Bulinski JC. Enhanced stability of microtubules enriched in detyrosinated tubulin is not a direct function of detyrosination level. J Cell

Biol. 1988;106(1):141-9. PubMed PMID: 3276710; PubMed Central PMCID: PMCPMC2114950.

123. Webster DR, Wehland J, Weber K, Borisy GG. Detyrosination of alpha tubulin does not stabilize microtubules in vivo. J Cell Biol. 1990;111(1):113-22. PubMed PMID: 1973168; PubMed Central PMCID: PMCPMC2116167.

124. Cook TA, Nagasaki T, Gundersen GG. Rho guanosine triphosphatase mediates the selective stabilization of microtubules induced by lysophosphatidic acid. J Cell Biol. 1998;141(1):175-85. PubMed PMID: 9531557; PubMed Central PMCID: PMCPMC2132729.

125. Nagasaki T, Gundersen GG. Depletion of lysophosphatidic acid triggers a loss of oriented detyrosinated microtubules in motile fibroblasts. J Cell Sci. 1996;109 (Pt 10):2461-9. PubMed PMID: 8923207.

126. Jiang K, Akhmanova A. Microtubule tip-interacting proteins: a view from both ends. Curr Opin Cell Biol. 2011;23(1):94-101. doi: 10.1016/j.ceb.2010.08.008. PubMed PMID: 20817499.

127. Bieling P, Kandels-Lewis S, Telley IA, van Dijk J, Janke C, Surrey T. CLIP-170 tracks growing microtubule ends by dynamically recognizing composite EB1/tubulin-binding sites. J Cell Biol. 2008;183(7):1223-33. doi: 10.1083/jcb.200809190. PubMed PMID: 19103809; PubMed Central PMCID: PMCPMC2606963.

128. Roll-Mecak A, Vale RD. Structural basis of microtubule severing by the hereditary spastic paraplegia protein spastin. Nature. 2008;451(7176):363-7. doi: 10.1038/nature06482. PubMed PMID: 18202664; PubMed Central PMCID: PMCPMC2882799.

129. Liao G, Gundersen GG. Kinesin is a candidate for cross-bridging microtubules and intermediate filaments. Selective binding of kinesin to detyrosinated tubulin and vimentin. J Biol Chem. 1998;273(16):9797-803. PubMed PMID: 9545318.

130. Langley RR, Fidler IJ. Tumor cell-organ microenvironment interactions in the pathogenesis of cancer metastasis. Endocr Rev. 2007;28(3):297-321. Epub 2007/04/06. doi: er.2006-0027 [pii]
10.1210/er.2006-0027. PubMed PMID: 17409287.

131. Steeg PS. Tumor metastasis: mechanistic insights and clinical challenges. Nat Med. 2006;12(8):895-904. Epub 2006/08/08. doi: nm1469 [pii]
10.1038/nm1469. PubMed PMID: 16892035.

132. Weiss L, Grundmann E, Torhorst J, Hartveit F, Moberg I, Eder M, et al. Haematogenous metastatic patterns in colonic carcinoma: an analysis of 1541 necropsies. J Pathol. 1986;150(3):195-203. Epub 1986/11/01. doi: 10.1002/path.1711500308. PubMed PMID: 3806280.

133. Mukhopadhyay R, Theriault RL, Price JE. Increased levels of alpha6 integrins are associated with the metastatic phenotype of human breast cancer cells. Clin Exp Metastasis. 1999;17(4):325-32. Epub 1999/11/02. PubMed PMID: 10545019.

134. Owens DM, Romero MR, Gardner C, Watt FM. Suprabasal alpha6beta4 integrin expression in epidermis results in enhanced tumourigenesis and disruption of TGFbeta signalling. J Cell Sci. 2003;116(Pt 18):3783-91. Epub 2003/08/07. doi: 10.1242/jcs.00725
jcs.00725 [pii]. PubMed PMID: 12902406.

135. Ramaswamy S, Ross KN, Lander ES, Golub TR. A molecular signature of metastasis in primary solid tumors. Nat Genet. 2003;33(1):49-54. Epub 2002/12/07. doi: 10.1038/ng1060
ng1060 [pii]. PubMed PMID: 12469122.

136. Jones PA, Baylin SB. The fundamental role of epigenetic events in cancer. Nat Rev Genet. 2002;3(6):415-28. Epub 2002/06/04. doi: 10.1038/nrg816
nrg816 [pii]. PubMed PMID: 12042769.

137. Chuang HY, Lee E, Liu YT, Lee D, Ideker T. Network-based classification of breast cancer metastasis. Mol Syst Biol. 2007;3:140. Epub 2007/10/18. doi: msb4100180 [pii]
10.1038/msb4100180. PubMed PMID: 17940530.

138. Khuon S, Liang L, Dettman RW, Sporn PH, Wysolmerski RB, Chew TL. Myosin light chain kinase mediates transcellular intravasation of breast cancer cells through the underlying endothelial cells: a three-dimensional FRET study. J Cell Sci. 2010;123(Pt 3):431-40. doi: 10.1242/jcs.053793. PubMed PMID: 20067998; PubMed Central PMCID: PMCPMC2816188.

139. Weis S, Cui J, Barnes L, Cheresh D. Endothelial barrier disruption by VEGF-mediated Src activity potentiates tumor cell extravasation and metastasis. J Cell Biol. 2004;167(2):223-9. Epub 2004/10/27. doi: jcb.200408130 [pii]
10.1083/jcb.200408130. PubMed PMID: 15504909.

140. Zhang Q, Liu T, Qin J. A microfluidic-based device for study of transendothelial invasion of tumor aggregates in realtime. Lab Chip. 2012;12(16):2837-42. Epub 2012/06/01. doi: 10.1039/c2lc00030j. PubMed PMID: 22648473.

141. Heyder C, Gloria-Maercker E, Entschladen F, Hatzmann W, Niggemann B, Zanker KS, et al. Realtime visualization of tumor cell/endothelial cell interactions during transmigration across the endothelial barrier. J Cancer Res Clin Oncol. 2002;128(10):533-8. Epub 2002/10/18. doi: 10.1007/s00432-002-0377-7. PubMed PMID: 12384796.

142. Fazakas C, Wilhelm I, Nagyoszi P, Farkas AE, Hasko J, Molnar J, et al. Transmigration of melanoma cells through the blood-brain barrier: role of endothelial

tight junctions and melanoma-released serine proteases. PLoS One. 2011;6(6):e20758. Epub 2011/06/16. doi: 10.1371/journal.pone.0020758
PONE-D-11-01986 [pii]. PubMed PMID: 21674054.

143. Brandt B, Heyder C, Gloria-Maercker E, Hatzmann W, Rotger A, Kemming D, et al. 3D-extravasation model -- selection of highly motile and metastatic cancer cells. Semin Cancer Biol. 2005;15(5):387-95. Epub 2005/08/02. doi: S1044-579X(05)00039-8 [pii]
10.1016/j.semcancer.2005.06.006. PubMed PMID: 16054390.

144. Mierke CT, Zitterbart DP, Kollmannsberger P, Raupach C, Schlotzer-Schrehardt U, Goecke TW, et al. Breakdown of the endothelial barrier function in tumor cell transmigration. Biophys J. 2008;94(7):2832-46. doi: 10.1529/biophysj.107.113613. PubMed PMID: 18096634; PubMed Central PMCID: PMCPMC2267111.

145. Iwanicki MP, Davidowitz RA, Ng MR, Besser A, Muranen T, Merritt M, et al. Ovarian cancer spheroids use myosin-generated force to clear the mesothelium. Cancer Discov. 2011;1(2):144-57. Epub 2012/02/04. doi: 10.1158/2159-8274.CD-11-0010. PubMed PMID: 22303516.

146. Mierke CT. Cancer cells regulate biomechanical properties of human microvascular endothelial cells. J Biol Chem. 2011;286(46):40025-37. Epub 2011/09/24. doi: M111.256172 [pii]
10.1074/jbc.M111.256172. PubMed PMID: 21940631.

147. Wittchen ES, Worthylake RA, Kelly P, Casey PJ, Quilliam LA, Burridge K. Rap1 GTPase inhibits leukocyte transmigration by promoting endothelial barrier function. J Biol Chem. 2005;280(12):11675-82. Epub 2005/01/22. doi: M412595200 [pii]
10.1074/jbc.M412595200. PubMed PMID: 15661741.

148. Mckenzie JAG, Ridley AJ. Roles of Rho/ROCK and MLCK in TNF-alpha-induced changes in endothelial morphology and permeability. Journal of Cellular Physiology. 2007;213(1):221-8. PubMed PMID: ISI:000249292000025.

149. Jannat RA, Robbins GP, Ricart BG, Dembo M, Hammer DA. Neutrophil adhesion and chemotaxis depend on substrate mechanics. J Phys Condens Matter. 2010;22(19):194117. Epub 2010/05/18. doi: 10.1088/0953-8984/22/19/194117. PubMed PMID: 20473350.

150. Oakes PW, Patel DC, Morin NA, Zitterbart DP, Fabry B, Reichner JS, et al. Neutrophil morphology and migration are affected by substrate elasticity. Blood. 2009;114(7):1387-95. Epub 2009/06/06. doi: blood-2008-11-191445 [pii]
10.1182/blood-2008-11-191445. PubMed PMID: 19491394.

151. Stroka KM, Aranda-Espinoza H. A biophysical view of the interplay between mechanical forces and signaling pathways during transendothelial cell migration. FEBS Journal. 2010;277(5):1145-58. PubMed PMID: ISI:000274312700010.

152. Mierke CT. Role of the endothelium during tumor cell metastasis: is the endothelium a barrier or a promoter for cell invasion and metastasis? J Biophys. 2008;2008:183516. doi: 10.1155/2008/183516. PubMed PMID: 20107573; PubMed Central PMCID: PMCPMC2809021.

153. Wang Y, Pelham R. Preparation of a flexible, porous polyacrylamide substrate for mechanical studies of cultured cells. Methods in Enzymology. 1998;298:489-96. PubMed PMID: ISI:000076246300039.

154. Stroka KM, Levitan I, Aranda-Espinoza H. OxLDL and substrate stiffness promote neutrophil transmigration by enhanced endothelial cell contractility and ICAM-1. J Biomech. 2012;45:1828-34. Epub 2012/05/09. doi: S0021-9290(12)00230-8 [pii] 10.1016/j.jbiomech.2012.04.011. PubMed PMID: 22560286.

155. Stroka KM, Vaitkus JA, Aranda-Espinoza H. Endothelial cells undergo morphological, biomechanical, and dynamic changes in response to tumor necrosis factor-alpha. European Biophysics Journal with Biophysics Letters. 2012;41(11):939-47. doi: Doi 10.1007/S00249-012-0851-3. PubMed PMID: ISI:000310074900002.

156. Norman LL, Aranda-Espinoza H. Cortical Neuron Outgrowth is Insensitive to Substrate Stiffness. Cellular and Molecular Bioengineering. 2010;3(4):398-414. doi: Doi 10.1007/S12195-010-0137-8. PubMed PMID: ISI:000285211500009.

157. Norman LL, Oetama RJ, Dembo M, Byfield F, Hammer DA, Levitan I, et al. Modification of Cellular Cholesterol Content Affects Traction Force, Adhesion and Cell Spreading. Cellular and Molecular Bioengineering. 2010;3(2):151-62. PubMed PMID: ISI:000277368900006.

158. Stroka KM, Aranda-Espinoza H. Effects of Morphology vs. Cell-Cell Interactions on Endothelial Cell Stiffness. Cellular and Molecular Bioengineering. 2011;4(1):9-27. Epub 2011/03/02. doi: 10.1007/s12195-010-0142-y. PubMed PMID: 21359128; PubMed Central PMCID: PMC3044329.

159. Shaw SK, Bamba PS, Perkins BN, Luscinskas FW. Real-time imaging of vascular endothelial-cadherin during leukocyte transmigration across endothelium. J Immunol. 2001;167(4):2323-30. Epub 2001/08/08. PubMed PMID: 11490021.

160. Norman L, Sengupta K, Aranda-Espinoza H. Blebbing dynamics during endothelial cell spreading. Eur J Cell Biol. 2011;90(1):37-48. Epub 2010/11/20. doi: 10.1016/j.ejcb.2010.09.013
S0171-9335(10)00204-9 [pii]. PubMed PMID: 21087809.

161. Norman LL, Brugues J, Sengupta K, Sens P, Aranda-Espinoza H. Cell blebbing and membrane area homeostasis in spreading and retracting cells. Biophys J. 2010;99(6):1726-33. Epub 2010/09/23. doi: 10.1016/j.bpj.2010.07.031
S0006-3495(10)00903-3 [pii]. PubMed PMID: 20858416.

162. Norman LL, Oetama RJ, Dembo M, Byfield F, Hammer DA, Levitan I, et al. Modification of Cellular Cholesterol Content Affects Traction Force, Adhesion and Cell Spreading. Cell Mol Bioeng. 2010;3(2):151-62. doi: 10.1007/s12195-010-0119-x. PubMed PMID: 21461187; PubMed Central PMCID: PMCPMC3066088.

163. Hayenga HN, Aranda-Espinoza H. Stiffness Increases Mononuclear Cell Transendothelial Migration. Cellular and Molecular Bioengineering. 2013;6(3):253-65. doi: Doi 10.1007/S12195-013-0284-9. PubMed PMID: ISI:000323109400001.

164. Breviario F, Caveda L, Corada M, Martin-Padura I, Navarro P, Golay J, et al. Functional properties of human vascular endothelial cadherin (7B4/cadherin-5), an endothelium-specific cadherin. Arterioscler Thromb Vasc Biol. 1995;15(8):1229-39. Epub 1995/08/01. PubMed PMID: 7627717.

165. Navarro P, Caveda L, Breviario F, Mandoteanu I, Lampugnani MG, Dejana E. Catenin-dependent and -independent functions of vascular endothelial cadherin. J Biol Chem. 1995;270(52):30965-72. Epub 1995/12/29. PubMed PMID: 8537353.

166. Mierke CT. Endothelial cell's biomechanical properties are regulated by invasive cancer cells. Molecular Biosystems. 2012;8(6):1639-49. doi: Doi 10.1039/C2mb25024a. PubMed PMID: ISI:000303776200004.

167. Lapis K, Paku S, Liotta LA. Endothelialization of embolized tumor cells during metastasis formation. Clin Exp Metastasis. 1988;6(1):73-89. Epub 1988/01/01. PubMed PMID: 3335082.

168. Crissman JD, Hatfield J, Schaldenbrand M, Sloane BF, Honn KV. Arrest and extravasation of B16 amelanotic melanoma in murine lungs. A light and electron microscopic study. Lab Invest. 1985;53(4):470-8. Epub 1985/10/01. PubMed PMID: 4046557.

169. Schmidt A, Ladage D, Steingen C, Brixius K, Schinkothe T, Klinz FJ, et al. Mesenchymal stem cells transmigrate over the endothelial barrier. Eur J Cell Biol. 2006;85(11):1179-88. Epub 2006/07/11. doi: S0171-9335(06)00108-7 [pii]
10.1016/j.ejcb.2006.05.015. PubMed PMID: 16824647.

170. Langer HF, Stellos K, Steingen C, Froihofer A, Schonberger T, Kramer B, et al. Platelet derived bFGF mediates vascular integrative mechanisms of mesenchymal stem cells in vitro. J Mol Cell Cardiol. 2009;47(2):315-25. Epub 2009/03/31. doi: S0022-2828(09)00116-3 [pii]
10.1016/j.yjmcc.2009.03.011. PubMed PMID: 19328809.

171. Teo GS, Ankrum JA, Martinelli R, Boetto SE, Simms K, Sciuto TE, et al. Mesenchymal stem cells transmigrate between and directly through tumor necrosis factor-alpha-activated endothelial cells via both leukocyte-like and novel mechanisms. Stem Cells. 2012;30(11):2472-86. Epub 2012/08/14. doi: 10.1002/stem.1198. PubMed PMID: 22887987; PubMed Central PMCID: PMC3479371.

172. Zervantonakis IK, Hughes-Alford SK, Charest JL, Condeelis JS, Gertler FB, Kamm RD. Three-dimensional microfluidic model for tumor cell intravasation and endothelial barrier function. Proc Natl Acad Sci U S A. 2012;109(34):13515-20. Epub 2012/08/08. doi: 1210182109 [pii]
10.1073/pnas.1210182109. PubMed PMID: 22869695; PubMed Central PMCID: PMC3427099.

173. Strell C, Lang K, Niggemann B, Zaenker KS, Entschladen F. Surface molecules regulating rolling and adhesion to endothelium of neutrophil granulocytes and MDA-MB-468 breast carcinoma cells and their interaction. Cellular and Molecular Life Sciences. 2007;64(24):3306-16. doi: Doi 10.1007/S00018-007-7402-6. PubMed PMID: ISI:000252219000015.

174. Ghislin S, Obino D, Middendorp S, Boggetto N, Alcaide-Loridan C, Deshayes F. LFA-1 and ICAM-1 expression induced during melanoma-endothelial cell co-culture favors the transendothelial migration of melanoma cell lines in vitro. BMC cancer. 2012;12:455. doi: 10.1186/1471-2407-12-455. PubMed PMID: 23039186; PubMed Central PMCID: PMC3495854.

175. van Grevenstein WM, Hofland LJ, Jeekel J, van Eijck CH. The expression of adhesion molecules and the influence of inflammatory cytokines on the adhesion of human pancreatic carcinoma cells to mesothelial monolayers. Pancreas. 2006;32(4):396-402. doi: 10.1097/01.mpa.0000220865.80034.2a. PubMed PMID: 16670622.

176. Zaman MH, Trapani LM, Sieminski AL, Mackellar D, Gong H, Kamm RD, et al. Migration of tumor cells in 3D matrices is governed by matrix stiffness along with cell-matrix adhesion and proteolysis. Proc Natl Acad Sci U S A. 2006;103(29):10889-94. Epub 2006/07/13. doi: 0604460103 [pii]
10.1073/pnas.0604460103. PubMed PMID: 16832052; PubMed Central PMCID: PMC1544144.

177. Alcaide P, Martinelli R, Newton G, Williams MR, Adam A, Vincent PA, et al. p120-Catenin prevents neutrophil transmigration independently of RhoA inhibition by impairing Src dependent VE-cadherin phosphorylation. Am J Physiol Cell Physiol. 2012;303(4):C385-95. Epub 2012/06/01. doi: ajpcell.00126.2012 [pii]
10.1152/ajpcell.00126.2012. PubMed PMID: 22648953; PubMed Central PMCID: PMC3422989.

178. Stroka KM, Hayenga HN, Aranda-Espinoza H. Human neutrophil cytoskeletal dynamics and contractility actively contribute to trans-endothelial migration. PLoS One. 2013;8(4):e61377. doi: 10.1371/journal.pone.0061377. PubMed PMID: 23626676; PubMed Central PMCID: PMCPMC3634075.

179. Vainer G, Vainer-Mosse E, Pikarsky A, Shenoy SM, Oberman F, Yeffet A, et al. A role for VICKZ proteins in the progression of colorectal carcinomas: regulating

lamellipodia formation. J Pathol. 2008;215(4):445-56. doi: 10.1002/path.2376. PubMed PMID: 18535985; PubMed Central PMCID: PMCPMC3148580.

180. Li Z, Wang L, Hays TS, Cai Y. Dynein-mediated apical localization of crumbs transcripts is required for Crumbs activity in epithelial polarity. J Cell Biol. 2008;180(1):31-8. doi: 10.1083/jcb.200707007. PubMed PMID: 18195099; PubMed Central PMCID: PMCPMC2213619.

181. Nagaoka K, Udagawa T, Richter JD. CPEB-mediated ZO-1 mRNA localization is required for epithelial tight-junction assembly and cell polarity. Nat Commun. 2012;3:675. doi: 10.1038/ncomms1678. PubMed PMID: 22334078; PubMed Central PMCID: PMCPMC4334452.

182. Ridley AJ. Life at the leading edge. Cell. 2011;145(7):1012-22. doi: 10.1016/j.cell.2011.06.010. PubMed PMID: 21703446.

183. Lo CM, Wang HB, Dembo M, Wang YL. Cell movement is guided by the rigidity of the substrate. Biophys J. 2000;79(1):144-52. doi: 10.1016/S0006-3495(00)76279-5. PubMed PMID: 10866943; PubMed Central PMCID: PMCPMC1300921.

184. Hamilla SM, Stroka KM, Aranda-Espinoza H. VE-cadherin-independent cancer cell incorporation into the vascular endothelium precedes transmigration. PLoS One. 2014;9(10):e109748. doi: 10.1371/journal.pone.0109748. PubMed PMID: 25275457; PubMed Central PMCID: PMCPMC4183660.

185. Dembo M, Wang YL. Stresses at the cell-to-substrate interface during locomotion of fibroblasts. Biophysical journal. 1999;76(4):2307-16. doi: 10.1016/S0006-3495(99)77386-8. PubMed PMID: 10096925; PubMed Central PMCID: PMC1300203.

186. Munevar S, Wang Y, Dembo M. Traction force microscopy of migrating normal and H-ras transformed 3T3 fibroblasts. Biophys J. 2001;80(4):1744-57. PubMed PMID: 11259288; PubMed Central PMCID: PMCPMC1301364.

187. Park HY, Trcek T, Wells AL, Chao JA, Singer RH. An unbiased analysis method to quantify mRNA localization reveals its correlation with cell motility. Cell Rep. 2012;1(2):179-84. doi: 10.1016/j.celrep.2011.12.009. PubMed PMID: 22832165; PubMed Central PMCID: PMCPMC4079260.

188. Tseng Q, Duchemin-Pelletier E, Deshiere A, Balland M, Guillou H, Filhol O, et al. Spatial organization of the extracellular matrix regulates cell-cell junction positioning. Proc Natl Acad Sci U S A. 2012;109(5):1506-11. doi: 10.1073/pnas.1106377109. PubMed PMID: 22307605; PubMed Central PMCID: PMCPMC3277177.

189. Paszek MJ, Zahir N, Johnson KR, Lakins JN, Rozenberg GI, Gefen A, et al. Tensional homeostasis and the malignant phenotype. Cancer Cell. 2005;8(3):241-54. doi: 10.1016/j.ccr.2005.08.010. PubMed PMID: 16169468.

190. Jaalouk DE, Lammerding J. Mechanotransduction gone awry. Nature reviews Molecular cell biology. 2009;10(1):63-73. doi: 10.1038/nrm2597. PubMed PMID: 19197333; PubMed Central PMCID: PMC2668954.

191. McGrail DJ, Kieu QM, Dawson MR. The malignancy of metastatic ovarian cancer cells is increased on soft matrices through a mechanosensitive Rho-ROCK pathway. J Cell Sci. 2014;127(Pt 12):2621-6. doi: 10.1242/jcs.144378. PubMed PMID: 24741068; PubMed Central PMCID: PMC4058108.

192. Kovacs M, Toth J, Hetenyi C, Malnasi-Csizmadia A, Sellers JR. Mechanism of blebbistatin inhibition of myosin II. J Biol Chem. 2004;279(34):35557-63. doi: 10.1074/jbc.M405319200. PubMed PMID: 15205456.

193. Ishizaki T, Uehata M, Tamechika I, Keel J, Nonomura K, Maekawa M, et al. Pharmacological properties of Y-27632, a specific inhibitor of rho-associated kinases. Mol Pharmacol. 2000;57(5):976-83. PubMed PMID: 10779382.

194. Engler AJ, Sen S, Sweeney HL, Discher DE. Matrix elasticity directs stem cell lineage specification. Cell. 2006;126(4):677-89. doi: 10.1016/j.cell.2006.06.044. PubMed PMID: 16923388.

195. Gundersen GG, Bulinski JC. Selective stabilization of microtubules oriented toward the direction of cell migration. Proc Natl Acad Sci U S A. 1988;85(16):5946-50. PubMed PMID: 3413068; PubMed Central PMCID: PMCPMC281882.

196. Guo WH, Frey MT, Burnham NA, Wang YL. Substrate rigidity regulates the formation and maintenance of tissues. Biophysical journal. 2006;90(6):2213-20. doi: 10.1529/biophysj.105.070144. PubMed PMID: 16387786; PubMed Central PMCID: PMC1386800.

197. Gu W, Katz Z, Wu B, Park HY, Li DL, Lin S, et al. Regulation of local expression of cell adhesion and motility-related mRNAs in breast cancer cells by IMP1/ZBP1. J Cell Sci. 2012;125(1):81-91. doi: 10.1242/jcs.086132. PubMed PMID: WOS:000300329100009.

198. Grinnell F, Rhee SM, Jiang HM, Ho CH. Microtubule function in fibroblast spreading is modulated according to the tension state of cell-matrix interactions. Faseb J. 2007;21(5):A635-A6. PubMed PMID: WOS:000245708505191.

199. Svitkina TM, Verkhovsky AB, McQuade KM, Borisy GG. Analysis of the actin-myosin II system in fish epidermal keratocytes: mechanism of cell body translocation. J Cell Biol. 1997;139(2):397-415. PubMed PMID: 9334344; PubMed Central PMCID: PMCPMC2139803.

200. Palazzo AF, Cook TA, Alberts AS, Gundersen GG. mDia mediates Rho-regulated formation and orientation of stable microtubules. Nat Cell Biol. 2001;3(8):723-9. doi: 10.1038/35087035. PubMed PMID: 11483957.

201. Palazzo AF, Joseph HL, Chen YJ, Dujardin DL, Alberts AS, Pfister KK, et al. Cdc42, dynein, and dynactin regulate MTOC reorientation independent of Rho-regulated microtubule stabilization. Curr Biol. 2001;11(19):1536-41. PubMed PMID: 11591323.

202. Fonrose X, Ausseil F, Soleilhac E, Masson V, David B, Pouny I, et al. Parthenolide inhibits tubulin carboxypeptidase activity. Cancer Res. 2007;67(7):3371-8. doi: 10.1158/0008-5472.CAN-06-3732. PubMed PMID: 17409447.

203. Palazzo AF, Eng CH, Schlaepfer DD, Marcantonio EE, Gundersen GG. Localized stabilization of microtubules by integrin- and FAK-facilitated Rho signaling. Science. 2004;303(5659):836-9. doi: 10.1126/science.1091325. PubMed PMID: 14764879.

204. Even-Ram S, Doyle AD, Conti MA, Matsumoto K, Adelstein RS, Yamada KM. Myosin IIA regulates cell motility and actomyosin-microtubule crosstalk. Nat Cell Biol. 2007;9(3):299-309. doi: 10.1038/ncb1540. PubMed PMID: 17310241.

205. Arakawa Y, Bito H, Furuyashiki T, Tsuji T, Takemoto-Kimura S, Kimura K, et al. Control of axon elongation via an SDF-1alpha/Rho/mDia pathway in cultured cerebellar granule neurons. J Cell Biol. 2003;161(2):381-91. doi: 10.1083/jcb.200210149. PubMed PMID: 12707308; PubMed Central PMCID: PMCPMC2172896.

206. Wen Y, Eng CH, Schmoranzer J, Cabrera-Poch N, Morris EJ, Chen M, et al. EB1 and APC bind to mDia to stabilize microtubules downstream of Rho and promote cell migration. Nat Cell Biol. 2004;6(9):820-30. doi: 10.1038/ncb1160. PubMed PMID: 15311282.

207. Wozniak MA, Desai R, Solski PA, Der CJ, Keely PJ. ROCK-generated contractility regulates breast epithelial cell differentiation in response to the physical properties of a three-dimensional collagen matrix. The Journal of cell biology. 2003;163(3):583-95. doi: 10.1083/jcb.200305010. PubMed PMID: 14610060; PubMed Central PMCID: PMC2173660.

208. Parekh A, Weaver AM. Regulation of cancer invasiveness by the physical extracellular matrix environment. Cell adhesion & migration. 2009;3(3):288-92. PubMed PMID: 19458499; PubMed Central PMCID: PMC2712813.

209. Parri M, Chiarugi P. Rac and Rho GTPases in cancer cell motility control. Cell communication and signaling : CCS. 2010;8:23. doi: 10.1186/1478-811X-8-23. PubMed PMID: 20822528; PubMed Central PMCID: PMC2941746.

210. Badiola I, Villace P, Basaldua I, Olaso E. Downregulation of discoidin domain receptor 2 in A375 human melanoma cells reduces its experimental liver metastasis ability. Oncology reports. 2011;26(4):971-8. doi: 10.3892/or.2011.1356. PubMed PMID: 21701781.

211. Valiathan RR, Marco M, Leitinger B, Kleer CG, Fridman R. Discoidin domain receptor tyrosine kinases: new players in cancer progression. Cancer metastasis reviews.

2012;31(1-2):295-321. doi: 10.1007/s10555-012-9346-z. PubMed PMID: 22366781; PubMed Central PMCID: PMC3351584.

212. Walsh LA, Nawshad A, Medici D. Discoidin domain receptor 2 is a critical regulator of epithelial-mesenchymal transition. Matrix biology : journal of the International Society for Matrix Biology. 2011;30(4):243-7. doi: 10.1016/j.matbio.2011.03.007. PubMed PMID: 21477649; PubMed Central PMCID: PMC3114285.

213. Whipple RA, Matrone MA, Cho EH, Balzer EM, Vitolo MI, Yoon JR, et al. Epithelial-to-mesenchymal transition promotes tubulin detyrosination and microtentacles that enhance endothelial engagement. Cancer research. 2010;70(20):8127-37. doi: 10.1158/0008-5472.CAN-09-4613. PubMed PMID: 20924103; PubMed Central PMCID: PMC3123454.

214. Whipple RA, Balzer EM, Cho EH, Matrone MA, Yoon JR, Martin SS. Vimentin filaments support extension of tubulin-based microtentacles in detached breast tumor cells. Cancer research. 2008;68(14):5678-88. doi: 10.1158/0008-5472.CAN-07-6589. PubMed PMID: 18632620; PubMed Central PMCID: PMC2859318.

215. Marella NV, Malyavantham KS, Wang J, Matsui S, Liang P, Berezney R. Cytogenetic and cDNA microarray expression analysis of MCF10 human breast cancer progression cell lines. Cancer research. 2009;69(14):5946-53. doi: 10.1158/0008-5472.CAN-09-0420. PubMed PMID: 19584277; PubMed Central PMCID: PMC2826242.

216. Kadota M, Yang HH, Gomez B, Sato M, Clifford RJ, Meerzaman D, et al. Delineating genetic alterations for tumor progression in the MCF10A series of breast cancer cell lines. PloS one. 2010;5(2):e9201. doi: 10.1371/journal.pone.0009201. PubMed PMID: 20169162; PubMed Central PMCID: PMC2821407.

217. Tang B, Vu M, Booker T, Santner SJ, Miller FR, Anver MR, et al. TGF-beta switches from tumor suppressor to prometastatic factor in a model of breast cancer progression. The Journal of clinical investigation. 2003;112(7):1116-24. doi: 10.1172/JCI18899. PubMed PMID: 14523048; PubMed Central PMCID: PMC198530.

218. Soule HD, Maloney TM, Wolman SR, Peterson WD, Jr., Brenz R, McGrath CM, et al. Isolation and characterization of a spontaneously immortalized human breast epithelial cell line, MCF-10. Cancer research. 1990;50(18):6075-86. PubMed PMID: 1975513.

219. Dawson PJ, Wolman SR, Tait L, Heppner GH, Miller FR. MCF10AT: a model for the evolution of cancer from proliferative breast disease. The American journal of pathology. 1996;148(1):313-9. PubMed PMID: 8546221; PubMed Central PMCID: PMC1861604.

220. Santner SJ, Dawson PJ, Tait L, Soule HD, Eliason J, Mohamed AN, et al. Malignant MCF10CA1 cell lines derived from premalignant human breast epithelial MCF10AT cells. Breast cancer research and treatment. 2001;65(2):101-10. PubMed PMID: 11261825.

221. Stephens PJ, Tarpey PS, Davies H, Van Loo P, Greenman C, Wedge DC, et al. The landscape of cancer genes and mutational processes in breast cancer. Nature. 2012;486(7403):400-4. doi: 10.1038/nature11017. PubMed PMID: 22722201; PubMed Central PMCID: PMC3428862.

222. Cancer Genome Atlas N. Comprehensive molecular portraits of human breast tumours. Nature. 2012;490(7418):61-70. doi: 10.1038/nature11412. PubMed PMID: 23000897; PubMed Central PMCID: PMC3465532.

223. Hayakawa K, Sato N, Obinata T. Dynamic reorientation of cultured cells and stress fibers under mechanical stress from periodic stretching. Exp Cell Res. 2001;268(1):104-14. doi: 10.1006/excr.2001.5270. PubMed PMID: 11461123.

224. Kaunas R, Nguyen P, Usami S, Chien S. Cooperative effects of Rho and mechanical stretch on stress fiber organization. Proc Natl Acad Sci U S A. 2005;102(44):15895-900. doi: 10.1073/pnas.0506041102. PubMed PMID: 16247009; PubMed Central PMCID: PMCPMC1276069.

225. Bulinski JC, Gundersen GG. Stabilization of post-translational modification of microtubules during cellular morphogenesis. Bioessays. 1991;13(6):285-93. doi: 10.1002/bies.950130605. PubMed PMID: 1892478.

226. Sabeh F, Shimizu-Hirota R, Weiss SJ. Protease-dependent versus -independent cancer cell invasion programs: three-dimensional amoeboid movement revisited. J Cell Biol. 2009;185(1):11-9. doi: 10.1083/jcb.200807195. PubMed PMID: 19332889; PubMed Central PMCID: PMCPMC2700505.